5-2017

Cation Exchange Processes Involving the Agricultural Antibiotic Tylosin in Soil and Soil Minerals

Jaime Jacinda Call
University of Tennessee, Knoxville, jcall1@utk.edu

To the Graduate Council:

I am submitting herewith a thesis written by Jaime Jacinda Call entitled "Cation Exchange Processes Involving the Agricultural Antibiotic Tylosin in Soil and Soil Minerals." I have examined the final electronic copy of this thesis for form and content and recommend that it be accepted in partial fulfillment of the requirements for the degree of Master of Science, with a major in Environmental and Soil Sciences.

Michael E. Essington, Major Professor

We have read this thesis and recommend its acceptance:

Jaehoon Lee, Jennifer M. DeBruyn

Accepted for the Council:
Dixie L. Thompson

Vice Provost and Dean of the Graduate School

(Original signatures are on file with official student records.)

Cation Exchange Processes Involving the Agricultural Antibiotic Tylosin in Soil and Soil Minerals

A Thesis Presented for the

Master of Science

Degree

The University of Tennessee, Knoxville

Jaime Jacinda Call

May 2017

DEDICATION

I first dedicate this thesis to my Mom, who was my cheerleader all of my life; and to my Dad, who first inspired my love of science.

Secondly, I dedicate this thesis to my husband, Benjamin, and my daughters, Rose and Marisa, who forgave the late nights and kept me focused on the finish line.

ACKNOWLEDGEMENTS

The completion of this work would not have been possible without the guidance and knowledge of my advisor, Michael Essington, who is not only my mentor but also a friend. I am indebted to my friend and mentor Joanne Logan who found support for me to attend and finish graduate school. I am grateful for the assistance of Melanie Stewart and Galina Melnichenko, not only in completing sample analysis but also for being great laboratory mates and friends. I am also grateful for Haley Koziol for being a hardworking undergraduate student who has become an integrated part of this thesis. I am thankful for the continual friendship and enthusiasm of my fellow graduate students who have come before me, and those still on the path to finishing. Countless thanks are owed to the many friends and family who have always encouraged me.

ABSTRACT

Tylosin (TYL) is a veterinary antibiotic that is used as a feed additive in swine production. Concentrations as high as 4.0 mg L^{-1} have been found in swine manure leachates. Tylosin is predominately a cationic species, due to the protonation of a dimethylamine moiety in pH < 7.5 solutions. The soil adsorption of TYL is influenced by pH, background electrolyte, and ionic strength, suggesting that ion exchange is an important retention mechanism. The objective of this study was to examine the exchange selectivity of TYL in competition with sodium and calcium in montmorillonite and vermiculite reference clays and in the Bt2 horizons of a west Tennessee Loring soil. Binary exchange studies were performed and exchange isotherms were developed to establish preference, to determine the Vanselow selectivity coefficient (K_V) as a function of exchange phase composition, and to determine the exchangeable and nonexchangeable forms of TYL. X-ray diffraction was used to evaluate TYL intercalation into reference and soil clay minerals. For TYLX-NaX exchange, the exchange isotherms indicated that TYL^+ was preferred over Na^+ by montmorillonite, but not by the Loring soil. For TYLX-CaX exchange, the exchange isotherms indicated that TYL^+ was preferred over Ca^{2+} by montmorillonite and the Loring soil. The K_V values were generally invariant with exchange phase composition for NaX to TYLX exchange on montmorillonite and soil clay minerals. However, the K_V values were variable with exchange phase composition for CaX to TYLX exchange. Tylosin adsorption was described by the Freundlich and partition models, with exchangeable TYL dominating in Na systems and nonexchangeable TYL in Ca systems. X-ray diffraction revealed TYL intercalation of the reference and soil clay minerals. The STx-1 expanded to 3 nm with

TYL intercalation, while the Libby vermiculite had no TYL intercalation. The d-value of TYL intercalated soil clay ranged from 1.7 nm to > 2 nm for the Ca and Na systems. The intercalation of TYL into soil and reference smectite suggests that this compound may be protected from microbial degradation. Conversely, the competition of TYL with common soil cations for exchange sites may result in enhance environmental mobility.

TABLE OF CONTENTS

LIST OF TABLES

LIST OF FIGURES

CHAPTER 1: INTRODUCTION

VETERINARY ANTIBIOTICS IN THE ENVIRONMENT

The presence of antibiotics in the environment has been shown to cause the development of antibiotic resistant bacteria in animal feces, milk, eggs, and meat (Teuber, 1999 and 2001). Since 2006, the European Parliament has heavily regulated the use of veterinary antibiotics (VA) in animal husbandry for nontherapeutic purposes, virtually banning these altogether (European Commission, 2003). Following suit, as of 2017, new legislative regulations for VAs in the United States have banned their use as prophylactics and for nontherapeutic purposes without the authorization of a veterinarian (U.S. Food and Drug Administration, 2015).

Prior to these new regulations, VAs were given to agricultural livestock for disease prevention, growth promotion, and other nontherapeutic purposes (Cohen, 1998; Kumar et al.,2005; Sarmah et al., 2006). Inefficient uptake and metabolism of antibiotics by animals results in the excretion of approximately 80% of the administered compounds in feces and urine (Levy, 1992; Alcock et al., 1999; Kolpin et al., 2002; Kemper, 2008). Thus, agricultural practices in animal husbandry and aquaculture have been found to be a major contributor of antibiotics to watersheds, where the antibiotics are exposed to the environment through manure fertilizers (Halling-Sorensen et al., 1998; Kolpin et al., 2002; Thiele-Bruhn, 2003; Harris et al., 2012). Livestock production creates an estimated 57.9 million metric tons of manure per year (Kummerer, 2003; Wang and Yates, 2008). Animal manure can be collected and stored in large lagoons resulting in the localized accumulation of antibiotics in the lagoons and in surface and groundwater surrounding the lagoons (Thiele-Bruhn, 2003).

Many studies have reported measureable amounts of antibiotics in soil, water, and plant samples. Kolpin et al. (2002) conducted a survey of U.S. streams for the presence of pharmaceuticals and found antibiotic concentrations of up to 0.7 μg L^{-1} in 27% of the streams sampled. The frequency of detection of antibiotics in surface waters was 50% higher than reproductive hormones (i.e. progesterone, testosterone, estriol and estrone). Sarmah et al. (2006) reported on an U.S. Geological Survey study where antibiotics were found in 21 samples out of 139 U.S. streams. Tylosin, a veterinarian antibiotic, was one of the top 3 pharmaceuticals that frequently occurred in the surface waters.

Plant uptake is one of the concerns associated with the environmental dispersement of antibiotics. Kumar et al. (2005) conducted a manure-fertilizer crop study with chlortetracycline (CTC), a commonly used veterinary antibiotic, where they found measureable amounts, 2 to 17 ng g^{-1}, of CTC in green onion, cabbage, and corn plant tissues. Further, tissue CTC concentrations were directly correlated to antibiotic presence in manure. Michelini et al. (2012) conducted a study using sulfadiazine (SMT), another commonly used veterinarian antibiotic. Corn and willow plants were grown in SMT-spiked soils in a greenhouse study. The SMT was mainly stored in the roots of both the corn and willow, and contributed to the lowered plant uptake of soil water and to reduced biomass production. In heavily SMT-spiked treatments, the adverse effects included corn plant death, and the willow had lower chlorophyll content and reduced carbon-nitrogen ratios. Batchelder (1982) conducted a greenhouse study of beans fertilized with antibiotic-laden manure. The manure was spiked with CTC and oxytetracycline (OTC) and bean plants were grown in sandy loam and clay loam soils.

He found soil characteristics to affect the impact of the antibiotics on plant growth and development. The bean plants grown in the clay loam did not show any growth or developmental differences with antibiotic treatment. However, reduced plant height and dry weight yields were observed in plants grown in the sandy loam treated with antibiotics. Batchelder (1982) hypothesized that the clay loam adsorbed the antibiotics limiting their availability to the bean plant.

TYLOSIN ANTIBIOTIC

Beausse (2004) identified the macrolides, fluoroquinolones, and sulfonamide antibiotic groups to be more widespread in the environment than other antibiotic groups, such as the tetracyclines and penicillins. Sarmah et al. (2006) found 54% of antimicrobial growth promoters administered to livestock is tylosin (TYL), a macrolide antibiotic. There are many mechanisms for antibiotics to become immobile or degraded in soil and water environments including photolysis, hydrolysis, thermolysis, adsorption, and biodegradation (Harris et al. 2012). Numerous studies have investigated the adsorptive behavior of antibiotic compounds, specifically TYL, by soil and soil separates (Allaire et al., 2006; Ter Laak et al., 2006; Sassman et al., 2007; Hu and Coats, 2009; Essington et al., 2010; Lee et al., 2014).

Veterinary-grade TYL (Figure A-1) is a mixture of macrolide antibiotics that are commonly used in swine and poultry production as a prophylactic (Fish and Carr, 1986). The compounds in the mixture include TYL, desmycosin, macrocin, and relomycin where TYL is the major component (Fish and Carr, 1986; Loke et al., 2002). Tylosin is a large organic compound with the molecular weight of 916.12 g mol^{-1} and a water

solubility of 5,000 mg L^{-1}. It has an octanol-water partition coefficient (K_{ow}) of 316 and a methylamine functional group that is protonated in neutral to acidic solutions (pK_a = 7.50, Figure A-1) (McFarland et al. 1997). The speciation of the methylamine functional group as a function of pH is illustrated in Figure A-2.

INTERCALATION OF CLAYS

How TYL and other veterinary antibiotics reside in soil and mineral structures can influence their fate and transport in the environment. In addition to adsorption studies, research has examined the intercalating clays with large organic compounds (Porubcan et al., 1977; Fejer et al., 2002; Chang et al., 2009; Parolo et al., 2008; Wang et al., 2010; Sun et al., 2013; Zhang et al., 2013; Kaur and Datta, 2013; Hou et al., 2014; Lv et al., 2015; Kedzierski et al., 2016; Aristilde et al., 2016). X-ray diffraction (XRD) and fourier transform infrared (FTIR) spectroscopy have been used to detect the presence these compounds and to characterize the binding mechanisms in mineral and soil structures. Montmorillonite, a 2:1 phyllosilicate smectite mineral is a common soil clay mineral and frequently used as an adsorption medium in organic compound retention studies. Montmorillonite has extensive surface area (~600 m^2 g^{-1}) and reactivity (CEC of 80 to 100 $cmol_c$ kg^{-1}) and can swell to accommodate large molecule (Madsen, 1977; Mercier and Detellier, 1994).

Studies involving the intercalation of montmorillonite with large organic compounds, such as peptides, deoxyribonucleic acid (DNA), and veterinary antibiotics (tetracycline, oxytetracycline, ciprofloxacin, and TYL) indicate that montmorillonite can expand to accommodate the compound. Kedzierski et al. (2016) intercalated Na-

montmorillonite (1.2 nm d value) with large dendrimeric peptide compounds and found d values to range from 1.48 to 3.09 nm. Hou et al. (2014) intercalated DNA into montmorillonite, where they reported a d value of 2.76 nm. Tetracycline expanded Na-, Ca-, and Mg-montmorillonite layers in pH 4 to 5 suspensions from 1.26 (Na-saturated) and 1.45 nm (Ca- and Mg-saturated) to 1.80 nm (Porubcan et al., 1977; Parolo et al., 2008; Chang et al., 2009; Aristilde et al., 2016).

While few studies have reported veterinary antibiotic intercalation into clay minerals, particularly the tetracyclins, there are limited studies that have examined TYL intercalation. Zhang et al. (2013) examined the intercalation of TYL into kaolinite and montmorillonite. Tylosin was added in various loadings to Na-montmorillonite and kaolinite samples in pH 4, 7, and 9 suspensions. As kaolinite is a non-expansive clay, there was no TYL intercalation reported. However, TYL moved into the montmorillonite layers and expansion from 1.19 nm (Na-saturated) to 1.62 nm was reported.

TYLOSIN ADSORPTION

Adsorption studies involving TYL have focused on characterizing adsorption by soil and soil minerals as a function of pH, ionic strength, background electrolyte type, organic matter content, and clay mineral content and type. Allaire et al. (2006) examined the adsorption kinetics of TYL in a sandy loam soil and a clay soil. Adsorption was examined at reaction times of 0.0-, 0.017-, 0.08-, 0.25-, 0.75-, 3-, 7-, 24-, and 48-hours. Tylosin reached adsorption equilibrium at 0.08 h (5 minutes) on the sandy loam and at 3 h on the clay soil. At equilibrium, the clay soil was found to adsorb 2.4 times more TYL than the sandy loam. It was concluded that TYL equilibrium could

be reached in less than 4 h under laboratory conditions, and that the extent of adsorption was dependent on soil clay content.

Ter Laak et al. (2006) investigated TYL adsorption by clay loam soil and a loamy sand soil using batch adsorption experiments as a function of pH and ionic strength. Sodium chloride and $CaCl_2$ were used as the background electrolytes, with concentrations ranging from 0.0 M to 0.2 M. The clay loam soil had more adsorption relative to the loamy sand at pH 6 and adsorption decreased with increasing pH. The authors postulated that the decreasing retention with increasing pH was due to the deprotonation and loss of the exchangeable, cationic form of tylosin (TYL^+). Tylosin adsorption also decreased with increasing ionic strength in both NaCl and $CaCl_2$ systems, and retention decreased in the $CaCl_2$ relative to the NaCl systems. Based on their findings, Ter Laak et al. (2006) concluded that cation exchange was the predominate adsorption mechanism for TYL.

Essington et al. (2010) examined the adsorption of TYL by montmorillonite and kaolinite as a function of pH, TYL concentrations, ionic strength, and background electrolyte type. Tylosin adsorption edge experiments were conducted in the 4 to 9 pH range and clay loadings were 0.3 g montmorillonite L^{-1} and 6.0 g kaolinite L^{-1}. In both the montmorillonite and kaolinite systems, the initial TYL concentration was 38 μmol L^{-1}. As pH increased, TYL adsorption was constant in the pH 4 to 7 range in the montmorillonite system at approximately 120 mmol kg^{-1}. As pH increased above 7, TYL adsorption decreased. Decreasing adsorption with increasing pH was associated with the loss of TYL^+. Unlike the montmorillonite system, TYL adsorption was at a maximum of 0.33 mmol kg^{-1} at pH 4 in the kaolinite system, then decreased with increasing pH

throughout the entire range of pH (4 to 9) examined. Surface complexation modeling indicated that TYL retention in both the montmorillonite and kaolinite systems could be predicted by employing only a cation exchange mechanism.

Essington et al. (2010) also performed adsorption isotherm experiments to examine the influence of ionic strength on TYL retention, as well as the effects of changing the background electrolyte type. Montmorillonite and kaolinite were added to TYL solutions containing the initial concentration range of 0.8 to 59 μmol L^{-1}. The solution-solid ratios were identical to the adsorption edge studies except with a range of ionic strengths (0.005, 0.01, and 0.05 mol L^{-1}) in $NaNO_3$ and an equilibrium pH of 5.6 in montmorillonite and 5.7 for kaollinite. To examine change in background electrolyte type, they repeated the adsorption isotherm experiments using 0.01 mol L^{-1} $Ca(NO_3)_2$ with an equilibrium pH of 5.0 in montmorillonite and 5.2 in kaolinite. For both montmorillonite and kaolinite, TYL retention was Langmuirian, where adsorption intensity decreased with increasing TYL surface coverage. Adsorption intensity also decreased when $Ca(NO_3)_2$ was substituted for $NaNO_3$ as the background electrolyte. The authors concluded these results indicated cation exchange was the main retention mechanism of TYL.

Lee et al. (2014) examined TYL retention by clay loam soils using batch adsorption isotherm experiments. For these, they used an initial concentration range of 1 to 3.2 μmol L^{-1} of TYL. The adsorption of TYL was Langmuirian; adsorption intensity decreased in intensity with increasing surface coverage. Further, TYL adsorption was greater in the subsurface soils compared to the surface soils. This increased adsorption by the subsurface soils was attributed to their greater clay content. Greater adsorption

occurred in the $NaNO_3$ systems compared to the $Ca(NO_3)_2$ systems, indicating that TYL^+ was competing with the cations for exchange sites. These findings were consistent with those of Essington et al. (2010) on montmorillonite and kaolinite, which also identified cation exchange as an important TYL retention mechanism.

Similar to the findings of Ter Laak et al. (2006), Essington et al. (2010) and Lee et al. (2014) reported an increase in TYL adsorption with increasing clay content. Greater TYL adsorption was observed by montmorillonite and subsurface soils (high CEC) relative to kaolinite and surface soils (low CEC). Retention decreased with increasing ionic strength, and decreased in the presence of a divalent cation relative to a monovalent. These findings indicate that an important retention mechanism for TYL is cation exchange.

CATION EXCHANGE AND TYLOSIN

Adsorption and mobility studies involving TYL suggest cation exchange as an important adsorption mechanism. Tylosin adsorption decreases with increasing ionic strength, is greater in Na systems relative to Ca systems, increases with increasing clay content and can be predicted by assuming electrostatic interactions with clay mineral surfaces (Essington et al., 2010; Lee et al., 2014). However, the cation exchange selectivity of TYL, relative to common soil cations, has not been examined. Exchange selectivity coefficients, which are conditional exchange equilibrium constants, are quantitative representations of cation exchange equilibrium and describe cation preference for the exchange complex (Essington, 2015). Cation exchange preference for a soil exchanger phase may be determined by developing an exchange isotherm: a

plot of the concentration of a cation on the exchange phase versus the concentration in solution at equilibrium (Essington, 2015). Binary exchange involving homoionic (NaX-TylX) or heteroionic (CaX_2-TylX) exchange are described by the reactions:

$$NaX + TYL^+ = TYLX + Na^+ \quad [1]$$

$$CaX_2 + 2TYL^+ = 2TYLX + Ca^{2+} \quad [2]$$

where X^- represents an equivalent of exchanger charge. The Vanselow equation is commonly used to describe cation preference and is used to calculate a true thermodynamic equilibrium constant for the exchange reaction (Essington, 2015). The Vanselow equation and the true equilibrium constant are represented by K_v and K_{ex}, and derived for the equilibrium exchange reaction in equation [1]:

$$K_V = \frac{N_{TYL}(Na^+)}{N_{Na}(TYL^+)} \quad [3]$$

$$K_{ex} = \frac{(TYLX)(Na^+)}{(NaX)(TYL^+)} \quad [4]$$

where N represents the mole fraction of the cation on the exchange phase and the parentheses denote ion activities (solution species) or exchanger phase activities. Vanselow's selectivity coefficient can be employed to generate the true exchange equilibrium constant (Essington, 2015). The K_V is also used to establish cation preference by comparing the exchange isotherm to a non-preference isotherm, which is a theoretical curve where $K_V = 1$. The non-preference isotherm graphically illustrates the condition when the Vanselow selectivity coefficient is unity.

RESEARCH OBJECTIVES

The objectives of this research are to examine the exchange selectivity of TYL in the B2t horizons of a west Tennessee soil and in reference vermiculite and montmorillonite systems. Binary exchange isotherms involving TYL-CaX and TYL-NaX exchange were developed to establish exchange preference, and to determine the distribution between exchangeable and nonexchangeable forms of the adsorbed TYL. An XRD study was performed to evaluate the intercalation of the reference and soil clay minerals by TYL.

REFERENCES

Alcock, R. E., Sweetman, A., and Jones, K.C. (1999). Assessment of organic contaminant fate in waste water treatment plants; I: selected compounds and physiochemical properties. Chemosphere, 38 (10), 2247-2262.

Allaire, S.E., Del Castillo, J. and Juneau, V. (2006). Sorption kinetics of chlortetracycline and tylosin on sandy loam and heavy clay soils. Journal of Environmental Quality, 35, 969-972.

Aristilde, L., Landson, B., Miehe-Brendle, J., Marichal, C., and Laurent, C., (2016). Enhanced interlayer trapping of a tetracycline antibiotic within montmorillonite layers in the presence of Ca and Mg. Journal of Colloid and Interface Science, 464, 153-149.

Batchelder, A.R. (1982). Chlortetracycline and oxytetracycline effects on plant growth and development in soil systems. Journal of Environmental Quality, 11(4), 675-678.

Beausse, J. (2004). Selected drugs in solid matrices: a review of environmental determination, occurrence, and properties of principal substances. Trends in Analytical Chemistry, 23(10-11), 753-761.

Chang, P.H., Li, Z., Jiang, W.T., and Jean, J.S. (2009). Adsorption and intercalation of tetracycline by swelling clay minerals. Applied Clay Science, 46, 27-36.

Cohen, M. L. (1998). Antibiotic use. In Antimicrobial Resistance: Issues and Options. Workshop Report. National Academy Press. Washington DC.

European Commission. (2003). Regulation (EC) No. 1831/2003 of the European Parliament and of the Council of 22 September 2003 on Additives for Use in Animal Nutrition.

Essington, M. E. (2015). Soil and water chemistry: An integrative approach, 2nd ed. CRC press, Boca Raton.

Essington, M. E., Lee, J., and Seo, Y. (2010). Adsorption of antibiotics by montmorillonite and kaolinite. Soil Science Society of America Journal, 74(5), 1577-1588.

Fejer, I., Mihaly, K., Istvan, E. and Dekany, I. (2002). Interaction of monovalent cationic drugs with montmorillonite. Colloid and Polymer Science, 280, 372-379.

Fish, B.J. and Carr, G.P.R. (1986). Pharmacopoeial procedure for the determination of tylosin factors by high-performance liquid chromatography. Journal of Chromatography, 353, 39-50.

Halling-Sorensen, B., Nors Nielson, S., Lanzky, P.F., Ingerslev, F., Holten Lutzhoft, H.C., and Jorensen, S.E. (1998). Occurrence, fate, and effects of pharmaceutical substances in the environment – a review. Chemosphere, 36, 357-393.

Harris, S.J., Cormican, M., and Cummins E. (2012). Antimicrobial residues and antimicrobial-resistant bacteria: impact on the microbial environment and risk to human health – a review. Human and Ecological Risk Assessment, 18, 767-809.

Hou, Y., Wu, P., Huang, Z., Ruan, B., Liu, P., and Zhu, N. (2014). Successful intercalation of DNA into CTAB-modified clay minerals for gene protection. Journal of Materials Science, 49(20), 7273-7281.

Hu, D., and Coats, J. R. (2009). Laboratory evaluation of mobility and sorption for the veterinary antibiotic, tylosin, in agricultural soils. Journal of Environmental Monitoring, 11(9), 1634-1638.

Kaur, M. and Datta, M. (2013). Adsorption equilibrium and kinetics of toxic dye-erythrosine B adsorption onto montmorillonite. Separation Science and Technology, 38, 1370-1381.

Kedzierski, M., Janiszewska, J., and Moszumanska, I. (2016). Dendrimeric peptide – montmorillonite intercalation compound. Polimery, 61(10), 677-682.

Kemper, N. (2008). Veterinary antibiotics in the aquatic and terrestrial environment. Ecological Indicators, 8(1), 1-13.

Kolpin, D. W., Furlong, E. T., Meyer, M. T., Thurman, E. M., Zaugg, S. D., Barber, L. B., and Buxton, H. T. (2002). Pharmaceuticals, hormones, and other organic wastewater contaminants in US streams, 1999-2000: A national reconnaissance. Environmental Science & Technology, 36(6), 1202-1211.

Kumar, K., Gupta, S.C., Baidoo, S.K., Chander, Y., and Rosen, C.J. (2005). Antibiotic uptake by plants from soil fertilized with animal manure. Journal of Environmental Quality, 34, 2082-2085.

Kummerer, K. (2003). Significance of antibiotics in the environment. Journal of Antimicrobial Chemotherapy, 52(1), 5-7.

Lee, J., Seo, Y., and Essington, M. E. (2014). Sorption and transport of veterinary pharmaceuticals in soil - a laboratory study. Soil Science Society of America Journal, 78(5), 1531-1543.

Levy, S.B. (1992) The antibiotic paradox. Plenum Press, New York.

Loke, M-L., Tjornelund, J., and Halling-Sorensen, B. (2002). Determination of the distribution coefficient (log K_d) of oxytetracycline, tylosin A, olaquindox and metronidazole in manure. Chemosphere, 48, 351-361.

Lv, G., Li, Z., Jiang, W.T., Change, P.H., and Liao, L. (2015). Interlayer configuration of ionic liquids in a ca-montmorillonite as evidenced by FTIR, TG-DTG, and XRD analyses. Materials Chemistry and Physics, 162, 417-424.

Madsen, F. T. (1977). Surface area measurements of clay minerals by glycerol sorption on a thermobalance. Thermochimica Acta, 21, 89-93.

McFarland, J.W., Berger, C.M., Froshauer, S.A., Hayashi, S. F., Hecker, S.J., Jaynes, B.H., Jefson, M.R., Kamicker, B.J., Lipinski, C.A., Lundy, K.M., Reese, C.P., and Vu, C.B. (1997). Quantitative structure - activity relationships among macrolide antibacterial agents: in vitro and in vivo potency against Pasteurella multocida. Journal of Medicinal Chemistry, 40 (9), 1340-1346.

Mercier, L. and Detellier, C. (1994). Intercalation of tetraalkylammonium cations into smectites and its application to internal surface area measurements. Clays and Clay Minerals, 42, 71-76.

Michelini, L., Reichel, R., Werner, W., Ghisi, R., and Thiele-Bruhn, S. (2012). Sulfadiazine uptake and effects on *Salix fragilis* L. and *Zea mays* L. plants. Water, Air, and Soil Pollution, 223, 5243-5257.

Parolo, M.E., Savini, M.C., Valles, J.M., Baschini, M.T., and Avena, M.J. (2008). Tetracycline adsorption on montmorillonite: pH and ionic strength effects. Applied Clay Science, 40, 179-186.

Porubcan, L.S., Serna, C.J., White, J.L., and Hem, S.L. (1977). Mechanism of adsorption of clindamycin and tetracycline by montmorillonite. Journal of Pharmaceutical Sciences, 67(8), 1081-1087.

Sarmah, A.K., Meyer, M.T., Boxall, A.B.A. (2006). A global perspective on the use, sales, exposure pathways, occurrence, fate and effects of veterinary antibiotics (VAs) in the environment. Chemosphere. 65, 725-759.

Sassman, S. A., Sarmah, A. K., and Lee, L. S. (2007). Sorption of tylosin A, D, and Aaldol and degradation of tylosin A in soils. Environmental Toxicology and Chemistry, 26(8), 1629-1635.

Sun, Z., Park, Y., Zheng, S., Ayoko, G.A., and Frost, R.L. (2013). XRD, TEM, and thermal analysis of Arizona ca-montmorillonite modified with didodecyldimethylammonium bromide. Journal of Colloid and Interface Science, 408, 75-81.

Ter Laak, T.L., Gebbink, W.A., and Tolls, J. (2006). The effect of pH and ionic strength on the sorption of sulfachloropyridzine, tylosin, and oxytetracycline to soil. Environmental Toxicology and Chemistry, 25(4), 904-911.

Teuber, M., 1999. Spread of antibiotic resistance with food-borne pathogens. Cell Mol. Life Sci. 56, 755–763.

Teuber, M., 2001. Veterinary use and antibiotic resistance. Curr. Opin. Mikrobiol. 4, 493–499.

Thiele-Bruhn, S. (2003). Pharmaceutical antibiotic compounds in soils - a review. Plant Nutrition and Soil Science, 166, 145-167.

U.S. Food and Drug Administration. (2015). Veterinary Feed Directive, 80 FR 31707 (3 June 2015). Federal Register: The Daily Journal of the United States. Web. 25 January 2017.

Wang, C.J, Li, Z., Jiang, W.T., Jean, J.S., and Liu, C.C. (2010). Cation exchange interaction between antibiotic ciprofloxacin and montmorillonite. Journal of Hazardous Materials, 183, 309-314.

Wang, Q. and Yates, S.R. (2008). Laboratory study of oxytetracycline degradation kinectics in animal manure and soil. Journal of Agricultural and Food Chemistry, 56, 1683-1688.

Zhang, Q., Yang, C., Huang, W., Dang, Z., and Shu, X. (2013). Sorption of tylosin on clay minerals. Chemosphere, 92, 2180-2186.

APPENDIX A: Chapter 1 Figures

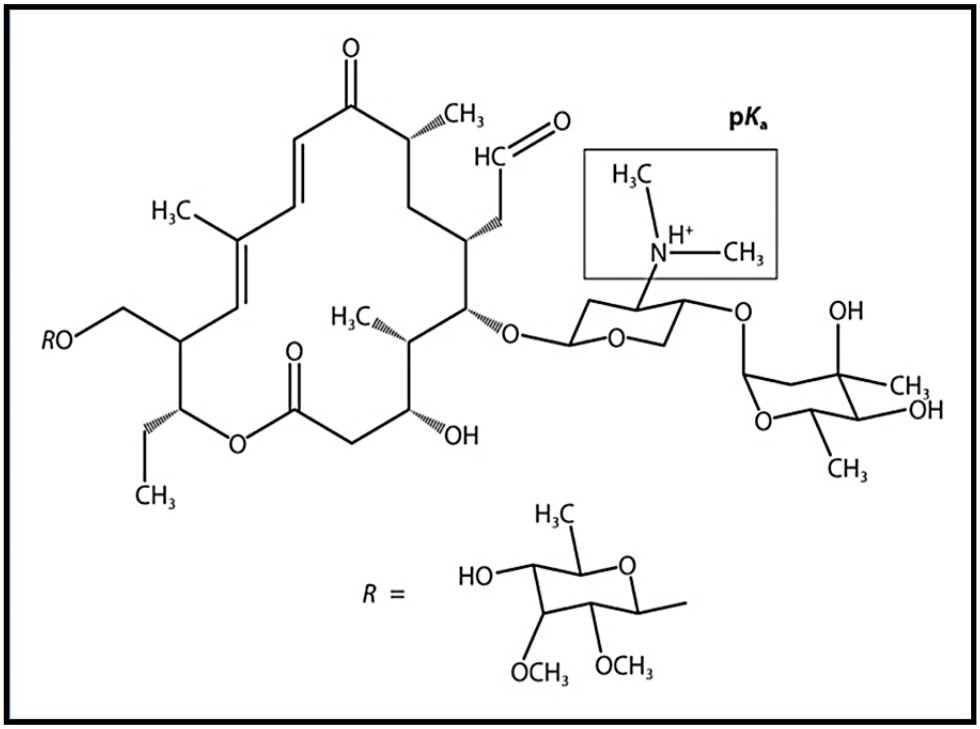

Figure A-1: Tylosin molecule with dimethylamine functional group boxed. The estimated octanol-water partition constant (K_{OW}) is 316, and the constant for the dissociation of the protonated dimethylamine is pK_a = 7.50 ± 0.13.

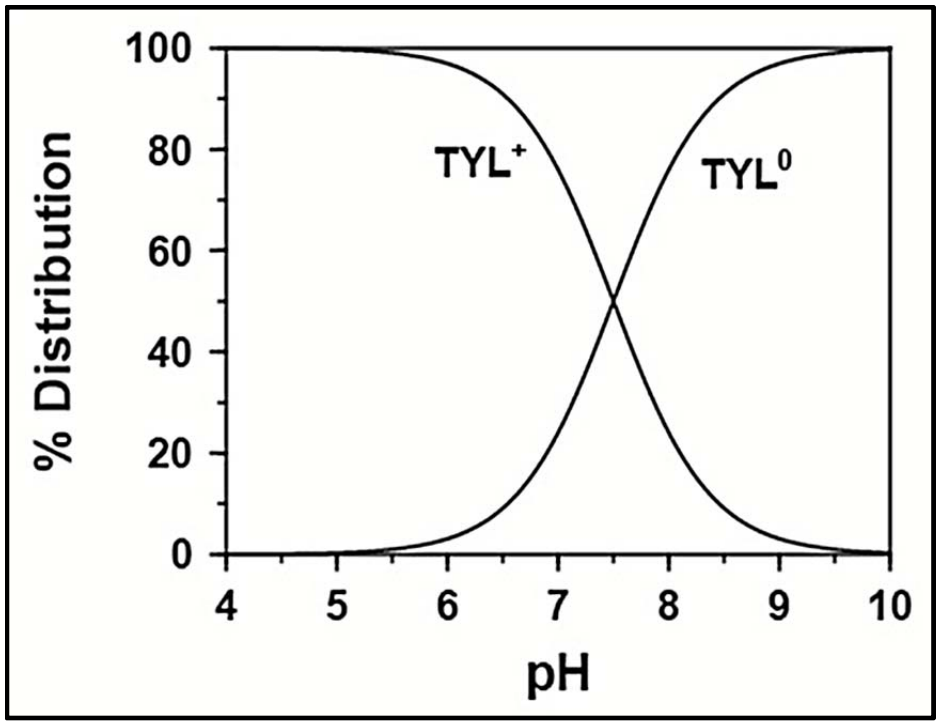

Figure A-2: Distribution diagram illustrating tylosin speciation as a function of pH.

CHAPTER 2: CATION EXCHANGE OF TYLOSIN BY MONTMORILLONITE AND VERMICULITE

ABSTRACT

Tylosin, an agricultural veterinary antibiotic, has been the focus of adsorption studies that use reference clay minerals (e.g., montmorillonite) to characterize potential mobility in the soil environment. These studies show TYL adsorption is a function of pH, ionic strength, background electrolyte type, organic matter content, and clay type, indicating ion exchange as an important adsorption mechanism. This study uses reference montmorillonite (STx-1) and Libby vermiculite minerals to develop binary exchange isotherms for TYLX-NaX and TYLX-CaX systems. The Vanselow selectivity coefficient (K_V) was calculated for each system to determine exchange phase preference for TYL. Adsorption isotherms were developed from the binary exchange studies to characterize the exchangeable and nonexchangeable forms of TYL. The isotherms were described using the Freundlich or partition models. In addition, x-ray diffraction was performed to evaluate TYL intercalation into the clay minerals. Binary exchange isotherms for STx-1 showed that TYL^+ was preferred over Na^+ and Ca^{2+}. The K_V was greater than 1 and generally invariant with exchange phase composition in the TYLX-NaX system, but variable in the TYLX-CaX system. Exchangeable TYL comprised a majority of total adsorbed TYL in the TYLX-NaX system; while nonexchangeable dominated total adsorbed TYL in the TYLX-CaX system. X-ray diffraction showed the expansion of STx-1 to approximately 3.0 nm when TYL occupied 75% of the exchange phase in the TYLX-NaX system. The STx-1 d value decreased with decreasing TYL on the exchange phase to 1.26 nm when Na-saturated. Tylosin intercalation was also observed in the TYLX-CaX system. In both the TYLX-NaX or TYLX-CaX systems, random and segregated interstratification of the STx-1 clay was

observed. Exchangeable TYL was not detected in the Libby vermiculite. Further, expansion of the vermiculite layers beyond 1.45 nm was not observed, indicating that TYL was not intercalated. Tylosin competes with common soil cations for the exchange complex of smectite clay, and the exchange behavior can be quantified by the Vanselow selectivity coefficient. Further, TYL intercalation into smectite in soil environments may limit the ability of soil microbes to degrade the compound, leading to longer soil residence times.

INTRODUCTION

The United States has recently regulated veterinary antibiotics (VA) by requiring veterinarian authorization for all uses (U.S. Food and Drug Administration, 2015). However, the longtime use of antibiotics is still an environmental concern. Before January 2017, VAs were used as prophylactics and for nontherapeutic purposes leading to their accumulation in manure fertilizers and dispersement in soil and water environments. Kolpin et al. (2002) and Sarmah et al. (2006) have reported tylosin (TYL), a commonly used agricultural antibiotic, in measurable amounts in surface waters.

Adsorption studies (Ter Laak et al., 2006; Essington et al., 2010; and Lee et al., 2014) have focused on antibiotics such as TYL because of their potential mobility in soil environments. These studies have characterized TYL adsorption by soil and soil minerals as a function of pH, ionic strength, background electrolyte type, organic matter content, and clay content and type. For example, Essington et al. (2010) conducted adsorption edge and adsorption isotherm studies of TYL by montmorillonite and

kaolinite. Greater TYL adsorption was observed by montmorillonite (high CEC) relative to kaolinite (low CEC). Retention decreased with increasing ionic strength, and decreased in the presence of divalent cations relative to monovalent. These findings indicate that an important retention mechanism for TYL is cation exchange. However, the cation exchange selectivity for TYL, relative to common soil cations, has not been examined.

The objectives of this study are to examine the exchange selectivity of TYL in reference vermiculite and montmorillonite systems. Binary exchange isotherms involving TYLX-CaX and TYLX-NaX were developed to establish exchange preference, and to determine the distribution between exchangeable and nonexchangeable forms of the adsorbed TYL. An XRD study was performed to evaluate the intercalation of vermiculite and montmorillonite by TYL.

MATERIALS AND METHODS

Chemicals

Veterinary-grade tylosin tartrate was obtained from Elanco (Greenfield, IN) for use in the exchange studies and consists of 95.5% tylosin, 3.1% desmycosin, and 1.4% macrocin. Analytical grade tylosin tartrate (98.8% tylosin) was obtained from Sigma-Aldrich and used as a standard for the chemical analysis of the equilibrium exchange systems. Other chemicals used include distilled-deionized water (carbon dioxide free, >18Ω; Barnstead E-pure system) and the analytical grade or better compounds (Fisher Scientific, Fair Lawn, NJ) sodium chloride, calcium chloride dihydrate, magnesium chloride hexahydrate, potassium phosphate monobasic, and acetonitrile.

Clay minerals

The reference montmorillonite (STx-1) was obtained from the Source Clay Minerals Repository at University of Missouri-Columbia. The source clay consists of ~67% smectite, 30% opal, and 3% quartz+feldspar+kaolinite+ talc (Chipera and Bish, 2001). The STx-1 was used as received and Na- , Ca-, or TYL-saturated with repeated centrifuge washes of 1.0 M NaCl or $CaCl_2$, or 0.004 M or 0.01 M tylosin. Libby vermiculite was obtained from Ward's Natural Science Establishment and consists of ~65% trioctahedral vermiculite, 28% biotite, 9% smectite, and 0.5% quartz (Alexiandes and Jackson, 1965). Particle size reduction was performed by combining the vermiculite with deionized water in a commercial blender. The suspension was blended in intervals of 30 minutes for a total of 3 hours. The vermiculite was then Na-saturated with repeated centrifuge washings of 1 M NaCl and the <50 μm sized particles were isolated using Stoke's Law sedimentation. The particle size distribution of the STx-1 and vermiculite separates was confirmed with a Becker Coulter LS 13320 Laser Diffraction Particle Size Analyzer (Brea, Ca) (Table B-1). The Na-saturated vermiculite was Ca- or TYL-saturated with repeated centrifuge washes of 1.0 M $CaCl_2$, 0.004 M or 0.01 M tylosin. The cation exchange capacity of the STx-1 and the Libby vermiculite samples were computed from the binary exchange studies.

Exchange Kinetics

A kinetic study was performed to determine NaX-TYLX equilibration times. Similar to the binary exchange isotherm study described below, 0.25 g STx-1 samples were Na-saturated and then 15 mL of 0.004 M TYL and 15 mL of 0.004 M Na were combined in 50-mL centrifuge tubes and the suspensions placed on an orbital shaker.

Triplicate samples were removed in time increments of 2, 6, 12, 24, 48, and 72 hours and then centrifuged with the supernatant filtered and analyzed for TYL, Na, and pH. Centrifuge tubes without solids were used to determine the total concentration of TYL added to the Na-saturated STx-1. The solids were centrifuged washed with deionized water to remove entrained salts (as determined by $AgNO_3$) and then washed 3 times with 1.0 M NH_4-acetate to determine the concentrations of Na and TYL associated with the exchange complex. The collected supernatant NH_4-acetate liquids were brought to a volume of 100 mL and filtered through qualitative-grade filter paper (Whatman #42). The NH_4-acetate extracts were stored under refrigeration until analysis.

Binary Exchange Isotherms

Binary exchange isotherms were developed using 0.25 g of either STx-1 or Libby vermiculite in 50 mL polyethylene centrifuge tubes. The exchange experiments were performed in triplicate. Clay mineral samples were initially TYL- or Na-saturated for TYLX-NaX binary exchange, or TYL- or Ca-saturated for TYLX-CaX exchange. The solids were introduced to 30 mL volume of solution containing varied ratios of TYL to Na, or TYL to Ca, such that the total normality was 0.004 N (Table B-2). Exchange experiments using a total normality of 0.01 N were also performed for TYL-Ca exchange. Centrifuge tubes without solids were used as a control for each exchange experiment. These control blanks were duplicated for each ratio in the experiment and used later to determine mass balance of original solutions, compute Cl and tartrate concentrations in ion speciation modeling, and to compute total adsorbed concentrations of TYL. The suspensions and the blanks were equilibrated for 18 hours on an orbital shaker at ambient temperature (20-22ºC). A kinetic study (described

above) indicated that exchange equilibrium was achieved in less than 2 hours; the 18 hour reaction time was chosen for convenience. Following the exchange equilibration period, the solution and solid phases were separated by centrifugation and the solution pH was determined. The solution was further clarified by filtration through a 0.45 μm membrane filter. Equilibrium solutions were stored under refrigeration until analysis. The remaining solids were centrifuge washed 3 times with deionized water to remove entrained soluble salts (as determined by $AgNO_3$ test), then repeatedly washed 3 times with 1.0 M NH_4-acetate (and the supernatant liquid collected) to remove the cations associated with the exchange complex. The collected supernatant NH_4-acetate liquids were brought to a volume of 100 mL and filtered through qualitative-grade filter paper (Whatman #42). The NH_4-acetate extracts were stored under refrigeration until analysis.

X-ray Diffraction Study

An x-ray diffraction study was performed to determine the location of adsorbed TYL in Na- and Ca-saturated STx-1 and Libby vermiculite. Solutions having differing TYL-Na or TYL-Ca ratios (with a total normality of 0.01 N) were equilibrated with Na- or Ca-saturated solids similar to the binary exchange study previously described. The solids were washed to remove entrained salts and a slurry mix for each ratio was created using DDI water to achieve a solid-solution ratio of 0.25 g to 20 mL. The solids were dispersed and allowed to sit undisturbed for a period of time computed by Stoke's Law to achieve a separation of <2 μm particles. The <2 μm samples were then pipetted onto glass slides and dried at room temperature. The slides were then placed in a desiccator over a saturated $MgCl_2$ solution and a relative humidity of 33% for a 24 h

period. X-ray diffraction was then preformed on the oriented-mount samples to determine d-values of the (001) spacing.

Analytical

A Hewlett-Packard Series 1100 (Hewlett-Packard Palo Alto, CA) HPLC coupled with ultraviolet detection was used to determine TYL concentrations using a procedure described by Essington et al. (2010) and Lee et al. (2014). An Ascentis C18 guard column (2 cm by 4.0 mm and 5 µm) and an Ascentis C18 analytical column (15 cm by 4.6 mm and 5 µm) with an injection volume of 100 µL and a flow rate of 1 mL min^{-1} was used. The mobile phase was an acetonitrile-0.01 M KH_2PO_4, pH 7.0 gradient ranging from 20:80 to 60:40 in 10 minutes, resulting in a TYL retention time of 7.8 minutes. A UV detector wavelength of 280 nm results a method detecting limit of 0.008 µmol L^{-1}. The Na and Ca concentrations were determined using a Perkin Elmer AAnalyst 800 atomic absorption spectrophotometer (Wellseley, PA). Sodium was analyzed with emission, while Ca with absorbance. The samples and standards were spiked with 12% lanthanum chloride ($LaCl_3$) solution using 0.1 mL for every 10 mL of sample. Sodium and Ca standards were made using atomic absorption standards from CPI International (Springfield, VA). Method detection limits for both Na and Ca were 0.01 mg L^{-1}.

X-ray diffraction (XRD) was used to determine the d-value of the (001) plane of the STx-1and Libby vermiculite saturated with varied ratios of TYLX-NaX and TYLX-CaX. X-ray diffractograms were generated using a Bruker Model D8 with Ni-filtered, Cu Kα radiation. The XRD operating parameters were set to 40 kV and 40 mA with a scan range of 2 to 12 °2θ, a step of 0.02 °2θ, and a count rate of 6 second per step.

A chemical equilibrium modeling program, Visual MINTEQ (VM), version 3.1 (Gustafsson, 2014) was used to compute the free cation concentrations of Na^+, Ca^{2+}, and TYL^+, as well as their single-ion activities. Input data for the speciation model included the equilibrium pH, and the total soluble concentrations of Na or Ca, TYL, Cl, and tartrate. The concentration of Cl was computed from the Na or Ca content of the blanks, and the concentration of tartrate was computed from the TYL content of the blanks. Table B-3 lists aqueous speciation reactions and log K_F values used by VM.

Data analysis

The concentrations of cations in the exchange phase are directly determined by NH_4 extraction. An exchange isotherm for TYL is a plot of the equivalent fraction of TYL^+ on the exchange phase (E_{TYLX}, y-axis) versus the equivalent fraction of TYL^+ in the equilibrium solution ($\tilde{E}_{TYL+}$, x-axis). A detailed description of the development of exchange isotherms is provided by Essington (2015). For NaX-TYLX exchange, E_{TYLX} is computed by,

$$E_{TYLX} = \frac{\{TYLX\}}{\{TYLX\}+\{NaX\}} \quad [1]$$

where {TYLX} and {NaX} are the mol kg^{-1} of TYL^+ and Na^+ on the exchange phase. Further,

$$E_{NaX} = 1 - E_{TYLX} \quad [2]$$

The equivalent fraction of TYL^+ in solution is,

$$\tilde{E}_{TYL^+} = \frac{[TYL^+]}{[TYL^+]+[Na^+]} \quad [3]$$

and,

$$\tilde{E}_{Na^+} = 1 - \tilde{E}_{TYL^+} \quad [4]$$

where [TYL^+] and [Na^+] are the mol L^{-1} of free cation in solution (computed using VM). A similar set of expressions describe the CaX-TYLX exchange systems:

$$E_{TYLX} = \frac{\{TYLX\}}{\{TYLX\}+2\{CaX_2\}} \quad [5]$$

$$E_{CaX} = 1 - E_{TYLX} \quad [6]$$

$$\tilde{E}_{TYL^+} = \frac{[TYL^+]}{[TYL^+]+2[Ca^{2+}]} \quad [7]$$

$$\tilde{E}_{Ca^{2+}} = 1 - \tilde{E}_{TYL^+} \quad [8]$$

Also plotted on the exchange isotherm is the non-preference isotherm, obtained from Essington (2015). For NaX-TYLX exchange, the non-preference isotherm is $E_{TYLX} = \tilde{E}_{TYL}{}^+$. For CaX-TYLX exchange, the non-preference isotherm is

$$E_{TYLX} = \left\{1 + \frac{2}{\Gamma\, TN}\left[\frac{1}{\tilde{E}^2_{TYL^+}} - \frac{1}{\tilde{E}_{TYL^+}}\right]\right\}^{-0.5} \quad [9]$$

where $= \frac{\gamma^2_{TYL^+}}{\gamma_{Ca^{2+}}}$, and the ɣ's are single-ion activity coefficients. The non-preference isotherm describes the condition where neither cation is preferred by the exchange phase. The non-preference condition is met when the Vanselow selectivity coefficient (K_V) for the exchange reaction is unity. For the $NaX + TYL^+ = TYLX + Na^+$ exchange reaction, K_V is,

$$K_V = \frac{N_{TYLX}(Na^+)}{N_{NaX}(TYL^+)} \quad [10]$$

For the $CaX_2 + 2TYL^+ = 2TYLX + Ca^{2+}$ exchange reaction, K_V is:

$$K_V = \frac{N^2_{TYLX}(Ca^{2+})}{N_{CaX_2}(TYL^+)^2} \quad [11]$$

In equations [10] and [11] the parentheses represent activity (obtained from VM) and N_{TYLX}, N_{NaX}, and N_{CaX_2}, are the mole fractions:

$$N_{TYLX} = \frac{\{TYLX\}}{\{TYLX\}+\{NaX\}} \; ; \quad N_{TYLX} = \frac{\{TYLX\}}{\{TYLX\}+\{CaX_2\}} \qquad [12]$$

$$N_{NaX} = 1 - N_{TYLX} \quad ; \quad N_{CaX_2} = 1 - N_{TYLX} \qquad [13]$$

A plot of ln K_V (Eqs. [10] or [11]) as a function of E_{TYLX} (Eq. [1] or [5]) provides a mechanism to determine true exchange equilibrium constant (K_{ex}) (Essington, 2015).

A mass balance was performed to determine the nonexchangeable concentration of adsorbed TYL. For initially Na^+- or Ca^{2+}-saturated clay, the mass of TYL added to the suspensions is determined from the blanks. The mass balance expression for TYL is (where m represents mmol): $m_{TYL_{total}} = m_{TYL_{aqueous}} + m_{TYL_{nonexchangeable}} + m_{TYL_{exchangeable}}$ where all m values except $m_{TYL_{nonexchangeable}}$ are directly measured. The nonexchangeable TYL concentration is $q_{TYL} = \frac{m_{TYL_{nonexchangeable}}}{m_S}$ where m_S is the mass of the adsorbant in kg. An adsorption isotherm is a plot of the amount of TYL adsorbed by the surface (q in mmol kg^{-1}, y-axis) versus the total concentration of TYL in the equilibrium solution (C_{eq} in mmol L^{-1}, x-axis). Adsorption isotherms were generated for total adsorbed TYL, nonexchangeable TYL, and exchangeable TYL and are modeled using the Freundlich equation:

$$q_{TYL} = K_F \, C_{eq}^N \qquad [14]$$

where q_{TYL} and C_{eq} are previously defined, K_F is the Freundlich adsorption constant, and N is a measure of the heterogeneity of surface sites and is constrained to lie

between 0 to 1. When N=1, Eq. [14] becomes the constant partition isotherm model and K_F becomes K_P, the partition coefficient. Values for K_F and N for each isotherm are generated using the linearized Freundlich equation:

$$\log q = \log K_F + N \log C_{eq} \quad [15].$$

Values for log K_F and N are determined by regressing log q on log C_{eq}, while K_P values are determined by regressing q on C_{eq}.

RESULTS AND DISCUSSION

Kinetics study

The total concentration of adsorbed TYL was greatest at 2 h with the adsorption equilibrium being obtained after 12 h (Figure B-1). The change in adsorbed TYL was not significant after the adsorption equilibrium time of 12 h ($p<0.01$). The result was similar to that of Allaire et al. (2006). They found absorbed concentrations to remain stable after a 3 h equilibration for the adsorption of TYL by sandy loam and heavy clay soils. Exchangeable TYL concentrations were stable after 2 h equilibrations, which is consistent with the general characteristic of exchange processes; they are instantaneous (Essington, 2015). Correspondingly, the Vaneslow selectivity coefficient was constant throughout the kinetic study with K_V = 2.40 ± 0.21 (Figure B-2). X-ray diffractograms of the intercalated STx-1 show d values of approximately 2.75 nm (Figure B-3). These d-values are substantially greater than the d-value for a Na^+-saturated smectite (1.2 nm), indicating TYL intercalation into the interlayers.

Binary Exchange Isotherms

For TYLX-NaX exchange by STx-1, the exchange isotherm shows there is more TYL^+ on the exchange phase than predicted by the nonpreference isotherm (Figure B-4). This indicates the STx-1 exchange phase prefers TYL^+ over Na^+. The Vanselow selectivity coefficient, ln K_V, for the initially Na-saturated system increases from 1.3 to 2.4 with increasing E_{TYLX} (Figure B-5). However, ln K_V decreases sharply from 2.1 to 0.7 as E_{TYLX} increases from 0.77 to 0.85 in the initially TYL-saturated system.

In the TYLX-CaX STx-1 exchange systems, the data for both the 0.004 and 0.01 N TN systems generally lie above the nonpreference isotherm indicating STx-1 prefers TYL^+ over Ca^{2+} (Figures B-6 and B-7). This is not an expected finding, as Ca^{2+} was preferred over monovalent cations (Sposito et al, 1983). This result also contradicts that of Fletcher et al. (1985). They showed montmorillonite strongly prefers the divalent cations Ca^{2+} and Mg^{2+} over Na^+. In the higher TN (0.01 N) TYL-saturated system, TYL was preferred by the surface through the range of surface coverage (Figure B-7). However, in the TN 0.004 N TYL-saturated system, Ca^{2+} was preferred when TYLX accounted for greater than approximately 40% of the exchange phase. The exchange selectivity for TYL^+ for both TN decreased as TYL^+ increased on the exchange phase (Figures B-8 and B-9). For the 0.004 N TYLX-CaX Ca-saturated system, ln K_V was discontinuous, as systems initially TYL-saturated and initially Ca-saturated do not follow the same trend. The ln K_V value significantly decreased from 6.0 to 2.1 as E_{TYLX} increased from 0.01 to 0.13. For the TYL-saturated system, ln K_V decreased from 4.0 to -0.09 as E_{TYLX} increased from 0.17 to 0.5. For the 0.01 N TYLX-CaX systems, ln K_V

was continuous (Figure B-9). The ln K_V value linearly decreased from 5.0 to 2.0 as E_{TYLX} increased from 0.06 to 0.33.

In the Libby vermiculite systems, both Na- and Ca-saturated, exchange isotherms were not developed, as TYLX was generally at or below detectable levels ($E_{TYLX} < 0.02$). Instead, adsorption isotherms were used to characterize TYL adsorption. This result is expected as vermiculite is not as expansive as montmorillonite, and TYL cannot access the vermiculite interlayers (Hsu and Bates, 1964).

Cation Exchange Capacity

The CEC values were determined for both STx-1 and Libby vermiculite exchange systems as a function of exchange phase composition. The reported CEC of STx-1 is 84.4 $cmol_c\ kg^{-1}$ (Fitch et al.,1995; Malekani et al., 1996; Bordon and Geese, 2001). The CEC for TYLX-NaX on initially Na-saturated STx-1 as a function of composition ranged from 32.18 (± 0.27) to 37.11 (± 0.72) $cmol_c\ kg^{-1}$ with a mean value of 35.0 $cmol_c\ kg^{-1}$ (Table B-4, Figure B-10). The CEC ranged from 58.59 (± 3.06) to 70.83 (± 2.51) and 46.48 (± 0.48) to 55.28 (± 0.14) $cmol_c\ kg^{-1}$ in the TYL-CaX systems in the 0.004 N and 0.01 N TN systems with mean values of 66.4 and 49.1 $cmol_c\ kg^{-1}$ for initially Ca-saturated STx-1 (Figures B-11 and B-12). Unlike the TYLX-NaX system, the CEC significantly decreased with increasing TYL on the exchange phase in the TYLX-CaX systems. The average CEC of the STx-1 exchange systems was a function of the equivalent fraction of TYLX, as affected by base cation type, TN, and initial cation saturation. The TYLX-NaX systems contain the greater E_{TYLX} values (Figure B-4)

relative to the TYLX-CaX systems (Figures B-6 and B-7). Correspondingly, the TYLX-NaX systems also have the lowest average CEC values, 35.0 $cmol_c\ kg^{-1}$ for initially Na-saturated, and 19.2 $cmol_c\ kg^{-1}$ for initially TYL-saturated. Higher E_{TYLX} also results in the lower CEC value for the initially TYL-saturated TYLX-NaX systems. The influence of initially cation saturation is also seen for the TYLX-CaX systems. An average CEC of 66.4 $cmol_c\ kg^{-1}$ was observed for the initially Ca-saturated, 0.004 N TN TYLX-CaX system, which is decreased to 45.7 $cmol_c\ kg^{-1}$ when the system was initially TYL-saturated. The higher TYL levels in the 0.01 N TN TYLX-CaX systems depresses the CEC further, to 49.1 $cmol_c\ kg^{-1}$ in the initially Ca-saturated systems and 42 $cmol_c\ kg^{-1}$ in the initially TYL-saturated.

Hsu and Bates (1964) reported a CEC of 115.6 $cmol_c\ kg^{-1}$ for Libby vermiculite. The CEC range for the TYLX-NaX Libby vermiculite was 90.45 (± 1.18) to 97.52 (± 2.04) $cmol_c\ kg^{-1}$ with a mean of 93.16 $cmol_c\ kg^{-1}$. A constant CEC was expected as there was no intercalation of TYL into the vermiculite layers. The CEC range for TYLX-CaX vermiculite was 83.31 (± 2.04) to 91.73 (± 1.82) with a mean of 89.78 $cmol_c\ kg^{-1}$, a value that is statistically similar to that for the TYLX-NaX system.

Adsorption Isotherms

The adsorption isotherms were developed to illustrate total, exchangeable, and nonexchangeable forms of TYL for each exchange system. Isotherms were described using the Freundlich (N<1) and constant partitioning models (N=1) (Eq. [14]). The adsorption constants are shown in Table B-5. For TYLX-NaX exchange on STx-1, exchangeable TYL accounted for approximately 72% of the total adsorbed at maximum

C_{eq} (Figure B-13). Nonexchangeable TYL, the TYL adsorbed by other than exchange mechanisms, accounted for approximately 75 mmol kg^{-1}; a value that was generally invariant through the C_{eq} range studied. The total and nonexchangeable TYL isotherms were modeled using the Freundlich equation, while the exchangeable TYL isotherm was modeled using the constant partition model (Table B-5, Figure B-14). Unlike the TYLX-NaX systems, nonexchangeable TYL dominated in the 0.004 N and 0.01 N TYLX-CaX systems (Figures B-15 and B-16). These isotherms were also modeled using the Freundlich (0.004 N system) and partition (0.01 N system) models (Figures B-17 and B-18). Less exchangeable TYL in both TN TYLX-CaX systems was most likely due to increased competition from Ca^{2+} for exchange sites. The nonexchangeable TYL for the TYLX-NaX STx-1 system, had a Freundlich constant (K_F) of 74.6 while the exchangeable TYL had a partition constant (K_P) of 285. The 0.004 N TYL-CaX STx-1 system had K_F values of 50 for exchangeable and 148 for nonexchangeable. The 0.01 N TYL-CaX STx-1 system had K_P values of 400 for exchangeable and 1487 for nonexchangeable.

The nonexchangeable TYL dominated the total adsorbed TYL in the TYLX-NaX and TYLX-CaX systems on the Libby vermiculite (Figures B-19 and B-20). For both TYLX-NaX and TYLX-CaX adsorption systems, the Freundlich model was used to model total and nonexchangeable TYL while the partition model was used for exchangeable TYL (Table B-4, Figures B-21 and B-22). The nonexchangeable TYL of the Na-saturated vermiculite had a K_F of 10.6, which is comparable to the STx-1 nonexchangeable TYL with a K_F of 74.6. The exchangeable TYL of Na-saturated vermiculite had a K_P of 1.66 while the STx-1 had K_P of 285. The nonexchangeable TYL

of the Ca-saturated system of vermiculite had a K_F of 6.83 and the exchangeable TYL had a K_P 0.12. These are also comparable to the Ca-saturated STx-1 systems especially the 0.01 N system which had a K_P of 400 for exchangeable TYL and K_P of 1487 for nonexchangeable TYL. The 0.004 N ca-saturated STx-1 system had a K_F of 50 for exchangeable TYL and K_F of 148 for nonexchangeable TYL.

X-ray Diffraction Study for Binary Exchange

The Libby vermiculite was not intercalated by TYL (Figure B-23). X-ray diffractions at 2.45 nm and 1.22 nm represent hydrobiotite (a regular interstratified biotite-vermiculite); at 1.1 nm, biotite; and 1.46 nm, vermiculite. These peaks do not deviate with increasing TYL. The d value of STx-1 increased from 1.26 nm for Na^+-saturated to 3.13 nm when TYLX was 75% of the exchange complex (Figure B-24). Zhang et al. (2013) was able to intercalate TYL into a montmorillonite species in a recent TYL adsorption study. However, their study parameters limited the XRD output to second order peaks, which is different from this study. Second order peaks tend to have less intensity if they are present at all. This study had parameters that captured first order peaks.

Based on the modeling study by Aristilde et al. (2010) of CTC intercalated smectite, the peak shift associated with increasing E_{TYLX} from 0 to 0.09 is due to the random interstratification of TYL into a predominately Na-saturated STx-1. Similarly, the peak shift from an E_{TYLX} of 0.75 to 0.55 is due to the random interstratification of Na^+ into a predominately TYL-saturated STx-1. The broad diffraction for E_{TYLX} = 0.25 represents the random interstratification between the two segregated end members;

primarily TYLX with minor NaX at 2.7 nm, and primarily NaX with minor TYLX at 1.58 nm. A similar response was observed for the TYLX-CaX systems (Figure B-25). Randomly interstratified CaX with minor amounts of TYLX occurs as E_{TYLX} increases from 0 to 0.04. The segregated interstratification occurs at E_{TYLX} = 0.13.

CONCLUSION

Tylosin exchange equilibrium on STx-1 was achieved after 2 h equilibrations while total adsorption equilibrium was achieved at 12 h. Tylosin participated in cation exchange on STx-1 in sodium and calcium systems as described by exchange isotherm studies. Exchangeable TYL was minor to below detectable levels in the Libby vermiculite due to greater layer charge and the limited expansiveness of the layers. Increasing TYL on the exchange phase decreased the CEC of STx-1. In both of TYLX-NaX and TYLX-CaX systems, TYL^+ was preferred by the STx-1 exchange phase. The Vanselow selectivity coefficient varied with exchange phase composition in both the TYLX-NaX and TYLX-CaX systems. Adsorbed TYL was partitioned into exchangeable and nonexchangeable forms and described by either the Freundlich or partition isotherm. Exchangeable TYL dominated the total adsorbed TYL in the TYLX-NaX system, while nonexchangeable TYL dominated in the TYLX-CaX systems. In the vermiculite systems, TYL adsorption was approximately 10% of that in STx-1 and exchangeable TYL was a minor component of the total adsorbed. X-ray diffraction illustrated the intercalation of TYL into the STx-1 interlayers, with the d-value of the 00l plane increasing with increasing E_{TYLX}. The d-value of Libby vermiculite was not

influenced by adsorbed TYL. These findings show the exchange complex of STx-1 thermodynamically prefers TYL^{+} over both Na^{+} and Ca^{2+}.

Tylosin is generally thermodynamically preferred by the smectite exchange phase. The Vanselow selectivity coefficient (K_V) does not change with surface composition in the binary TYLX-NaX soil system; however, K_V is variable with composition in the TYLX-CaX soil system. Thus, in soil environments, which are commonly dominated by Ca^{2+}, K_V cannot be used as a predictive tool. The intercalation of tylosin into smectite interlayers may also provide a level of protection for the tylosin molecule, reducing bioaccessibilty and increasing longevity in affected soils.

REFERENCES

Alexiades, C. A., and Jackson, M. L. (1965). Quantitative determination of vermiculite in soils. Soil Science Society of America Journal, 29, 522-527

Allaire, S.E., Del Castillo, J. and Juneau, V. (2006). Sorption kinetics of chlortetracycline and tylosin on sandy loam and heavy clay soils. Journal of Environmental Quality, 35, 969-972.

Aristilde, L., Landson, B., Miehe-Brendle, J., Marichal, C., and Laurent, C., (2016). Enhanced interlayer trapping of a tetracycline antibiotic within montmorillonite layers in the presence of Ca and Mg. Journal of Colloid and Interface Science, 464, 153-149.

Borden, D and Giese, R. F. (2001) Baseline studies of the clay minerals society source clays: cation exchange capacity measurements by the ammonia-electrode method. Clays and Clay Minerals 49 (50), 444-445.

Chipera, S.J. and Bish, D. L. (2001) Baseline studies of the clay minerals society source clays: powder X-ray diffraction analyses. Clays and Clay Minerals 49(5), 398-409.

Essington, M. E. (2015). Soil and water chemistry: An integrative approach, 2nd ed. CRC press, Boca Raton.

Essington, M. E., Lee, J., and Seo, Y. (2010). Adsorption of antibiotics by montmorillonite and kaolinite. Soil Science Society of America Journal, 74(5), 1577-1588.

Fitch, A., Du, J., Gan, H. and Stucki, J.W. (1995). Effect of clay charge on swelling: A clay-modified electrode study. Clays and clay minerals, 43(5), 607-614.

Fletcher, P., Sposito, G., and LeVesque, C.S. (1984). Sodium-calcium-magnesium exchange reactions on a montmorillonitic soil: I: Binary exchange reactions. Soil Science Society of America Journal, 48(5), 1016-1021.

Gustafsson, J.P. (2014). Visual MINTEQ (Version 3.1). http://vminteq.lwr.kth.se/.

Hsu, P.H. and Bates, T.F. (1964). Fixation of hydroxy-aluminum polymers by vermiculite. Soil Science Society of America Journal, 28(6), 763-769.

Kolpin, D. W., Furlong, E. T., Meyer, M. T., Thurman, E. M., Zaugg, S. D., Barber, L. B., and Buxton, H. T. (2002). Pharmaceuticals, hormones, and other organic wastewater contaminants in US streams, 1999-2000: A national reconnaissance. Environmental science & technology, 36(6), 1202-1211.

Lee, J., Seo, Y., and Essington, M. E. (2014). Sorption and transport of veterinary pharmaceuticals in soil - a laboratory study. Soil Science Society of America Journal, 78(5), 1531-1543.

Malekani, K., Rice, J.A., and JAR-SYoNG, L.I.N. (1996). Comparison of techniques for determing the fractal dimensions of clay minerals. Clays and clay minerals, 44(5), 677-685.

Sarmah, A.K., Meyer, M.T., Boxall, A.B.A. (2006). A global perspective on the use, sales, exposure pathways, occurrence, fate and effects of veterinary antibiotics (VAs) in the environment. Chemosphere. 65, 725-759.

Sposito, G., Holtzclaw, K. M., Jouany, C., and Charlet, L. (1983). Cation selectivity in sodium-calcium, sodium-magnesium, and calcium-magnesium exchange on Wyoming bentonite at 298 K. Soil Science Society of America Journal, 47(5), 917-921.

Ter Laak, T.L., Gebbink, W.A., and Tolls, J. (2006). The effect of pH and ionic strength on the sorption of sulfachloropyridzine, tylosin, and oxytetracycline to soil. Environmental Toxicology and Chemistry, 25(4), 904-911.

U.S. Food and Drug Administration. (2015). Veterinary Feed Directive, 80 FR 31707 (3 June 2015). Federal Register: The Daily Journal of the United States. Web. 25 January 2017.

Zhang, Q., Yang, C., Huang, W., Dang, Z., and Shu, X. (2013). Sorption of tylosin on clay minerals. Chemosphere, 92, 2180-2186.

APPENDIX B: Chapter 2 Tables and Figures

Table B-1. Particle size distributionof the Libby vermiculite and STx-1 smectite used in the exchange studies.

Sample	Avg Mean (µm)	Avg Median (µm)	Avg SD (µm)	Avg d10 (µm)	Avg d90 (µm)
Libby Verm	47	30.7	44.9	6.97	115
STx-1	24.2	15.0	25.6	2.65	58.6

Table B-2: Volume (in mL) ratios of tylosin and NaCl or $CaCl_2$ solutions added to each 50 mL tube of solid for 0.004 and 0.01 total normalities.

Starting out Tyl-Saturated				Starting out NaCl or $CaCl_2$-Saturated			
Tyl-Na†		Tyl-Ca‡		Tyl-Na†		Tyl-Ca‡	
0.004 M Tyl	0.004 M NaCl	0.004 M Tyl	0.002 M $CaCl_2$	0.004 M Tyl	0.004 M NaCl	0.004 M Tyl	0.002 M $CaCl_2$
0	30	0	30	5	25	5	25
5	25	5	25	10	20	10	20
10	20	10	20	15	15	15	15
15	15	15	15	20	10	20	10
20	10	20	10	25	5	25	5
25	5	25	5	30	0	30	0

† For 0.01 M TN systems, the solution concentrations are 0.01 M Tyl and 0.01 M NaCl

‡ For 0.01 M TN systems, the solution concentrations are 0.01 M Tyl and 0.005 $CaCl_2$

Table B-3: Aqueous speciation reactions and association constant (log K_f) values used in Visual MINTEQ.

Reaction	log K_f
$Ca^{2+} + Cl^- = CaCl^+$	0.4
$Ca^{2+} + H^+ + Tartrate^{2-} = CaHTartrate^+$	5.86
$Ca^{2+} + H_2O = CaOH^+ + H^+$	-12.697
$Ca^{2+} + Tartrate^{2-} = CaTartrate\ (aq)$	2.8
$2H^+ + Tartrate^{2-} = H_2Tartrate^0\ (aq)$	7.402
$H^+ + Tartrate^{2-} = HTartrate^-$	4.366
$H^+ + Tyl^- = HTyl^0$	7.5
$Na^+ + Cl^- = NaCl^0\ (aq)$	-0.3
$Na^+ + Tartrate^{2-} + H^+ = NaHTartrate^0\ (aq)$	4.58
$Na^+ + H_2O = NaOH^0\ (aq) + H^+$	-13.897
$Na^+ + Tartrate^{2-} = NaTartrate^-$	0.90
$H_2O = H^+ + OH^-$	-13.997

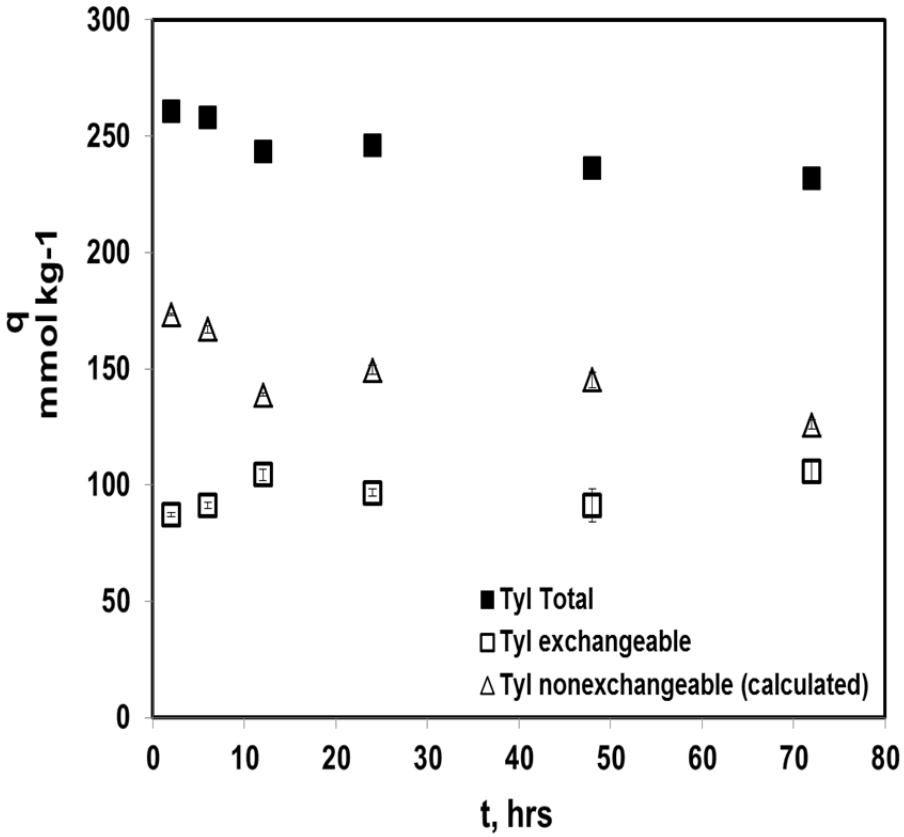

Figure B-1: Total, exchangeable, and nonexchangeable (calculated) tylosin as a function of equilibration time for the TYLX-NaX STx-1 system. Error bars represent ± 1 standard deviation.

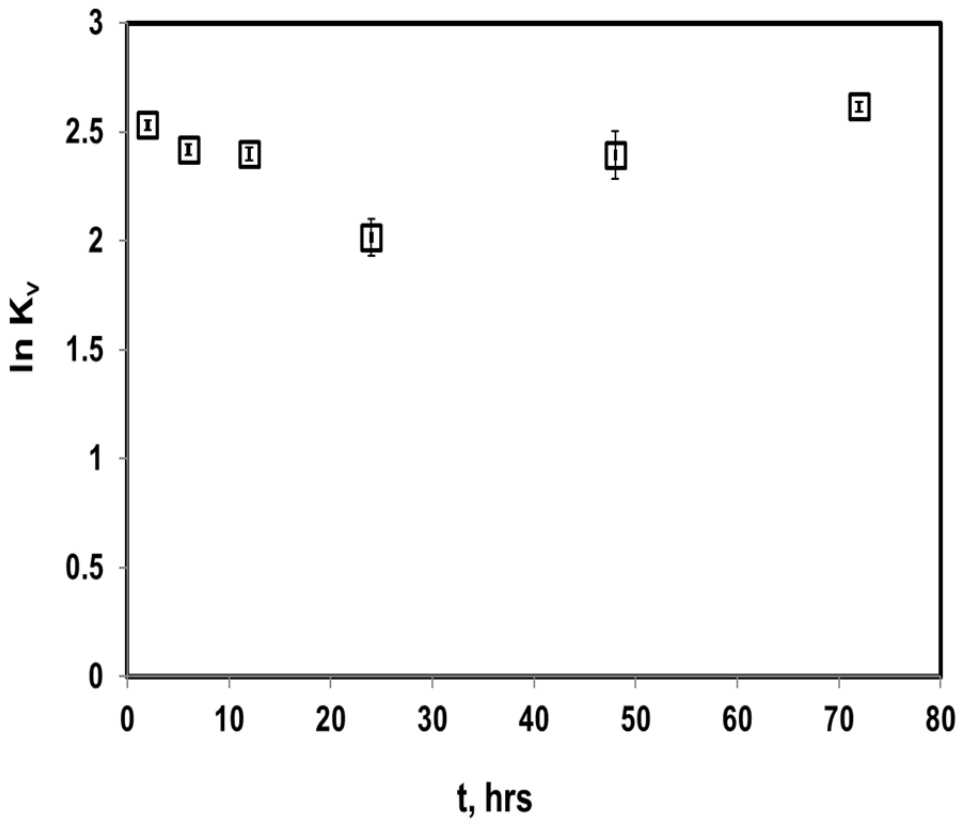

Figure B-2: The Vanselow selectivity coefficient as of function of equilibration time for the TYLX-NaX STx-1 system. The error bars represent ± 1 standard deviation.

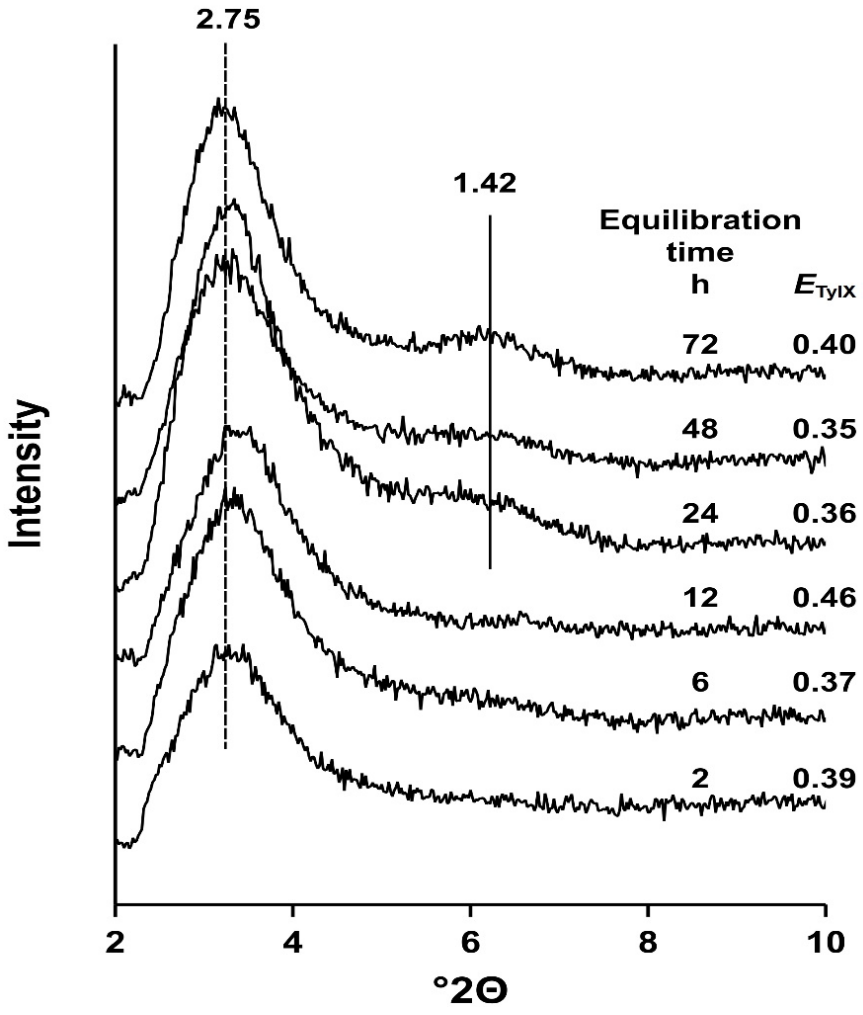

Figure B-3: X-ray diffractograms of STx-1 for TYLX-NaX exchange as a function of equilibration time and the equivalent fraction of tylosin on the exchange phase (E_{TYLX}). The d values for the primary and secondary diffractions are given in nm.

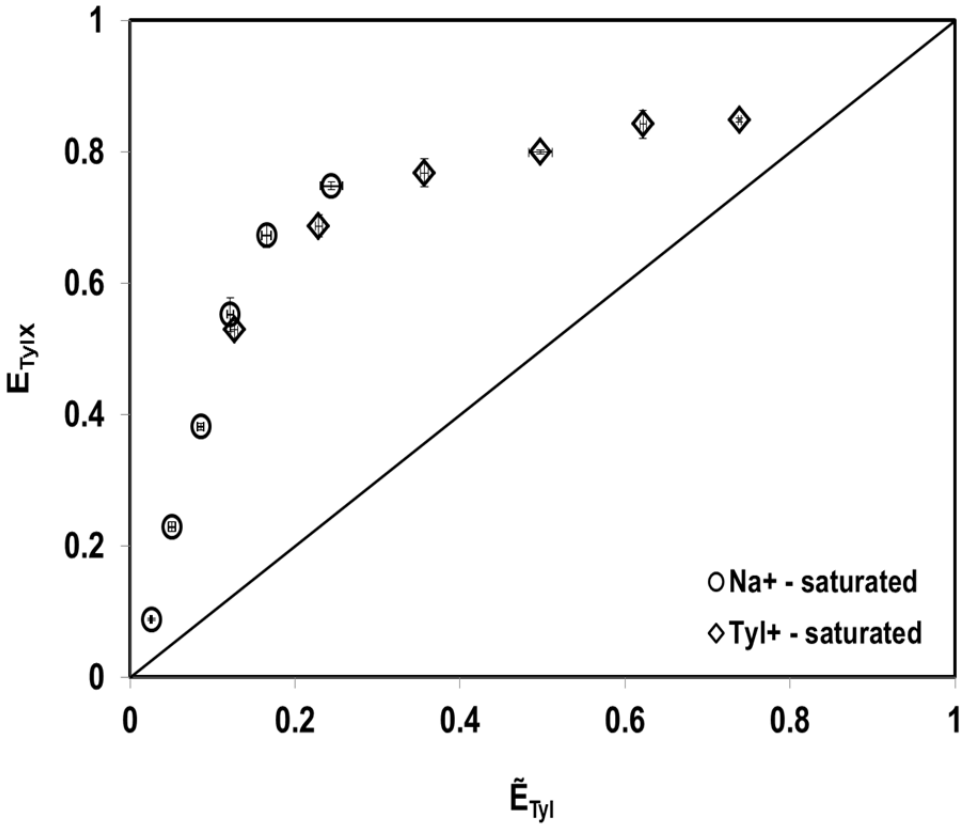

Figure B-4: Exchange isotherms for TYLX-NaX STx-1 systems. Error bars represent ± 1 standard deviation.

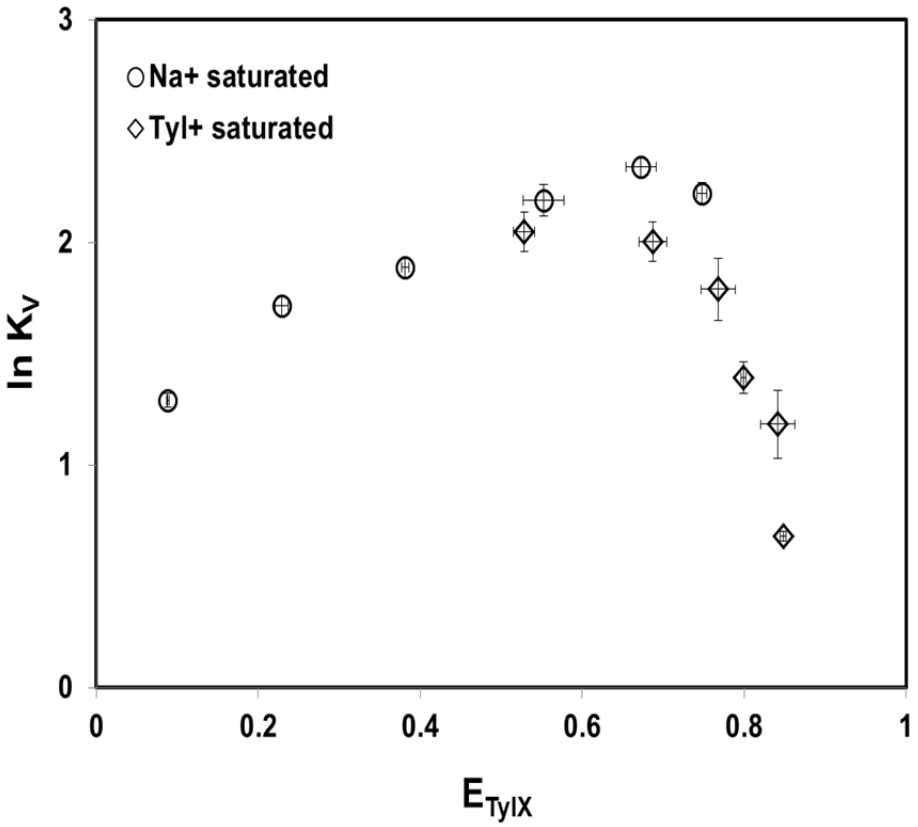

Figure B-5: Tylosin- and Na-saturated exchange selectivity for the TYLX-NaX STx-1 system. Error bars represent ± 1 standard deviation.

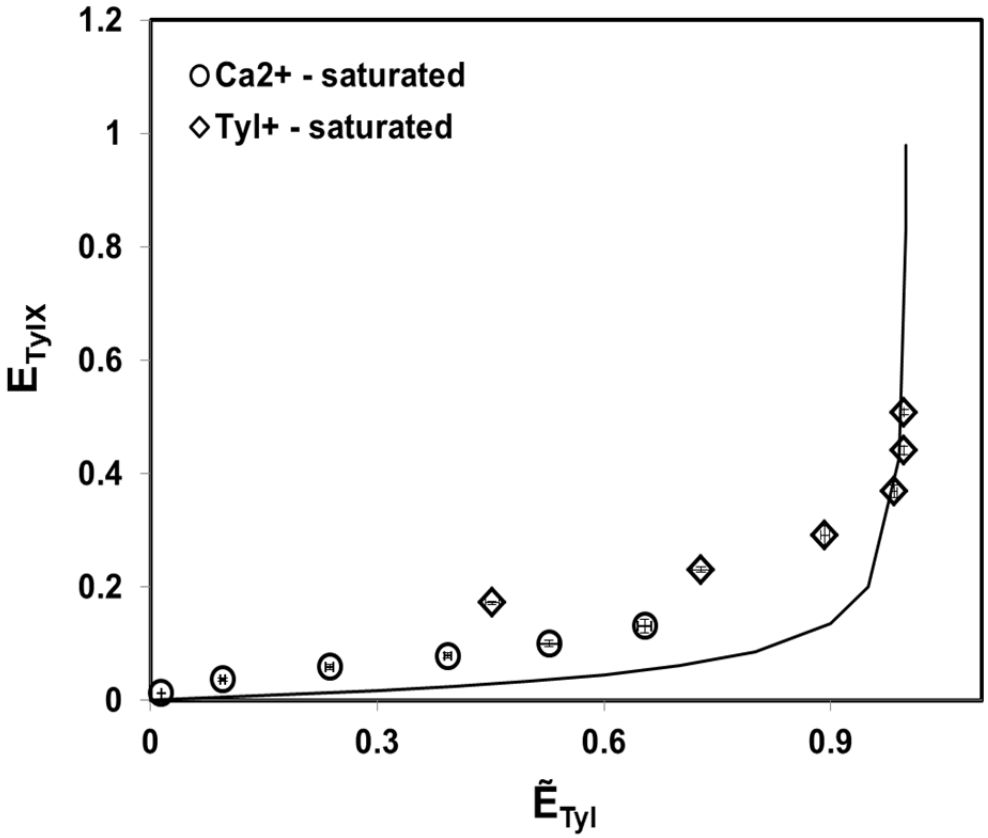

Figure B-6: Exchange isotherms for 0.004 N total normality TYLX-CaX STx-1 system. Error bars represent ± 1 standard deviation.

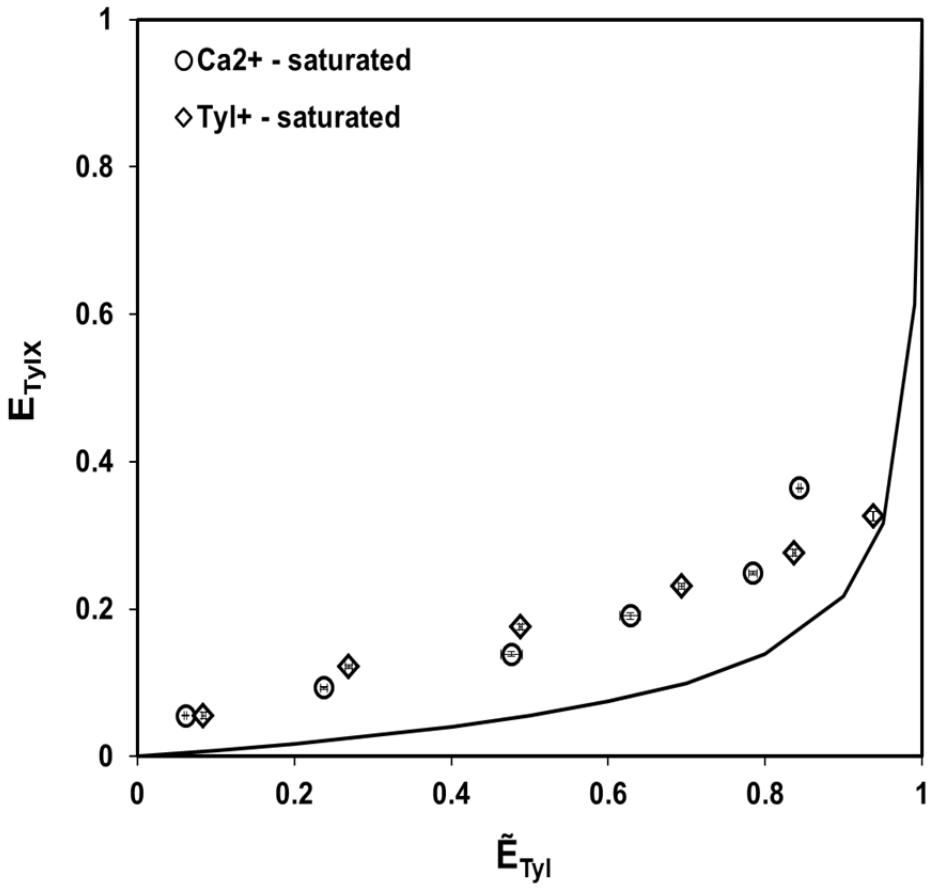

Figure B-7: Exchange isotherms for 0.01 N total normality TYLX-CaX STx-1 systems. Error bars represent ± 1 standard deviation.

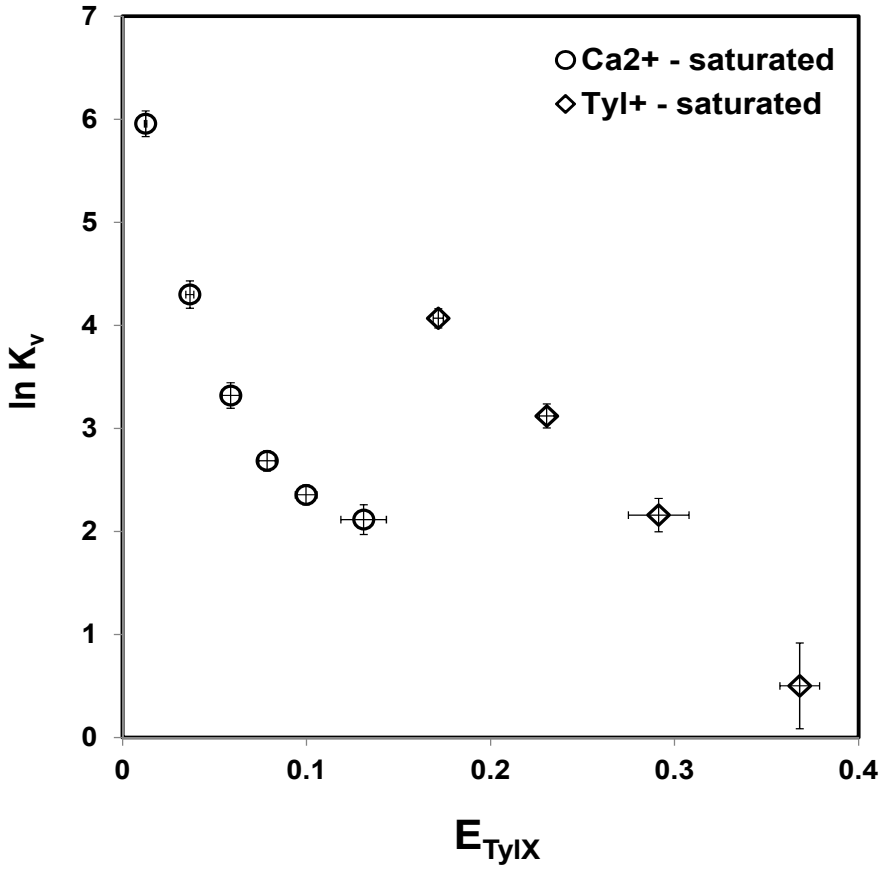

Figure B-8: Tylosin- and Ca-saturated exchange selectivity for 0.004 N TYLX-CaX STx-1 systems. Error bars represent ± 1 standard deviation.

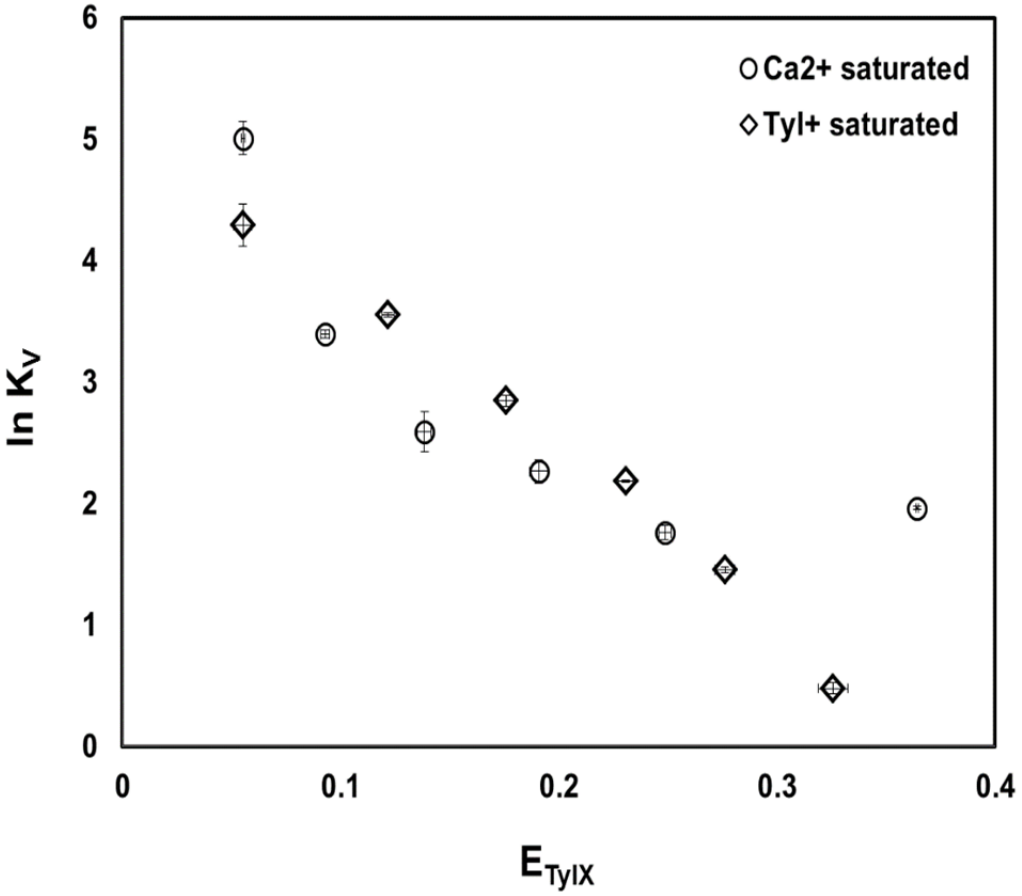

Figure B-9: Tylosin- and Ca-saturated exchange selectivity for 0.01 N TYLX-CaX STx-1 systems. Error bars represent ± 1 standard deviation.

Table B-4: Average cation exchange capacity calculated from STx-1 binary exchange studies.

System	CEC ($cmol_c\ kg^{-1}$)
TYLX-NaX, Na-saturated	35.0
TYLX-NaX, TYL-saturated	19.2
TYLX-CaX, Ca-saturated, 0.004 N	66.4
TYLX-CaX, TYL-saturated, 0.004 N	45.7
TYLX-CaX, Ca-saturated, 0.01 N	49.1
TYLX-CaX, TYL-saturated, 0.01 N	42.0

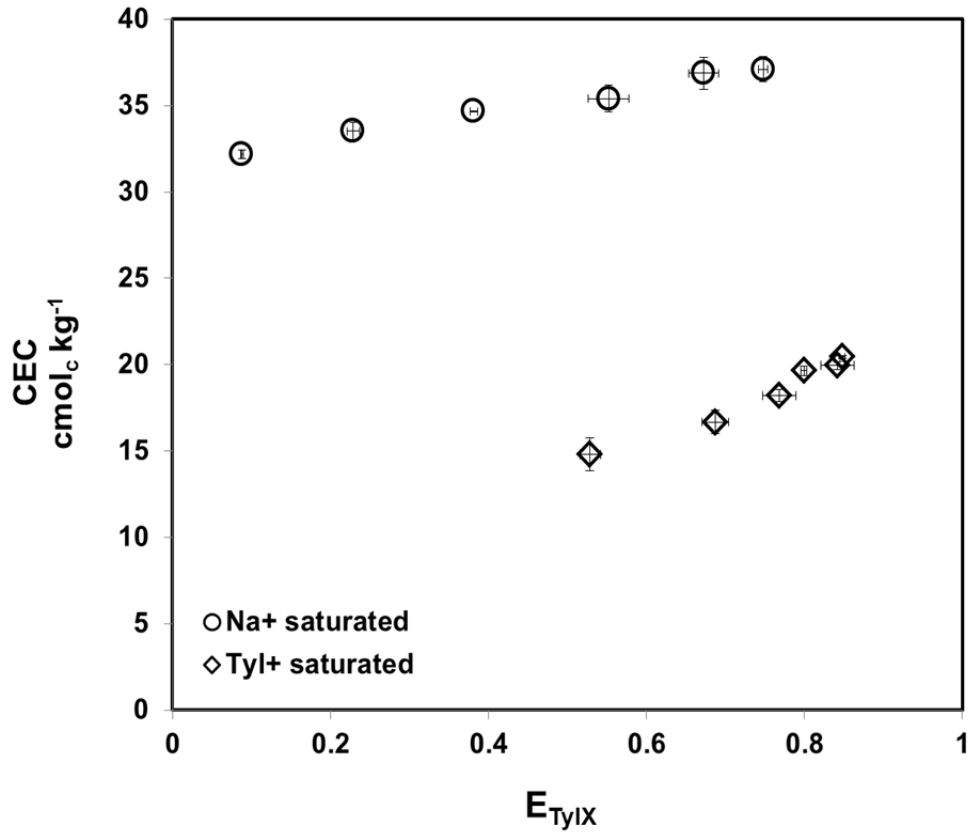

Figure B-10: Cation exchange capacity for TYLX-NaX STx-1 system as a function of the equivalent fraction of TYLX. Error bars represent ± 1 standard deviation.

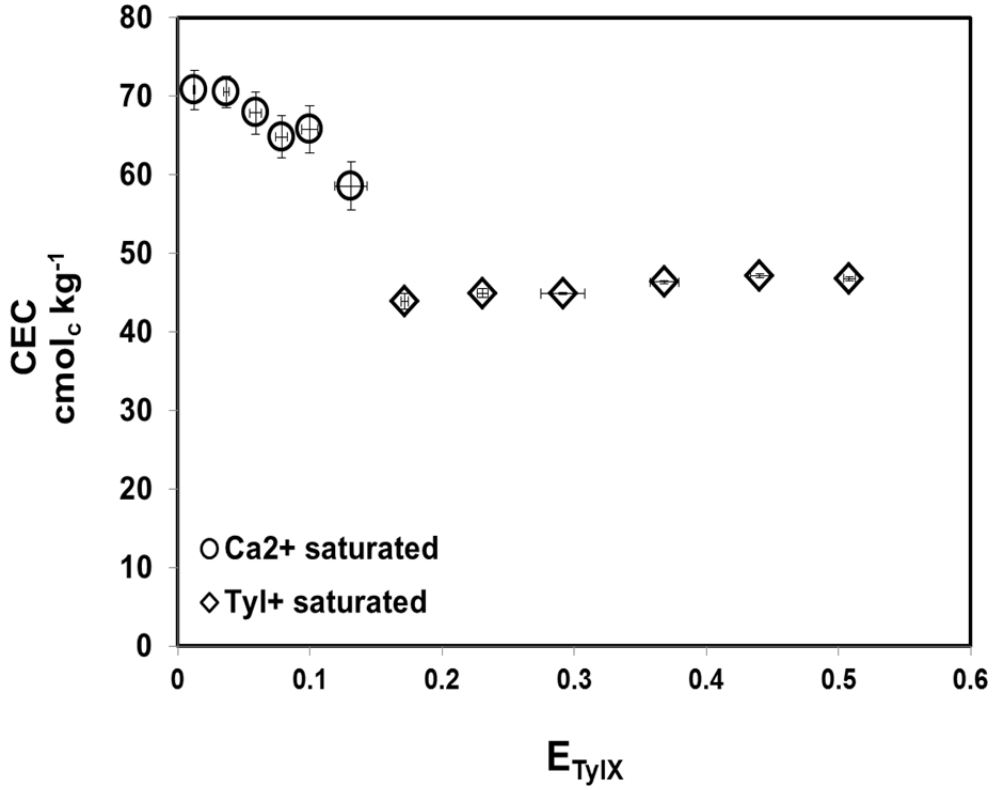

Figure B-11: Cation exchange capacity for 0.004 N TYLX-CaX STx-1 systems as a function of the equivalent of TYLX. Error bars represent ± 1 standard deviation.

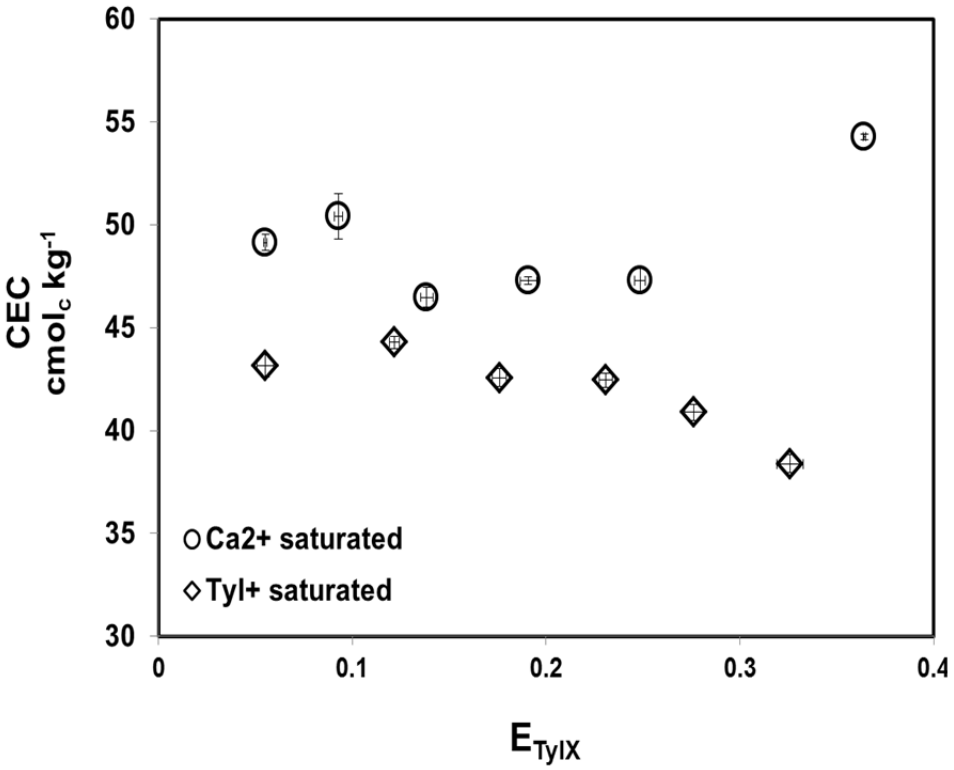

Figure B-12: Cation exchange capacity for 0.01 N TYLX-CaX STx-1 systems as a function of the equivalent fraction of TYLX. Error bars represent ± 1 standard deviation.

Table B-5: Adsorption constants generated from Freundlich and partition models for STx-1 and Libby vermiculite systems.

Exchange	Tylosin	log K_F	K_F	N	R^2	K_P	R^2
Na-saturated STx-1	total	2.57	369	0.74	0.97	--	--
	exchangeable	--	--	--	--	285	0.90
	nonexchangeable	1.87	74.6	0.24	0.79	--	--
0.004 N Ca-saturated STx-1	total	2.30	199	0.34	0.98	--	--
	exchangeable	1.70	50.1	0.58	0.97	--	--
	nonechangeable	2.17	148	0.28	1.00	--	--
0.01 N Ca-saturated STx-1	total	--	--	--	--	1887	0.91
	exchangeable	--	--	--	--	400	1.00
	nonechangeable	--	--	--	--	1487	0.86
Na-saturated Libby vermiculite	total	1.07	11.7	0.87	0.95	--	--
	exchangeable	--	--	--	--	1.66	0.90
	nonexchangeable	1.02	10.6	0.80	0.95	--	--
Ca-saturated Libby vermiculite	total	0.84	6.95	0.97	0.86	--	--
	exchangeable	--	--	--	--	0.12	0.84
	nonexchangeable	0.83	6.83	0.97	0.86	--	--

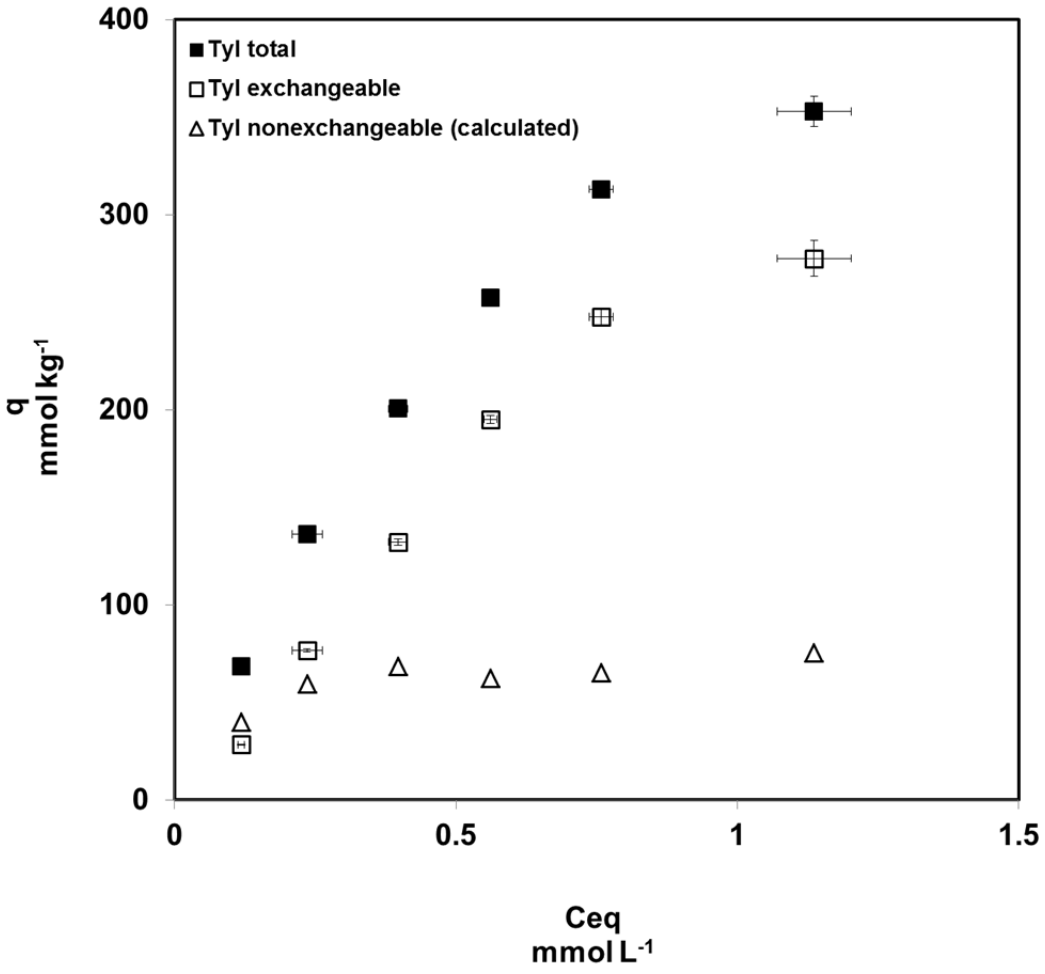

Figure B-13: Tylosin adsorption isotherms for the TYLX-NaX STx-1 system. Error bars represent ± 1 standard deviation.

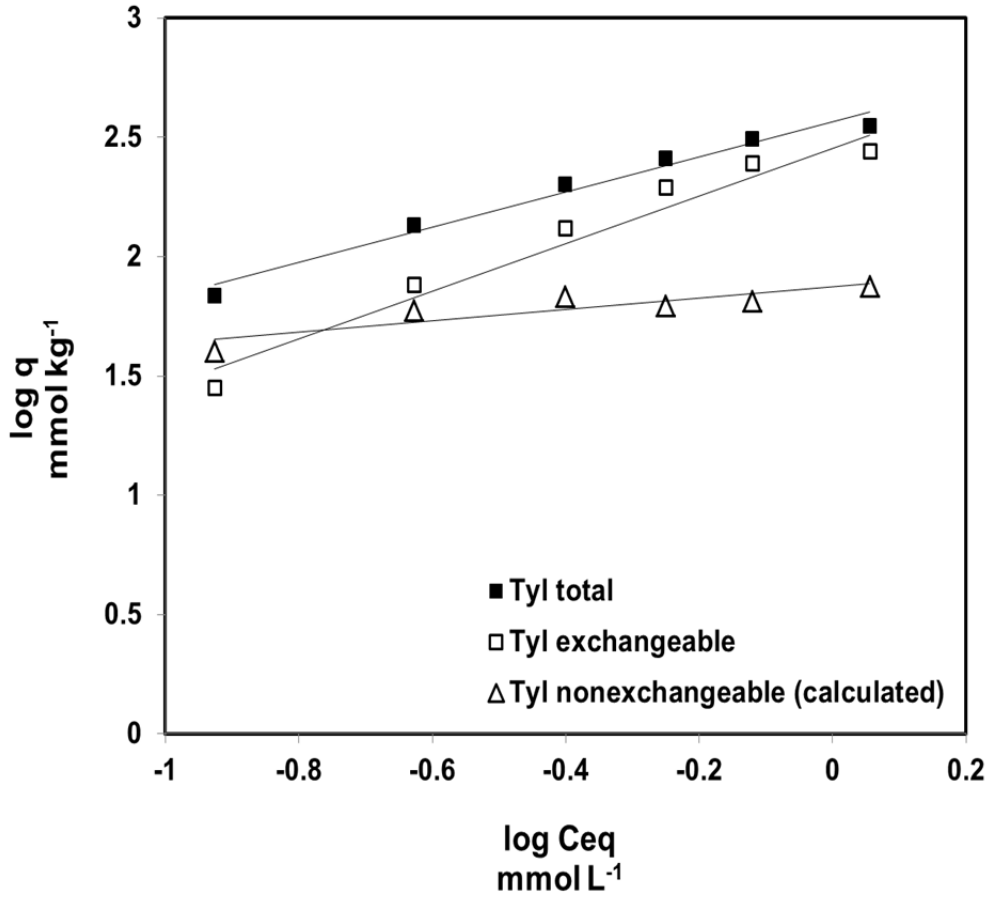

Figure B-14: Freundlich isotherms for the TYLX-NaX STx-1 system. The lines represent the Freundlich (TYL total and TYL nonexchangeable) or the partition (TYL exchangeable) isotherm models.

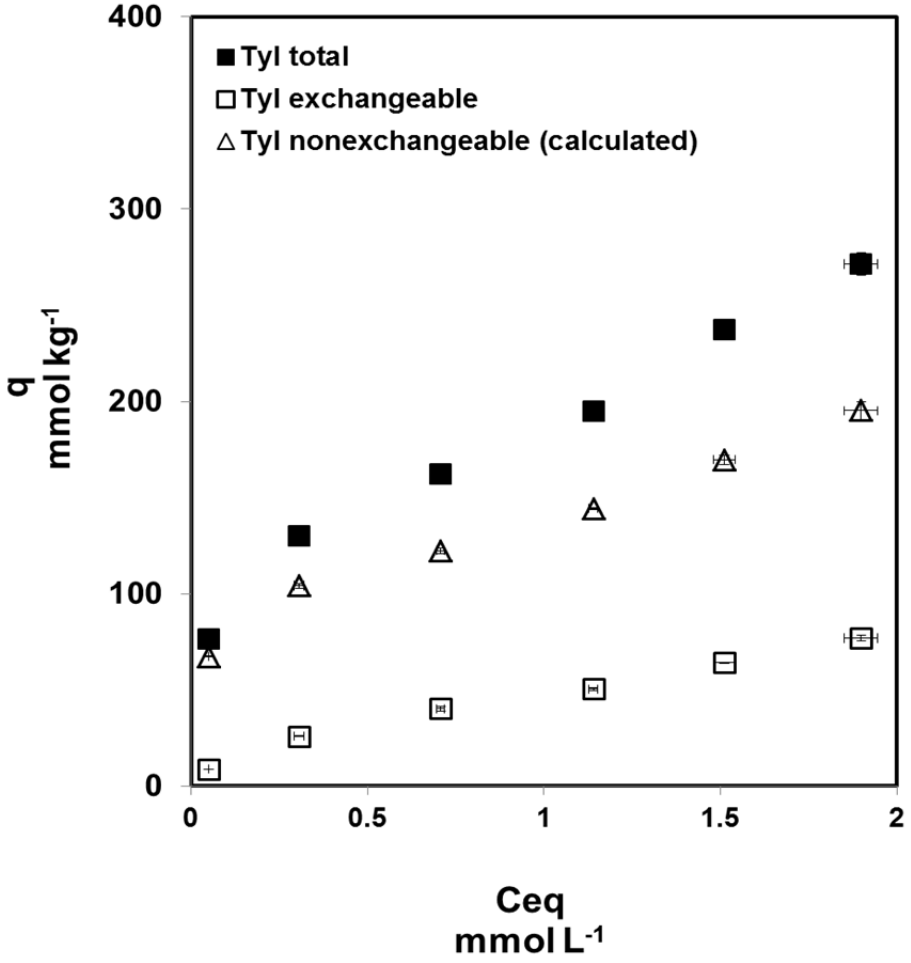

Figure B-15: The tylosin adsorption isotherms for 0.004 N TYLX-CaX STx-1 system. Error bars represent ± 1 standard deviation.

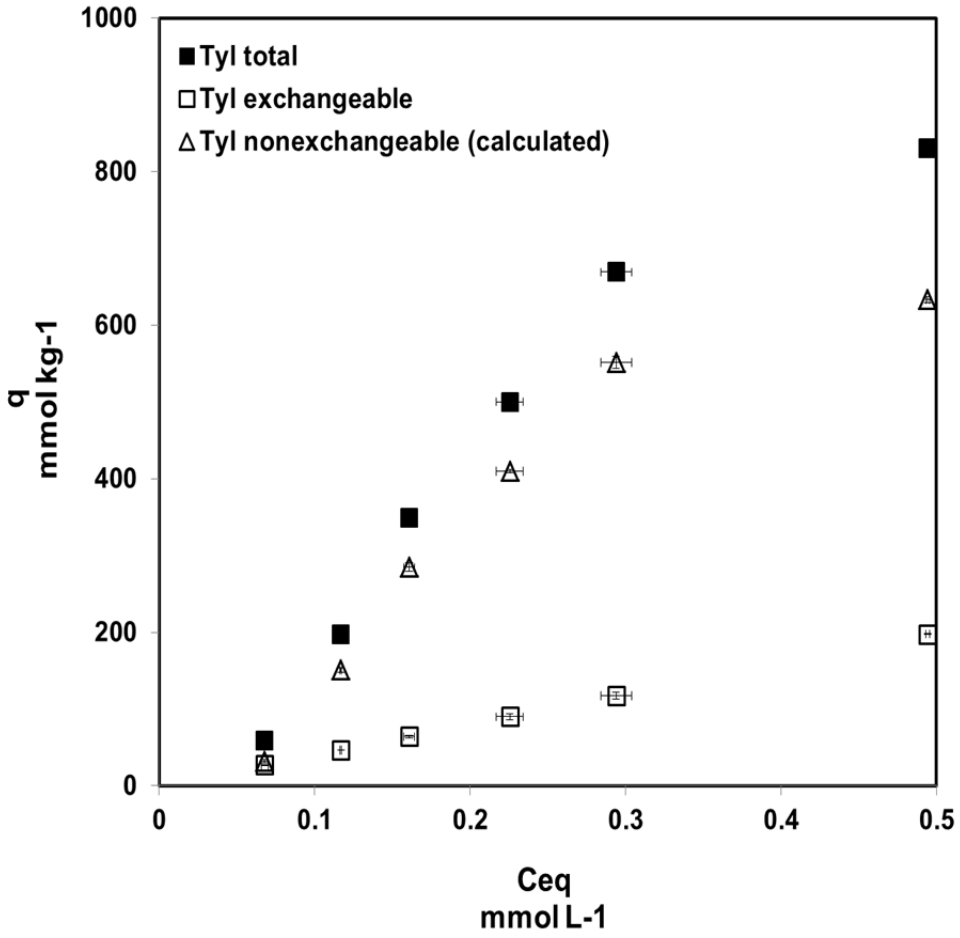

Figure B-16: The tylosin adsorption isotherms for 0.01 N TYLX-CaX STx-1 system. Error bars represent ± 1 standard deviation.

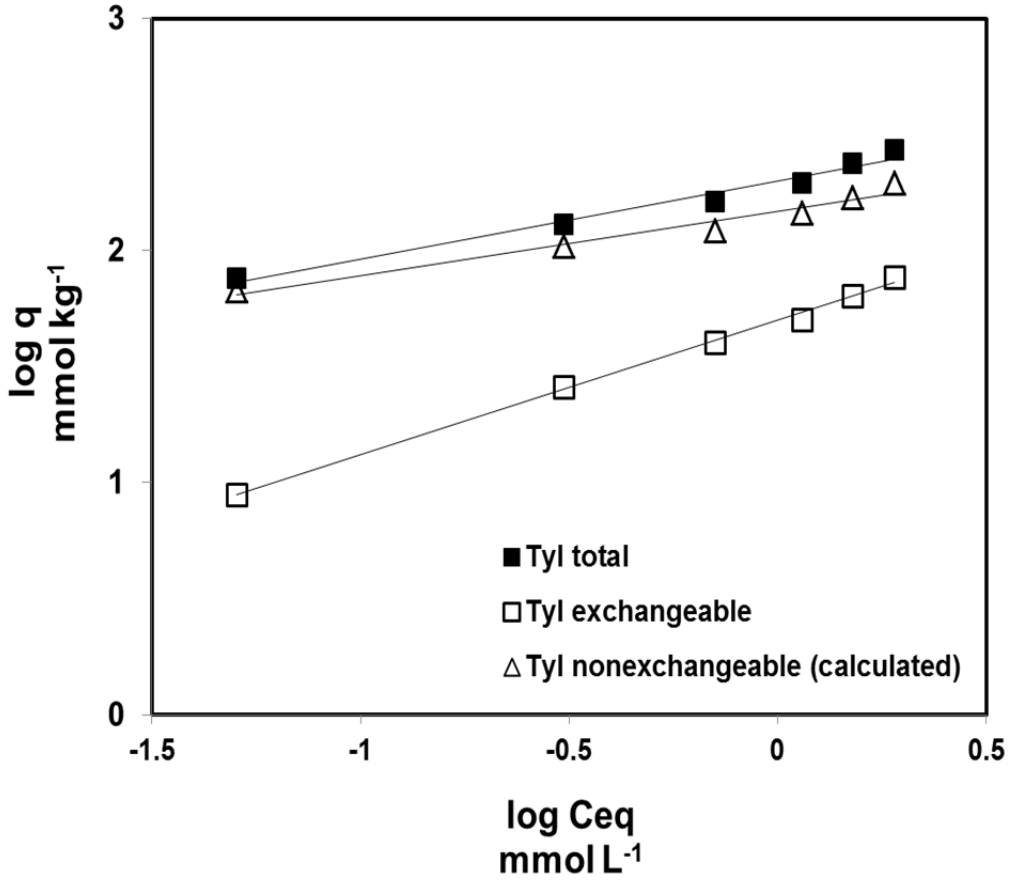

Figure B-17: Freundlich isotherms for the 0.004 N TYLX-CaX STx-1 system. The lines represent the Freundlich isotherm models.

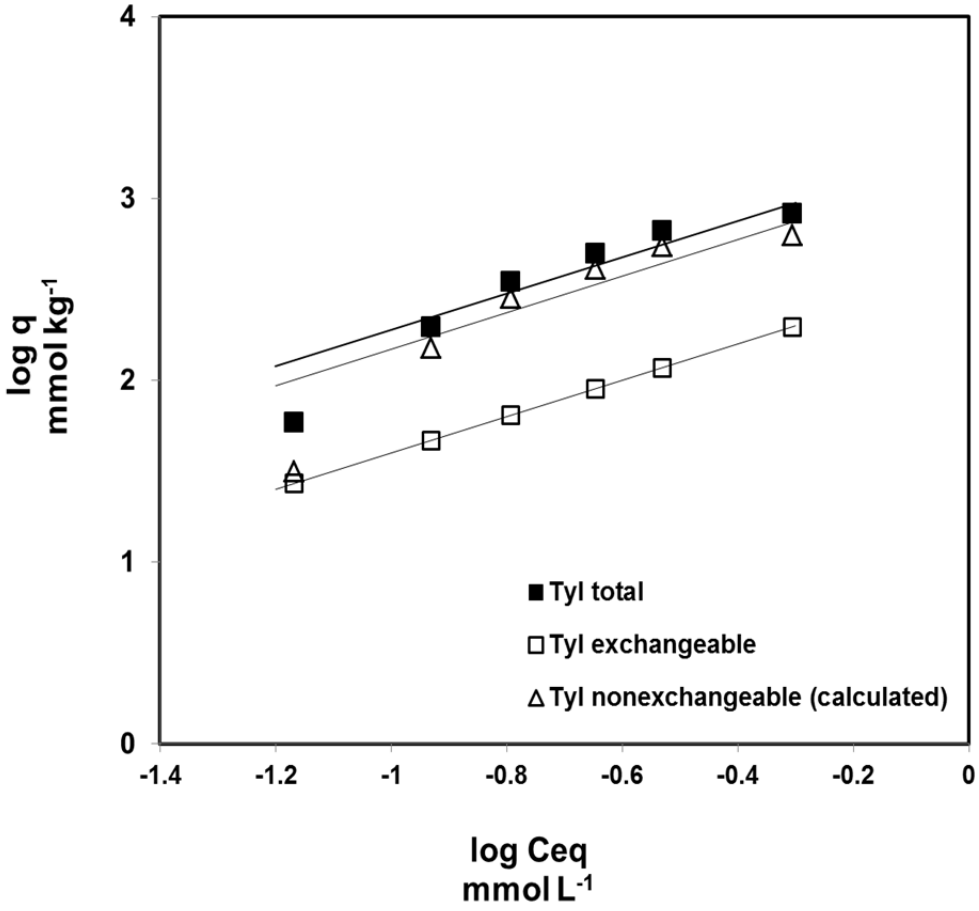

Figure B-18: Freundlich isotherms for the 0.01 N TYLX-CaX STx-1 system. The lines represent the partition isotherm models.

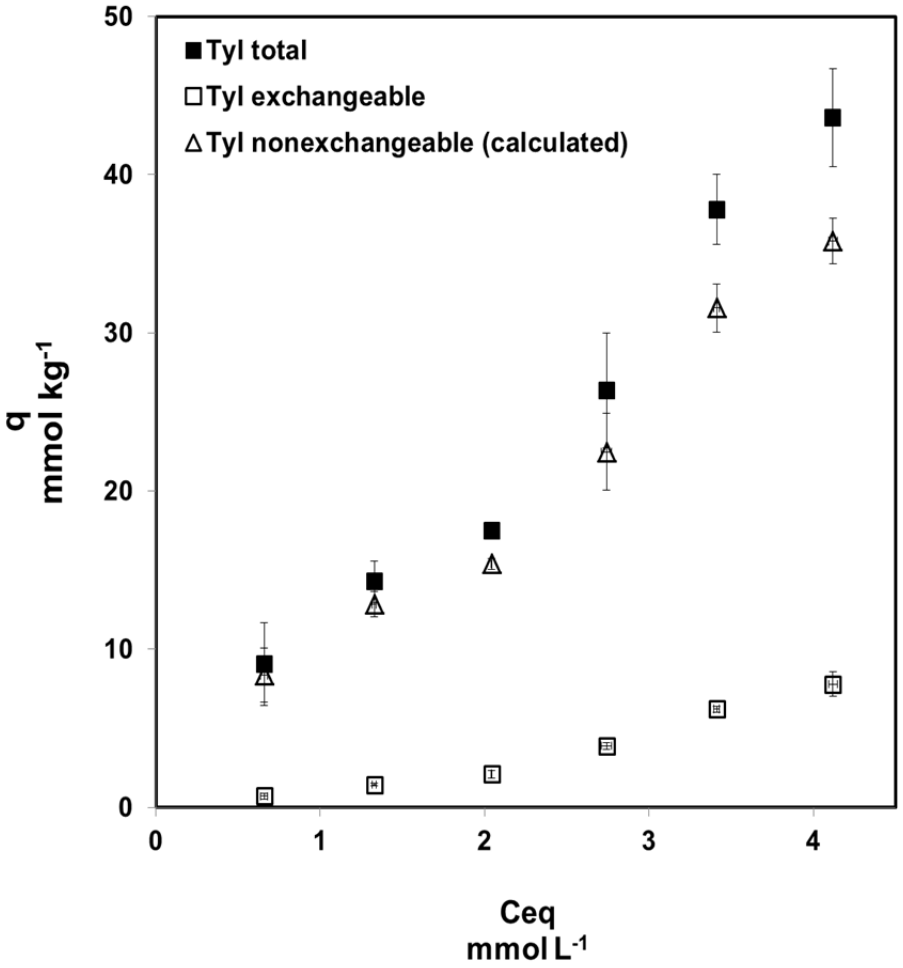

Figure B-19: The tylosin adsorption isotherms for TYLX-NaX Libby vermiculite. Error bars represent ± 1 standard deviation.

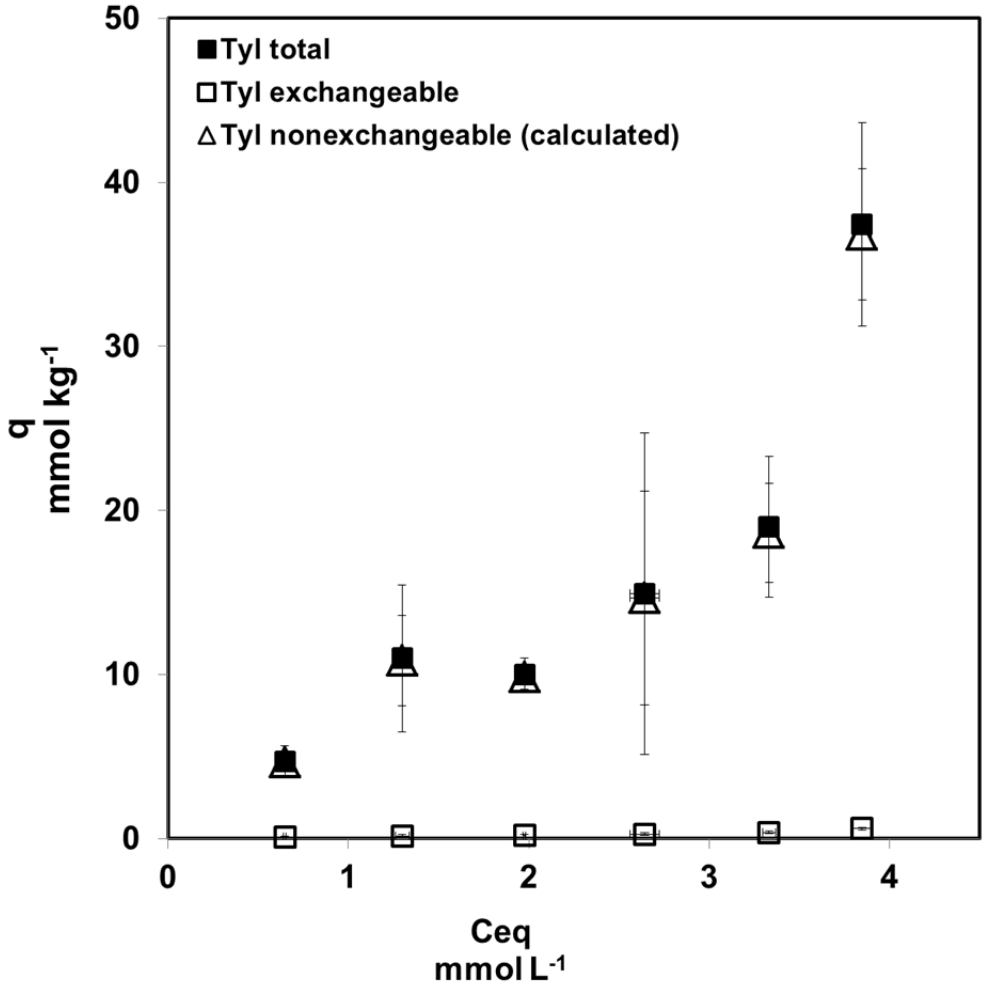

Figure B-20: The tylosin adsorption isotherms for TYLX-CaX Libby vermiculite system. Error bars represent ± 1 standard deviation.

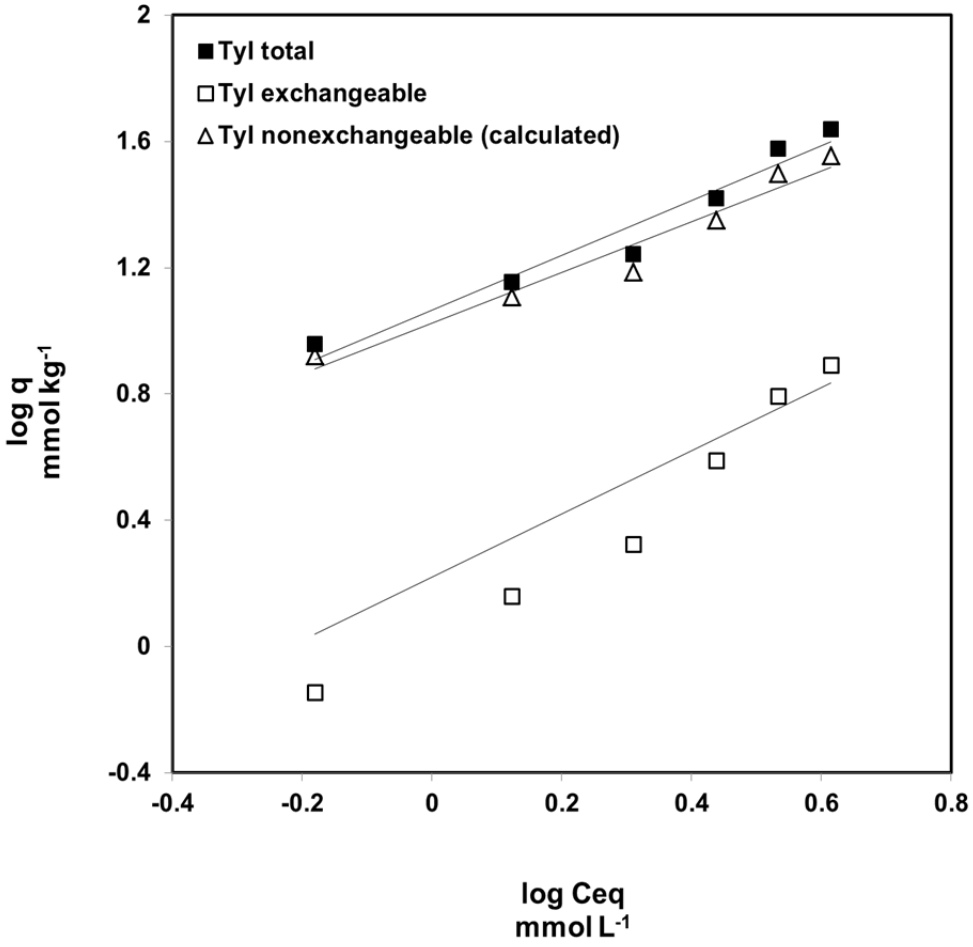

Figure B-21: Freundlich isotherms for the TYLX-NaX Libby vermiculite system. The lines represent the Freundlich (TYL total and TYL nonexchangeable) or the partition (TYL exchangeable) isotherm models.

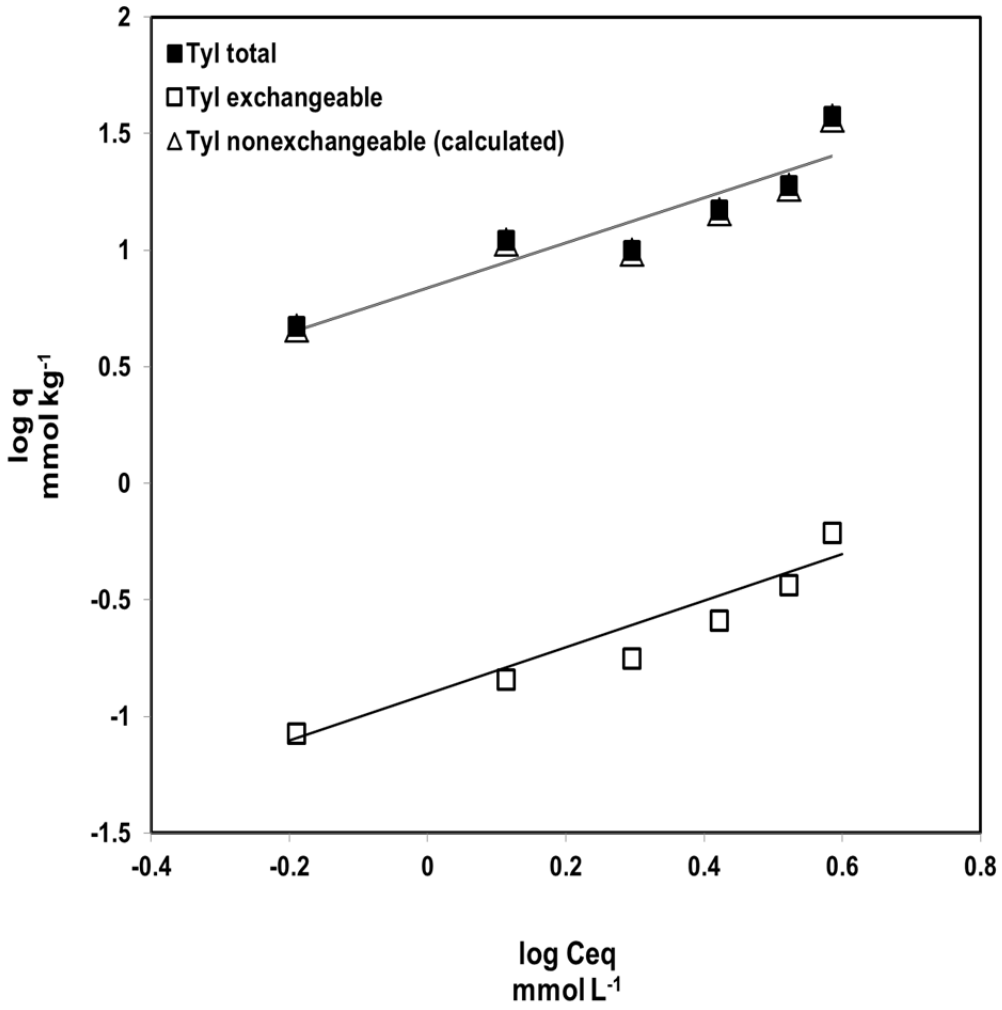

Figure B-22: Freundlich isotherms for the TYLX-CaX Libby vermiculite system. The lines represent the Freundlich (TYL total and TYL nonexchangeable) or the partition (TYL exchangeable) isotherm models.

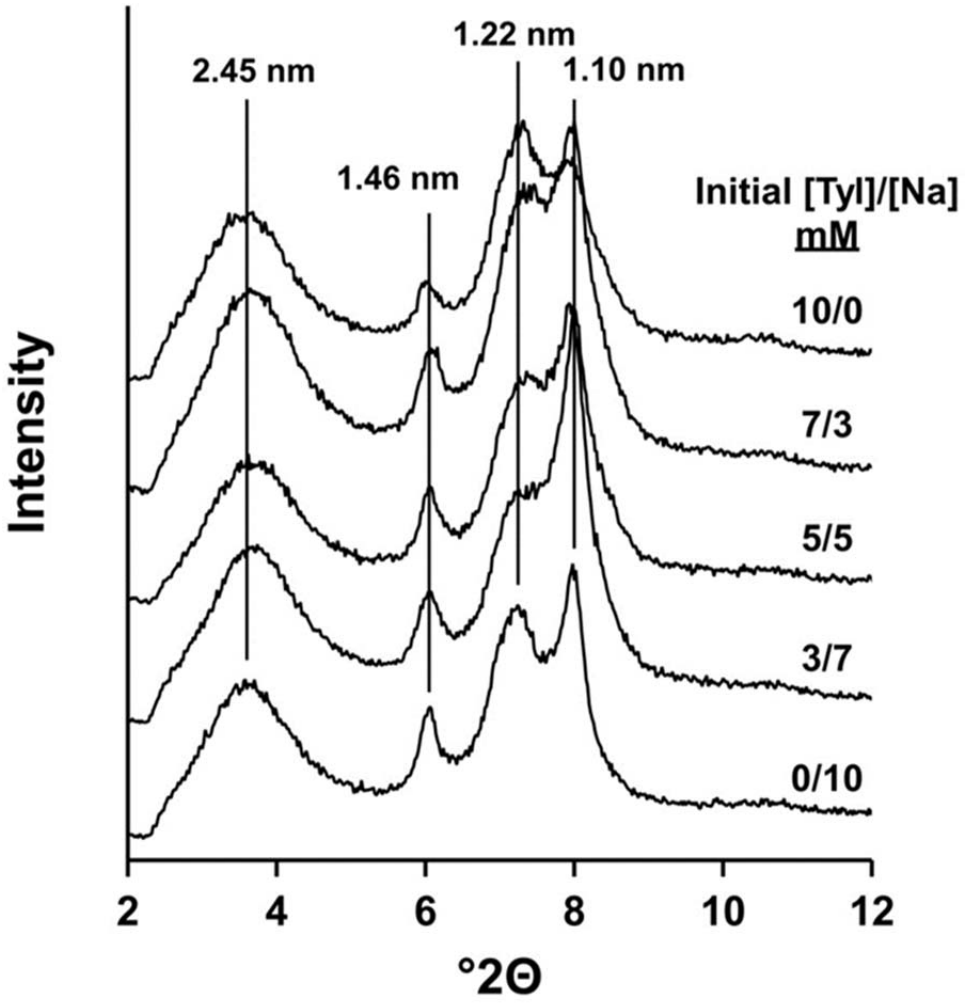

Figure B-23: X-ray diffractograms of TYLX-NaX Libby vermiculite as a function of initial tylosin suspension concentration and a total normality of 0.01 N.

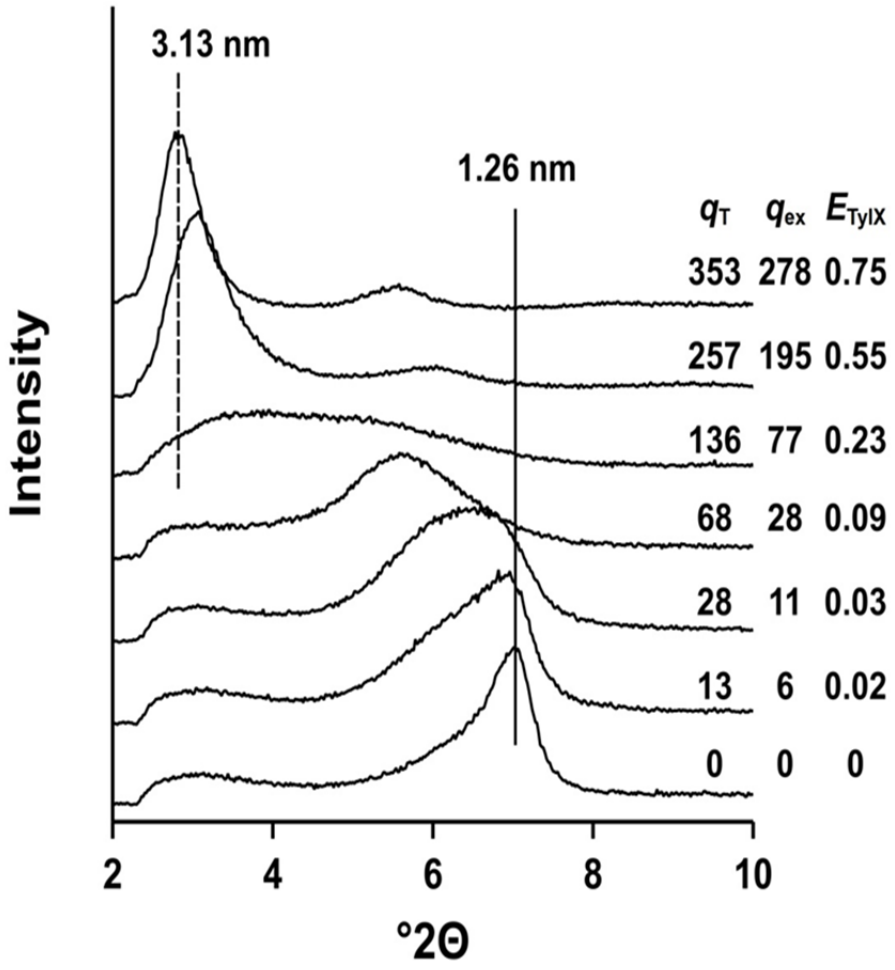

Figure B-24: X-ray diffractograms of TYLX-NaX STx-1 as a function of the equivalent fraction of TYLX in 0.004 N system.

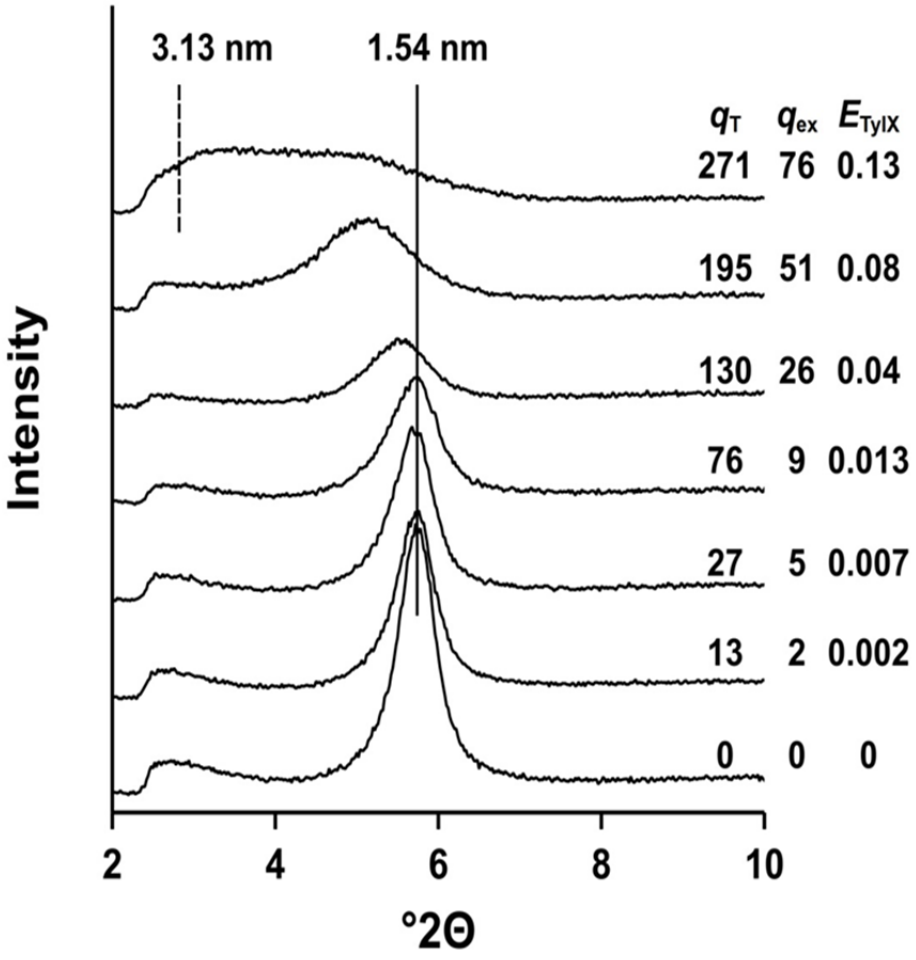

Figure B-25: X-ray diffractograms of TYLX-CaX STx-1 as a function of the equivalent fraction of TYLX in 0.004 N system.

CHAPTER 3: CATION EXCHANGE OF TYLOSIN IN A LOESS-DERIVED WEST TENNESSEE SOIL

ABSTRACT

Tylosin (TYL) is a commonly used agricultural antibiotic that has been reported in measurable amounts in surface waters. Tylosin retention by agricultural soils is a function of pH, ionic strength, background electrolyte type, organic matter content, and clay content and type. These findings indicate that ion exchange is an important mechanism for TYL retention. This study examines ion exchange involving TYL using clay-sized particles from two Bt2 horizon depths (15-30 and 30-46 cm depths) of a west Tennessee Loring soil. Binary exchange isotherms were developed to study TYL exchange in Na and Ca systems. The Vanselow selectivity coefficient (K_V) was calculated for each system to determine exchange phase preference for TYL. Adsorption isotherms were developed from the binary exchange studies to display exchangeable and nonexchangeable TYL. The adsorption isotherms were described with the Freundlich and partition models. In addition, x-ray diffraction was performed to evaluate TYL intercalation into the soil clay minerals. For the TYLX-NaX exchange system, the exchange phase did not prefer TYL^+ or Na^+ for either Bt2 horizon. However, TYL^+ was preferred over Ca^{2+} in the TYLX-CaX system for both horizons. The K_V is invariant for the TYLX-NaX and the TYLX-CaX exchange systems. For both depths, exchangeable TYL comprised a majority of total adsorbed in the TYLX-NaX system, while nonexchangeable TYL comprised a majority of total adsorbed in the TYLX-CaX system. In the TYLX-NaX system, TYL intercalation resulted in d values of 2.77 nm (15-30 cm depth) and 2.37 nm (30-46 cm depth). In the TYLX-CaX system, d values of 1.60 nm (15-30 cm depth) and 1.63 nm (30-46 cm depth) were observed. The intercalation of TYL into the soil clay minerals indicates that this substance may be protected from

microbial degradation. However, the competition of TYL with common soil cations for exchange sites may result in enhance environmental mobility.

INTRODUCTION

The longtime use of veterinary antibiotics (VA) in agricultural systems has led to the concern of their accumulation in manure fertilizers and soil and water environments. Kolpin et al. (2002) and Sarmah et al. (2006) have reported tylosin, a commonly used agricultural antibiotic, in measurable amounts in surface waters. Adsorption studies have focused on antibiotics such as tylosin because of their mobility in soil environments (Ter Laak et al., 2006; Sassman et al., 2007; Essington et al., 2010; and Lee et al., 2014).

Adsorption studies involving TYL have focused on characterizing adsorption by soil and soil minerals as a function of pH, ionic strength, background electrolyte type, organic matter content, and clay content and type. For example, Allaire et al. (2006) conducted an adsorption kinetics study on TYL with sandy loam and clay soils. The soils differed greatly in their particle size distribution; therefore, TYL adsorption was correlated with particle size. The authors found that adsorption equilibrium occurred in less than 48 h. After 1 h, TYL adsorption was constant to 100 h. They also found that TYL adsorption was 2.4 times greater on the clay soil than the sandy soil, which indicates TYL adsorption is dependent on clay content and particle size. Kolz et al. (2005) came to a similar conclusion. They studied tylosin adsorption using manure slurries from open and closed (or anaerobic) swine manure lagoons and used the Freundlich model to characterize the adsorption isotherms. The samples were divided

into solids (< 2 mm) and colloids (< 1.2 μm). The closed lagoon solids had a K_F of 39.4 while the colloids had a K_F of 67.7. The open lagoon solids had a K_F 99.5 and the colloids had a K_F of 182.5. TYL adsorption is influenced by soil surface area. Smaller particle-sized soils, which have a higher surface area, generated greater TYL adsorption.

Ter Laak et al. (2006) conducted TYL batch adsorption isotherms studies using clay loam and loamy sand soils. Tylosin adsorption was determined to be strongly pH dependent and adsorption decreased as pH increased to 9.0 and decreased with increasing ionic strength of the background electrolyte, indicating ion exchange as the adsorption mechanism. The adsorption isotherms were fit with the Freundlich model with the clay loam K_F being 85 and the loamy sand K_F being 6.8.

Lee et al. (2014) conducted batch adsorption isotherm studies of TYL by surface and subsurface clay loam and sandy loam soils. Greater TYL adsorption was observed by the clay loam (higher clay content and higher CEC) relative to sandy loam (lower clay content and lower CEC) soils. Further, they observed greater retention in surface soils, exhibiting lower clay content but greater organic matter content. Tylosin adsorption decreased with increasing ionic strength, retention was greater to Na^+ background electrolyte relative to Ca^{2+}. Tylosin adsorption for both soils was described as Langmuirian, as adsorption intensity decreased with increasing surface coverage.

The experimental findings indicate that an important retention mechanism for TYL in soil is cation exchange. However, the cation exchange selectivity of TYL, relative to common cations in soil systems, has not been examined. The objectives of this research are to examine the exchange selectivity of TYL in the B2t horizons of a

west Tennessee soil. Binary exchange isotherms involving TYL-Ca and TYL-Na were developed to establish exchange preference, and to determine the distribution between exchangeable and nonexchangeable forms of the adsorbed TYL. An XRD study was performed to evaluate the intercalation of soil clays by TYL.

MATERIALS AND METHODS

Chemicals

Veterinary-grade tylosin tartrate was obtained from Elanco (Greenfield, IN) for use in the exchange studies and consists of 95.5% tylosin, 3.1% desmycosin, and 1.4% macrocin. Analytical grade tylosin tartrate (98.8% tylosin) was obtained from Sigma-Aldrich and used as a standard for the chemical analysis of the equilibrium exchange systems. Other chemicals used include distilled-deionized (DDI) water (carbon dioxide free, >18Ω; Barnstead E-pure system) and the analytical grade or better compounds (Fisher Scientific, Fair Lawn, NJ) sodium chloride, calcium chloride dihydrate, magnesium chloride hexahydrate, potassium phosphate monobasic, and acetonitrile.

Soils

Soil samples from the Milan Research and Education Center in Milan, TN were used in this study. The samples were obtained from the 15-30 cm and 30-46 cm depth increments of a Loring soil (Oxyaquic Fragiudalfs). These depth increments represent the B2t horizons of the soil and contain approximately 12% to 15% clay. The clay mineralogy of the Loring soil was verified through x-ray diffraction (described below). The soil samples were air dried, disaggregated, passed through a 2 mm sieve, and then

Na-saturated by repeated centrifuge washings with 1 M NaCl. The <2 μm size separate was isolated using Stoke's Law sedimentation with Na-saturated soil. The clay fraction was repeatedly centrifuge washed with DDI water to remove entrained salt, then freeze-dried. The particle size distribution of the Loring soil size separates were determined with a Becker Coulter LS 13320 Laser Diffraction Particle Size Analyzer (Brea, Ca) and shown in Table C-1. The samples were Ca- or TYL-saturated with repeated centrifuge washes of 1.0 M $CaCl_2$, or 0.004 M or 0.01 M tylosin.

Binary Exchange Isotherms

Binary exchange isotherms were developed using 0.5 g of the Loring clay in 50 mL polyethylene centrifuge tubes. The exchange experiments were performed in triplicate. Soil samples were initially TYL- or Na-saturated for TYL-Na binary exchange, or TYL- or Ca-saturated for TYL-Ca exchange. The soils were introduced to 30 mL volume of solution containing varied ratios of TYL to Na, or TYL to Ca, such that the total normality was 0.004 N (Table C-2). Centrifuge tubes without soils were used as controls for each exchange experiment. These control blanks were duplicated for each ratio in the experiment and used later to determine mass balance of original solutions, determine total Cl and tartrate concentrations for ion speciation modeling, and to compute total adsorbed concentration of TYL. The suspensions and the blanks were equilibrated for 18 hours on an orbital shaker at ambient temperature (20-22ºC). Kinetics study described in Chapter 2 indicated that exchange equilibrium in a reference smectite system was achieved in less than 2 hours; the 18 hour reaction time was chosen for convenience. Following the exchange equilibration period, the solution and

solid phases were separated by centrifugation and the solution pH was determined. The solution was further clarified by filtration through a 0.45 µm membrane filter. Equilibrium solutions were stored under refrigeration until analysis. The remaining solids were centrifuge washed 3 times with DDI water to remove entrained soluble salts (as determined by $AgNO_3$ test), then repeatedly washed 3 times with 1.0 M NH_4-acetate (and the supernatant liquid collected) to remove the exchangeable cations. The collected supernatant NH_4-acetate liquids were brought to a volume of 100 mL and filtered through qualitative-grade filter paper (Whatman #42). The NH_4-acetate extracts were stored under refrigeration until analysis.

Clay mineralogy

To determine clay mineralogy of the Loring clay fraction (15-30 cm and 30-46 cm depths), samples were sequentially treated to remove cementing agents with pH 5.0 ammonium acetate (carbonate removal and Na-saturation), hydrogen peroxide (organic matter and manganese oxide removal), and sodium-citrate-dithionite (iron oxide removal) as described by Jackson (2005). For each depth, 5 cation saturations and heat treatments were performed: potassium-saturated and dried at room temperature (K-room), potassium-saturated and treated at 300ºC (K-300), potassium-saturated and treated at 550ºC (K-550), magnesium-saturated and dried at room temperature (Mg-room), and magnesium-saturated treated with glycol (Mg-glycol).

In preparation for clay mineralogical analysis, 2 g of each of the 15-30 cm and 30-46 cm depths were weighed into 250 mL centrifuge bottles. To each sample, 50 mL of 1 N pH 5 sodium acetate (NaOAc) was added. The samples were digested at 80ºC

for 30 minutes and centrifuged (supernatant decanted). The pH 5 NaOAc and digestion step was repeated for a total of 3 times. The samples were then transferred to a 600 mL beaker where 5 mL of 30% hydrogen peroxide (H_2O_2) was added and the suspension stirred at room temperature for 10 minutes. Once the frothing subsided, the samples were heated to 80ºC and an additional 15 mL of H_2O_2 was added. Samples were covered and digested for 4 hours at 80ºC and then transferred to 250 mL centrifuge bottles where they were repeatedly centrifuge washed 3 times with pH 5 1N NaOAc. The samples were then centrifuge washed with 95% methanol and followed by 99% methanol. The samples were then repeatedly washed with DDI water to remove the methanol. To each bottle, 40 mL of 0.3 M sodium-citrate and 5 mL of 1 M sodium bicarbonate were added and heated to 80ºC. One g additions of sodium dithionite were gradually added while stirring for a final total of 3 g. After the final 1 g addition of sodium dithionite, the samples were digested for 15 minutes and then centrifuge washed twice with a mixture of 10 mL of saturated sodium chloride and 10 mL of acetone. After the final wash, excess liquid was removed and sufficient DDI water added to divide each depth into 2 centrifuge bottles. Excess liquid was removed and the samples stored under refrigeration.

The disaggregated clays were repeatedly centrifuge washed 4 times with either 1 M KCl and 1 M $MgCl_2$ and then centrifuge washed 3 times with DDI water to remove excess soluble salt (as determined by $AgNO_3$ test). The soils were kept in a slurry mix and pipetted onto quartz slides and dried overnight at room temperature. The slides were then placed in a desiccator over saturated $MgCl_2$ and a relative humidity of 33%. Potassium-saturated slides were then placed in a muffle furnace at 330ºC or 550ºC for

2 hours. For the Mg-glycol saturation, a Mg-saturated soil suspension was combined with glycol and the mixture placed on a quartz slide. The Mg-glycol slide was placed inside the desiccator over a beaker of glycol and allowed to dry. X-ray diffraction was then preformed to determine d-values of the (00l) spacings of the layer silicates.

Both surface and subsurface Loring soils displayed similar clay mineralogy (Figures C-1 and C-2). The Mg-saturation showed peaks at approximately 1.47 and >2.0 nm representing smectite and an interstratifed mica-smectite. Upon gylcolation, expansion of the 1.47 nm peak to 1.7 to 1.8 nm confirms the presence of smectite. The 1.0 nm peak present in all treatments indicates the occurrence of mica, and the disappearance of the 0.7 nm peak upon heating to 550°C indicates kaolinite.

X-ray Diffraction Study

An x-ray diffraction study was performed to determine the location of adsorbed TYL in Na- and Ca-saturated Loring clays. Solutions having differing TYL-Na or TYL-Ca ratios (with a total normality of 0.01 N) were equilibrated with Na- or Ca-saturated solids similar to the binary exchange study previously described. Following equilibration, the soils were centrifuge washed to remove entrained salts. A slurry mix (0.5 g of soil to 20 mL DDI water) for each ratio was created using DDI water. Samples were then pipetted onto glass slides and dried at room temperature overnight. The slides were then placed in a desiccator over a saturated $MgCl_2$ solution (33% relative humidity) for an additional 24 h period. X-ray diffraction was then preformed to determine d-values of the (00l) spacing.

Analytical

A Hewlett-Packard Series 1100 (Hewlett-Packard Palo Alto, CA) HPLC coupled with ultraviolet detection was used to determine TYL concentrations using a procedure described by Essington et al. (2010) and Lee et al. (2014). An Ascentis C18 guard column (2 cm by 4.0 mm and 5 µm) and an Ascentis C18 analytical column (15 cm by 4.6 mm and 5 µm) with an injection volume of 100 µL and a flow rate of 1 mL min^{-1} was used. The mobile phase was an acetonitrile-0.01 M KH_2PO_4, pH 7.0 gradient ranging from 20:80 to 60:40 in 10 minutes, results in a tylosin retention time of 7.8 minutes. A UV detector wavelength of 280 nm results a method detecting limit of 0.008 µmol L^{-1}. The Na and Ca concentrations were determined using a Perkin Elmer AAnalyst 800 atomic absorption spectrophotometer (Wellseley, PA). Sodium was analyzed with emission while Ca with absorbance. The samples and standards were spiked with 12% lanthanum chloride ($LaCl_3$) solution using 0.1 mL for every 10 mL of sample. Sodium and Ca standards were made using atomic absorption standards from CPI International (Springfield, VA). Method detection limits for both Na and Ca were 0.01 mg L^{-1}.

X-ray diffraction (XRD) was used to determine the clay mineralogy and the d value of the (001) plane of the Loring soil clay minerals with varied ratios of TYLX-NaX and TYLX-CaX. X-ray diffractograms were generated using a Bruker Model D8 with Ni-filtered, Cu Kα radiation. The XRD operating parameters were set to 40 kV and 40 mA with a scan range of 2 to 12° 2θ, a step of 0.02 °2θ, and a count rate of 6 second per step.

A chemical equilibrium modeling program, Visual MINTEQ (VM), version 3.1 (Gustafsson, 2014) was used to compute the free cation concentrations of Na^+, Ca^{2+},

and TYL^+, as well as their single-ion activities. Input data for the speciation model included the equilibrium pH, and the total soluble concentrations of Na or Ca, tylosin, Cl, and tartrate. The concentration of Cl was computed from the Na or Ca content of the blanks, and the concentration of tartrate was computed from the tylosin content of the blanks. Table C-3 lists the aqueous speciation reactions and log K_f values used by VM.

Data analysis

The concentrations of cations in the exchange phase are directly determined by NH_4 extraction. An exchange isotherm for TYL is a plot of the equivalent fraction of TYL^+ on the exchange phase (E_{TYLX}, y-axis) versus the equivalent fraction of TYL^+ in the equilibrium solution ($\tilde{E}_{TYL+}$, x-axis). A detailed description of the development of exchange isotherms is provided by Essington (2015). For NaX-TYLX exchange, E_{TYLX} is computed by,

$$E_{TYLX} = \frac{\{TYLX\}}{\{TYLX\}+\{NaX\}} \quad [1]$$

where {TYLX} and {NaX} are the mol kg^{-1} of TYL^+ or Na^+ on the exchange phase. Further,

$$E_{NaX} = 1 - E_{TYLX} \quad [2]$$

The equivalent fraction of TYL^+ in solution is,

$$\tilde{E}_{TYL^+} = \frac{[TYL^+]}{[TYL^+]+[Na^+]} \quad [3]$$

and,

$$\tilde{E}_{Na^+} = 1 - \tilde{E}_{TYL^+} \quad [4]$$

where $[TYL^+]$ and $[Na^+]$ are the mol L^{-1} of free cation in solution (computed using VM). A similar set of expressions describe the CaX-TYLX exchange systems:

$$E_{TYLX} = \frac{\{TYLX\}}{\{TYLX\}+2\{CaX_2\}} \quad [5]$$

$$E_{CaX} = 1 - E_{TYLX} \quad [6]$$

$$\tilde{E}_{TYL^+} = \frac{[TYL^+]}{[TYL^+]+2[Ca^{2+}]} \quad [7]$$

$$\tilde{E}_{Ca^{2+}} = 1 - \tilde{E}_{TYL^+} \quad [8]$$

Also plotted on the exchange isotherm is the non-preference isotherm, obtained from Essington (2015). For NaX-TYLX exchange, the non-preference isotherm is $E_{TYLX} = \tilde{E}_{TYL}{}^{+}$. For CaX-TYLX exchange, the non-preference isotherm is

$$E_{TYLX} = \left\{1 + \frac{2}{\Gamma TN}\left[\frac{1}{\tilde{E}^2_{TYL^+}} - \frac{1}{\tilde{E}_{TYL^+}}\right]\right\}^{-0.5} \quad [9]$$

where $= \frac{\gamma^2_{TYL^+}}{\gamma_{Ca^{2+}}}$, and the ɣ's are single-ion activity coefficients. The non-preference isotherm describes the condition where neither cation is preferred by the exchange phase. The non-preference condition is met when the Vanselow selectivity coefficient (K_V) for the exchange reaction is unity. For the $NaX + TYL^+ = TYLX + Na^+$ exchange reaction, K_V is,

$$K_V = \frac{N_{TYLX}(Na^+)}{N_{NaX}(TYL^+)} \quad [10]$$

For the $CaX_2 + 2TYL^+ = 2TYLX + Ca^{2+}$ exchange reaction, K_V is:

$$K_V = \frac{N^2_{TYLX}(Ca^{2+})}{N_{CaX_2}(TYL^+)^2} \quad [11]$$

In equations [10] and [11] the parentheses represent activity (obtained from VM) and N_{TYLX}, N_{NaX}, and N_{CaX_2}, are the mole fractions:

$$N_{TYLX} = \frac{\{TYLX\}}{\{TYLX\}+\{NaX\}} \quad ; \quad N_{TYLX} = \frac{\{TYLX\}}{\{TYLX\}+\{CaX_2\}} \qquad [12]$$

$$N_{NaX} = 1 - N_{TYLX} \quad ; \quad N_{CaX_2} = 1 - N_{TYLX} \qquad [13]$$

A plot of ln K_V (Eqs. [10] or [11]) as a function of E_{TYLX} (Eq. [1] or [5]) provides a mechanism to determine true exchange equilibrium constant (K_{EX}) (Essington, 2015).

A mass balance was performed to determine the nonexchangeable concentration of adsorbed TYL. For initially Na^+- or Ca^{2+}-saturated clay, the mass of TYL added to the suspensions is determined from the blanks. The mass balance expression for TYL is (where m represents mmol): $m_{TYL_{total}} = m_{TYL_{aqueous}} + m_{TYL_{nonexchangeable}} + m_{TYL_{exchangeable}}$ where all m values except $m_{TYL_{nonexchangeable}}$ are directly measured. The total adsorbed TYL concentration is $q_{TYL} = \frac{m_{TYL_{total}}}{m_S}$ where m_S is the mass of the adsorbant in kg. An adsorption isotherm is a plot of the amount of TYL adsorbed by the surface (q in mmol kg^{-1}, y-axis) versus the total concentration of TYL in the equilibrium solution (C_{eq} in mmol L^{-1}, x-axis). Adsorption isotherms were generated for total adsorbed TYL, nonexchangeable TYL, and exchangeable TYL and are modeled using the constant partition equation:

$$q_{TYL} = K_P \, C_{eq} \qquad [14]$$

where q_{TYL} and C_{eq} are previously defined and K_P is the partition constant. K_P for each isotherm is generated using least square linear regression analysis.

RESULTS AND DISCUSSION

Binary Exchange Isotherms

For TYLX-NaX exchange, the exchange isotherm for both the surface and subsurface soils shows little to no preference for TYL^+ or Na^+ in the system (Figure C-3). This is an unexpected result as the STx-1 (Chapter 2) preferred TYL^+ over Na^+. There is a slight preference for TYL^+ when the system was initially Na-saturated while there was no preference to a slight preference for Na^+ when initially TYL-saturated. The ln K_V values for both soil depths are generally constant for the Na-saturated soils and changes little with increasing E_{TYLX} (Figure C-4, Figure C-5). However, as TYL decreases on the exchange phase, from E_{TYLX} of 0.5 to 0.1, the ln K_V for TYL-saturated at the 15-30 cm depth ranges from -0.5 to 1.5, and from -0.1 to 1.3 for the 30-46 depth.

For the TYLX-CaX exchange system for both depths, the exchange isotherm shows there is more TYL^+ on the exchange than predicted by the nonpreference isotherm (Figure C-5). This indicates the Loring soil prefers TYL^+ over Ca^{2+}. This is similar to what was found in Chapter 2 for the TYLX-CaX exchange on STx-1. The exchange selectivity (ln K_V) for the 15-30 cm and 30-46 cm depths decrease with increasing TYL on the exchange phase. For the Ca-saturated 15-30 cm depth ln K_V is 2.8 when E_{TYLX} is 0.05, the ln K_V linearly decreases to 1.2 as E_{TYLX} increases to 0.12 (Figure C-7). For the TYL-saturated 15-30 depth, ln K_V is 3.5 when E_{TYLX} is approximately 0.1, and ln K_V linearly decreases to 0 when E_{TYLX} is at 0.4 This trend is also seen with the Ca-saturated 30-46 cm depth for both Ca- and TYL-saturated systems (Figure C-8). The Ca-saturated ln K_V is 3.2 when E_{TYLX} is approximately 0.025 and then linearly decreases to 1.8 when E_{TYLX} is approximately 0.1. The TYL-saturated

ln K_V is 3.6 and linearly decreases to 0.4 E_{TYLX} increases from 0.4 to approximately 0.35.

Cation Exchange Capacity

The CEC was determined for the Loring soil exchange system as a function of exchange phase composition. The initially Na-saturated TYLX-NaX system had an average CEC of 10.3 $cmol_c\ kg^{-1}$ for the 15-30 cm depth and 15.8 $cmol_c\ kg^{-1}$ for the 30-46 cm depth (Figures C-9 and C-10). However, in the initially TYL-saturated systems the CEC decreases to 3.45 $cmol_c\ kg^{-1}$ in the 15-30 depth and 4.81 $cmol_c\ kg^{-1}$ in the 30-46 cm depths. The TYLX-CaX system had an average CEC of 46.6 $cmol_c\ kg^{-1}$ for the 15-30 cm depth and 37.4 $cmol_c\ kg^{-1}$ for the 30-46 cm depth (Figures C-11 and C-12). In the initially TYL-saturated TYLX-CaX system, the CEC was 4.08 cmolc kg-1 for 15-30 and 5.94 cmolc kg-1 for 30-46 cm depths. The CEC differed between the TYLX-NaX and TYLX-CaX systems due to the differing concentrations of exchangeable TYL. Within each depth, the CEC is generally constant with increasing TYL on the exchange phase. For the 15-30 cm depth in the TYLX-NaX systems, the CEC was 13.3 $cmol_c\ kg^{-1}$ when E_{TYLX} was less than 0.1 (Figure C-9). The CEC decreased slightly to 10.6 $cmol_c\ kg^{-1}$ and remained constant as E_{TYLX} increased to 0.4. For the 30-46 cm depth, the CEC was 18.6 $cmol_c\ kg^{-1}$ when E_{TYLX} was less than 0.1 (Figure C-10). As E_{TYLX} increased to 0.4, the CEC decreased slightly to 14.5 $cmol_c\ kg^{-1}$.

For the 15-30 cm depth in the TYLX-CaX systems, the CEC was 50.4 $cmol_c\ kg^{-1}$ when E_{TYLX} was 0.01 (Figure C-11). The CEC decreased slightly to 42.1 $cmol_c\ kg^{-1}$ as E_{TYLX} increased to 0.07. For the 30-46 cm depth, the CEC was generally constant.

When E_{TYLX} was 0.02, the CEC was 38.5 $cmol_c\ kg^{-1}$ and decreased slightly to 36.0 $cmol_c\ kg^{-1}$ when E_{TYLX} increased to 0.1 (Figure C-12).

Adsorption Isotherms

The adsorption isotherms were developed to illustrate total, exchangeable, and nonexchangeable forms of TYL for each exchange system at each soil depth. Isotherms were described using the constant partitioning model and the adsorption constants (K_P) are shown in Table C-4. For the TYLX-NaX exchange system, the amount of exchangeable TYL adsorbed increased with depth (Figures C-13 and C-14). The TYLX-CaX adsorption isotherms were similar to the TYLX-NaX system because exchangeable TYL increased with increasing depth (Figures C-15 and C-16). However, the increase of percentage was small as depth increased.

The partitioning model best fit the adsorption isotherms for both depths of TYLX-NaX and TYLX-CaX exchange systems except for the TYL nonexchangeable in the 30-46 cm of TYLX-CaX exchange system. The K_P values for TYL total and TYL exchangeable in the TYLX-NaX systems were 34 and 12.2 (15-30 cm depth) and 58 and 25 (30-46 cm depth), respectively. The K_P values for the TYL exchangeable in the TYLX-CaX systems were 19 and 11 (15-30 cm depth) and 26 and 16.4 (30-46 cm depth), respectively. The K_P values for the TYL total and TYL exchangeable increased as depth increased. However, with increasing cation charge of Na^+ to Ca^{2+}, the K_P values decreased for both TYL total and TYL exchangeable.

X-ray Diffraction Study for Binary Exchange

Loring soils are composed of smectite, interstratified smectite-mica, mica, and kaolinite. The intercalation of smectite by TYL is expected, as inferred from the STx-1 finding presented in Chapter 2, and because exchangeable TYL is a significant fraction of the total adsorbed. The intercalation of TYL into the soil smectite expanded the soil smectite d value to 2.7 nm (Figure C-17). This was only detectable in the TYLX-NaX system and when E_{TYLX} was greater than 0.2. In the Na-saturated soil clays, the d value shifted from 1.30 nm to approximately 2.7 nm when TYL^+ occupied 40% of the exchange complex. In the Ca-saturated soil clays, the d-value shifted from 1.45 nm to 1.6 nm when TYL^+ occupied 10% of the exchange complex (Figure C-18).

CONCLUSION

Tylosin participated in cation exchange on the surface and subsurface horizons of the Loring soil from west Tennessee. Similar to the findings in Chapter 2, exchange phase composition had little effect on the cation exchange capacity of both soil depths within a given exchange system. However, the CEC of initially TYL-saturated systems was significantly lower than initially Na- or Ca-saturated systems, indicating that TYL masks the CEC of the soil. In the TYLX-NaX system, neither Na^+ nor TYL^+ were preferred by the soil exchange phase, while in the TYL-CaX systems TYL^+ was preferred. This differed from the findings in Chapter 2 where for both TYLX-NaX and TYLX-CaX exchange systems, the STx-1 exchange surface preferred TYL^+. The Vaneslow selectivity coefficient did not vary with exchange phase composition in the TYLX-NaX system but did vary in the TYLX-CaX system. Adsorbed TYL was divided

into exchangeable and nonexchangeable forms and the adsorption isotherms were described by the partition model. Exchangeable TYL composed half of the total adsorbed in both depths of the TYLX-CaX system and the 30-46 cm depth in the TYLX-NaX system. Nonexchangeable TYL dominated the 15-30 cm depth in the TYLX-NaX system. The XRD study revealed the intercalation of TYL into the soil layers where more TYL intercalation occurred in the Na-saturated system compared to the Ca-saturated system.

Tylosin is generally thermodynamically preferred by the soil smectite exchange phase. The Vanselow selectivity coefficient (K_V) does not change with surface composition in the binary TYLX-NaX soil system; however, K_V is variable with composition in the TYLX-CaX soil system. Thus, in soil environments, which are commonly dominated by Ca^{2+}, K_V cannot be used as a predictive tool. Tylosin mobility in Ca-dominated soils is highly likely. However, the intercalation of tylosin into soil smectite interlayers may provide a level of protection for the tylosin molecule, reducing bioaccessibilty and increasing longevity in affected soils.

REFERENCES

Allaire, S. E., Del Castillo, J., and Juneau, V. (2006). Sorption kinetics of chlortetracycline and tylosin on sandy loam and heavy clay soils. Journal of Environmental Quality, 35, 969-972.

Essington, M. E. (2015). Soil and water chemistry: An integrative approach, 2nd ed. CRC press, Boca Raton.

Essington, M. E., Lee, J., and Seo, Y. (2010). Adsorption of antibiotics by montmorillonite and kaolinite. Soil Science Society of America Journal, 74(5), 1577-1588.

Gustafsson, J.P. (2014). Visual MINTEQ (Version 3.1). http://vminteq.lwr.kth.se/.

Jackson, M. L. (2005). Soil chemical analysis: advanced course. UW-Madison Libraries Parallel Press.

Kolpin, D. W., Furlong, E. T., Meyer, M. T., Thurman, E. M., Zaugg, S. D., Barber, L. B., and Buxton, H. T. (2002). Pharmaceuticals, hormones, and other organic wastewater contaminants in US streams, 1999-2000: A national reconnaissance. Environmental science & technology, 36(6), 1202-1211.

Kolz, A.C., Ong, S.K., and Moorman, T.B. (2005). Sorption of tylosin onto swine manure. Chemosphere, 60, 284-289.

Lee, J., Seo, Y., and Essington, M. E. (2014). Sorption and transport of veterinary pharmaceuticals in soil - a laboratory study. Soil Science Society of America Journal, 78(5), 1531-1543.

Sarmah, A.K., Meyer, M.T., Boxall, A.B.A. (2006). A global perspective on the use, sales, exposure pathways, occurrence, fate and effects of veterinary antibiotics (VAs) in the environment. Chemosphere. 65, 725-759.

Sassman, S. A., Sarmah, A. K., and Lee, L. S. (2007). Sorption of tylosin A, D, and Aaldol and degradation of tylosin A in soils. Environmental Toxicology and Chemistry, 26(8), 1629-1635.

Ter Laak, T.L., Gebbink, W.A., and Tolls, J. (2006). The effect of pH and ionic strength on the sorption of sulfachloropyridzine, tylosin, and oxytetracycline to soil. Environmental Toxicology and Chemistry, 25(4), 904-911.

APPENDIX C: Chapter 3 Tables and Figures

Table C-1: Particle size distribution of 15-30 cm and 30-46 cm Loring soil depth increments.

Sample	Avg Mean (µm)	Avg Median (µm)	Avg SD (µm)	Avg d10 (µm)	Avg d90 (µm)
15-30 cm soil	56.38	44.59	51.70	2.52	133.23
30-46 cm soil	78.52	71.35	55.69	6.01	158.63

Table C-2: Volume (in mL) ratios of tylosin and NaCl or $CaCl_2$ solutions added to each 50 mL tube of solid for 0.004 N.

Starting out Tyl-Saturated				Starting out NaCl or $CaCl_2$-Saturated			
Tyl-Na		Tyl-Ca		Tyl-Na		Tyl-Ca	
0.004 M Tyl	0.004 M NaCl	0.004 M Tyl	0.002 M $CaCl_2$	0.004 M Tyl	0.004 M NaCl	0.004 M Tyl	0.002 M $CaCl_2$
0	30	0	30	5	25	5	25
5	25	5	25	10	20	10	20
10	20	10	20	15	15	15	15
15	15	15	15	20	10	20	10
20	10	20	10	25	5	25	5
25	5	25	5	30	0	30	0

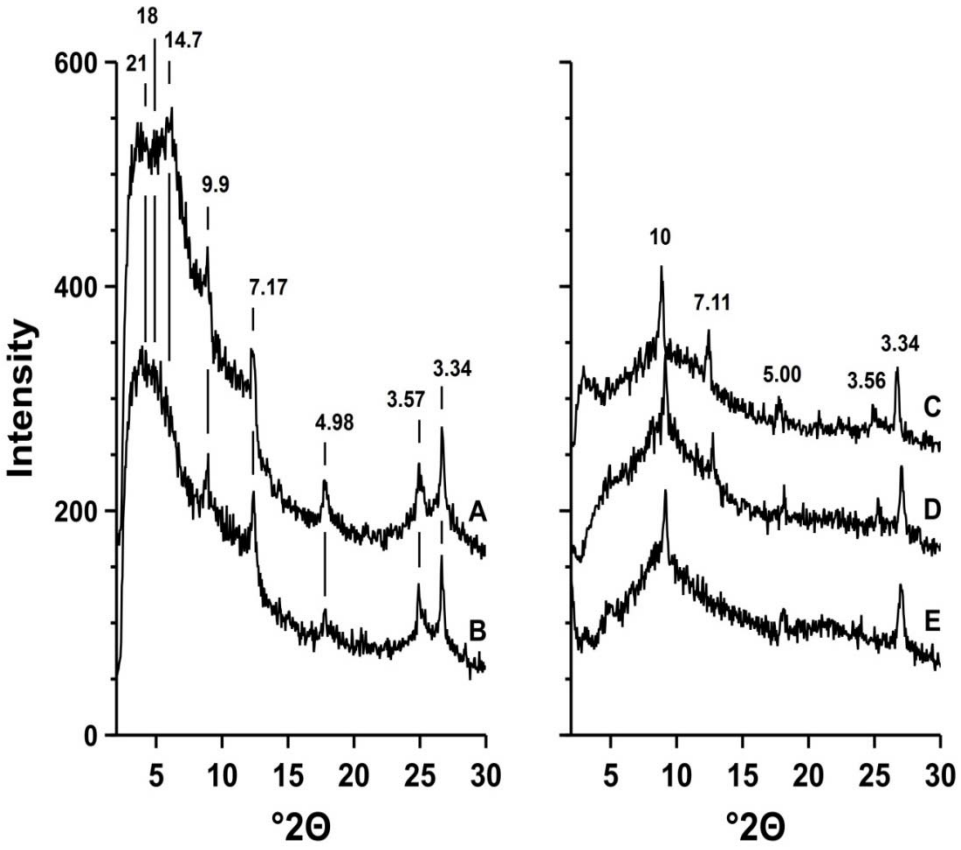

Figure C-1: X-ray mineralogy diffractograms of 15-30 cm depth Loring soil. (A) Mg-saturation, (B) Mg-glycol, (C) K-saturation, room temperature, (D) K-saturation, 300ºC, (E) K-saturation, 550ºC. Diffraction peaks are identified by their d values, in nm.

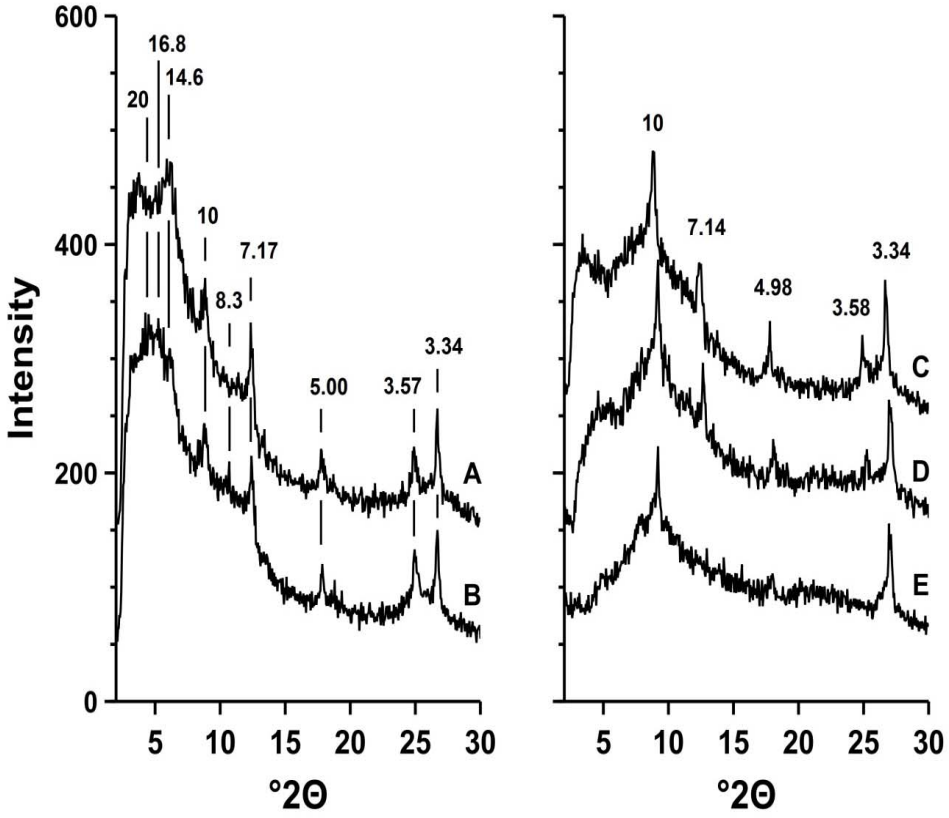

Figure C-2: X-ray mineralogy diffractograms of 30-46 cm depth Loring soil. (A) Mg-saturation, (B) Mg-glycol, (C) K-saturation, room temperature, (D) K-saturation, 300ºC, (E) K-saturation, 550ºC. Diffraction peaks are identified by their d values, in nm.

Table C-3: Aqueous speciation reactions and association constants (log K_F) values used in Visual MINTEQ.

Reaction	log K_f
$Ca^{2+} + Cl^- = CaCl^+$	0.4
$Ca^{2+} + H^+ + Tartrate^{2-} = CaHTartrate^+$	5.86
$Ca^{2+} + H_2O = CaOH^+ + H^+$	-12.697
$Ca^{2+} + Tartrate^{2-} = CaTartrate\ (aq)$	2.8
$2H^+ + Tartrate^{2-} = H_2Tartrate^0\ (aq)$	7.402
$H^+ + Tartrate^{2-} = HTartrate^-$	4.366
$H^+ + Tyl^- = HTyl^0$	7.5
$Na^+ + Cl^- = NaCl^0\ (aq)$	-0.3
$Na^+ + Tartrate^{2-} + H^+ = NaHTartrate^0\ (aq)$	4.58
$Na^+ + H_2O = NaOH^0\ (aq) + H^+$	-13.897
$Na^+ + Tartrate^{2-} = NaTartrate^-$	0.90
$H_2O = H^+ + OH^-$	-13.997

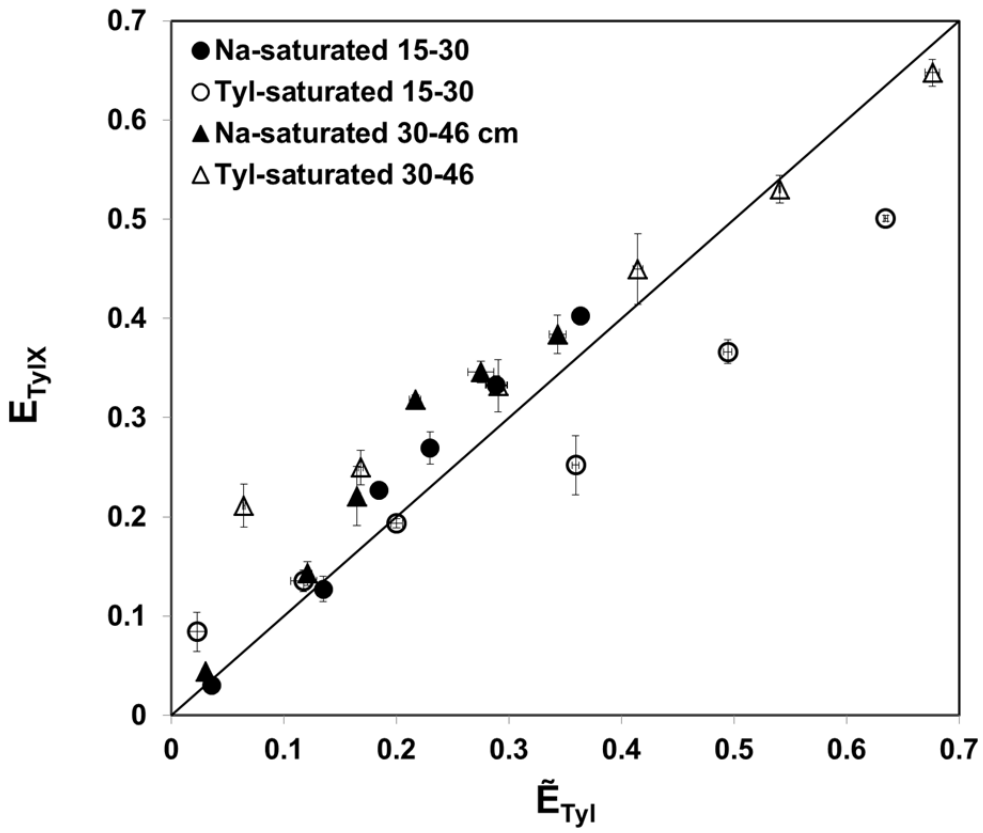

Figure C-3: Exchange isotherms of TYLX-NaX for 15-30 cm and 30-46 cm Loring soil.

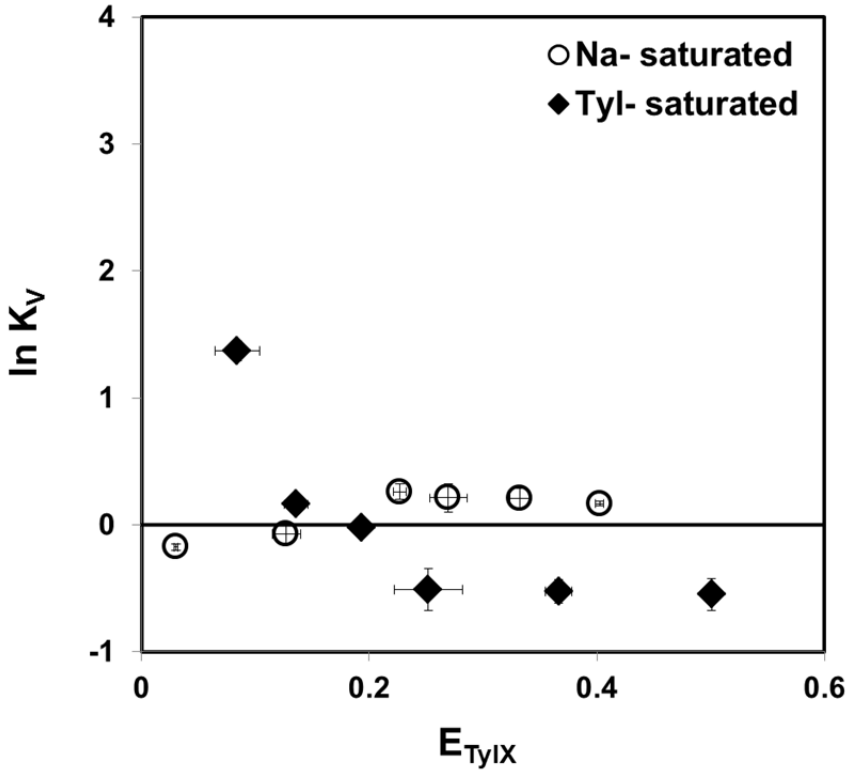

Figure C-4: Exchange selectivity and nonpreference line of TYLX-NaX for the 15-30 cm depth of Loring soil.

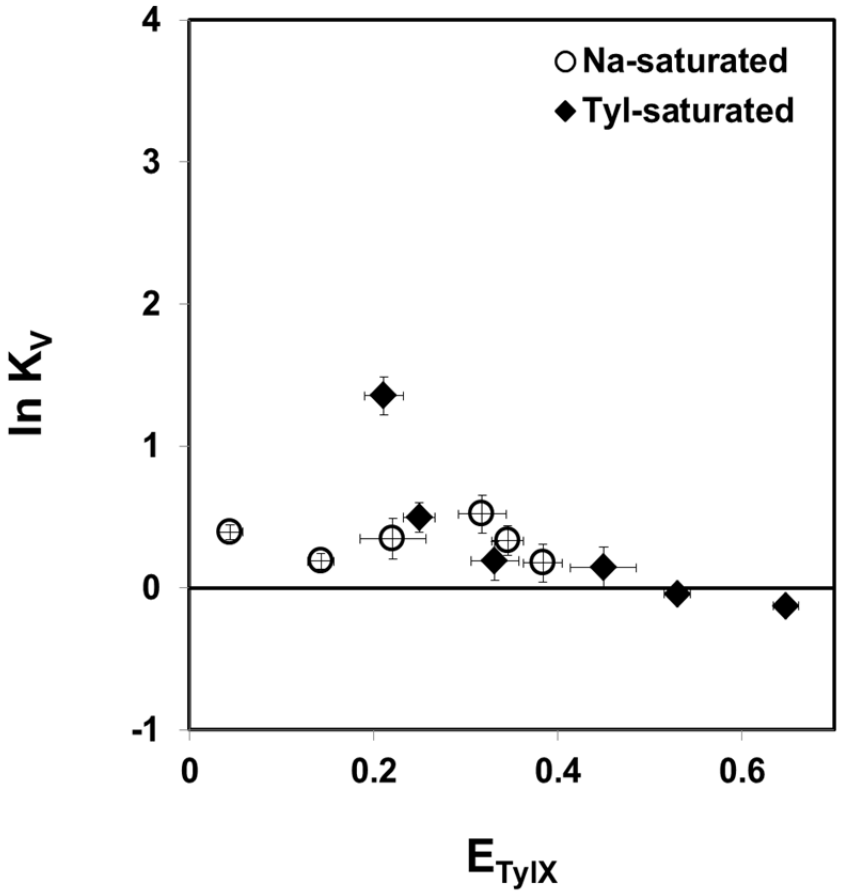

Figure C-5: Exchange selectivity and nonpreference line of TYLX-NaX for the 30-46 cm depth of Loring soil.

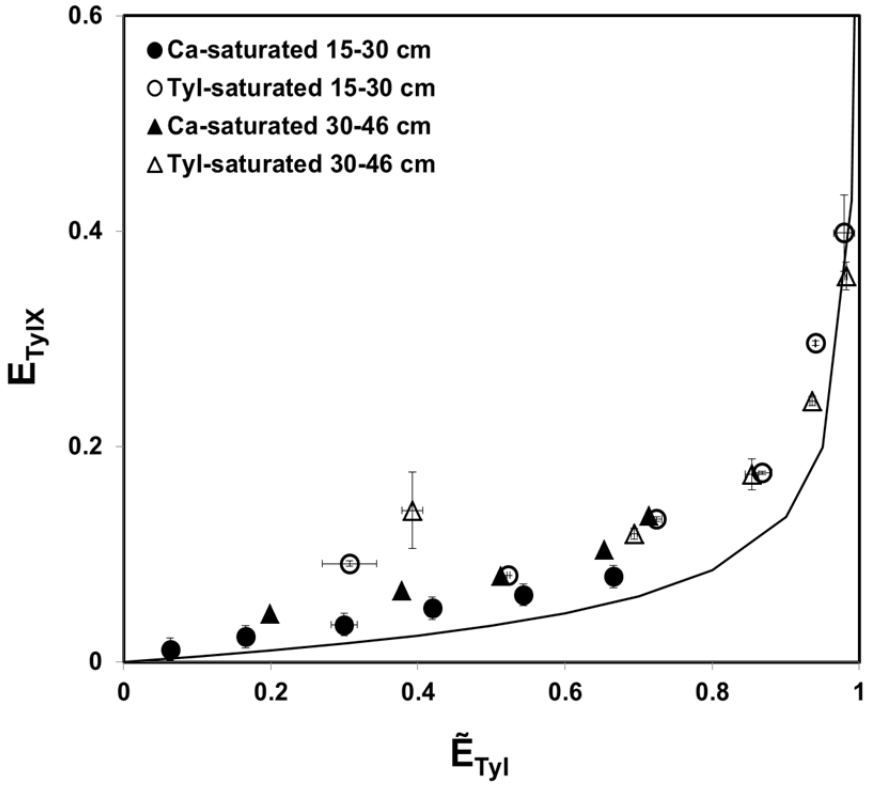

Figure C-6: Exchange isotherms of TYLX-CaX for 15-30 cm and 30-46 cm depths of Loring soil.

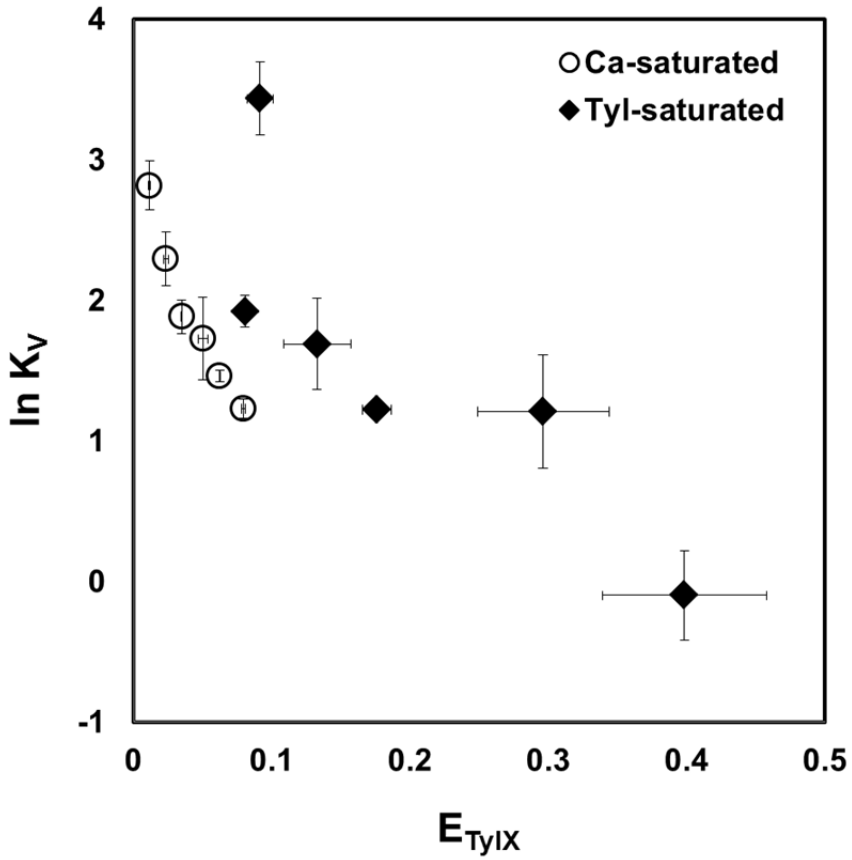

Figure C-7: Exchange selectivity of TYLX-CaX for 15-30 cm depth of Loring soil.

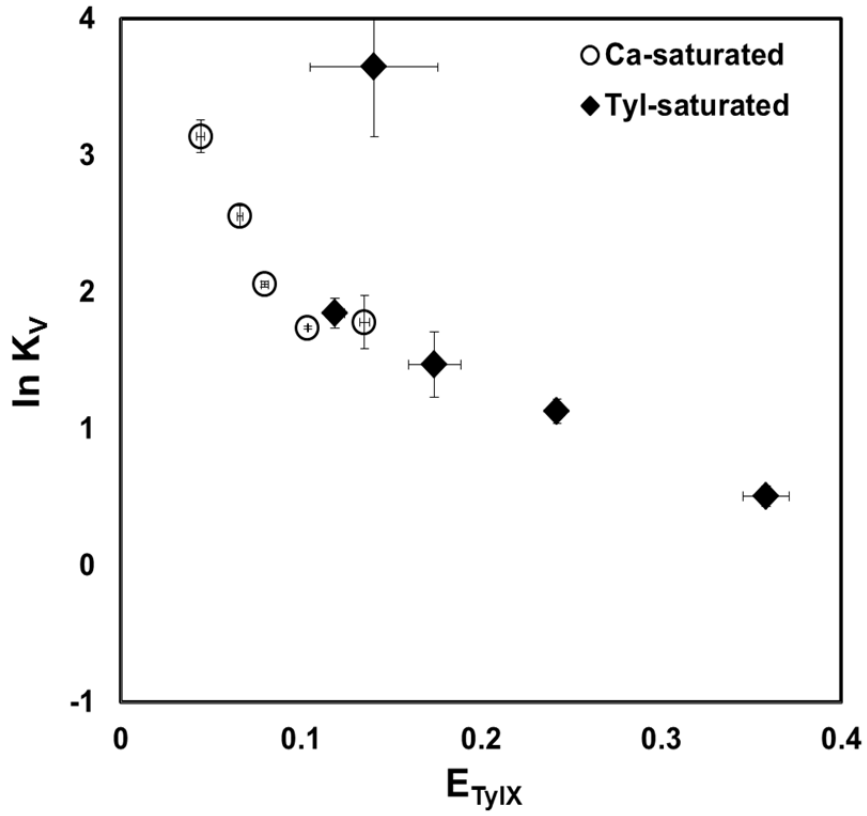

Figure C-8: Exchange selectivity of TYLX-CaX for 30-46 cm depth of Loring soil.

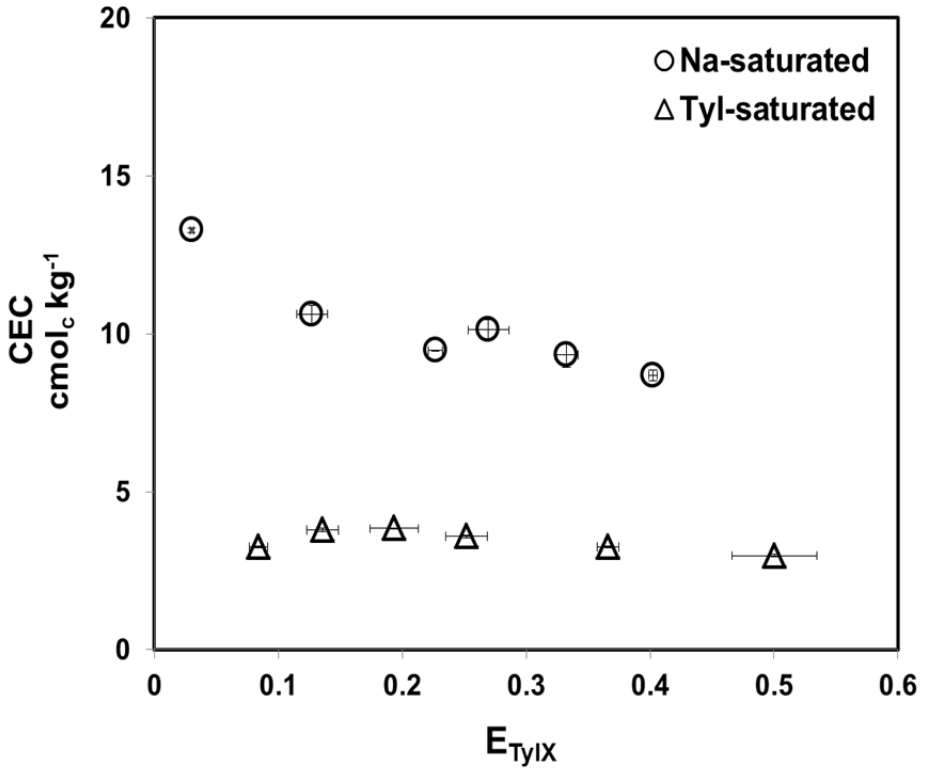

Figure C-9: Cation exchange capacity of TYLX-NaX for 15-30 cm depth of Loring soil.

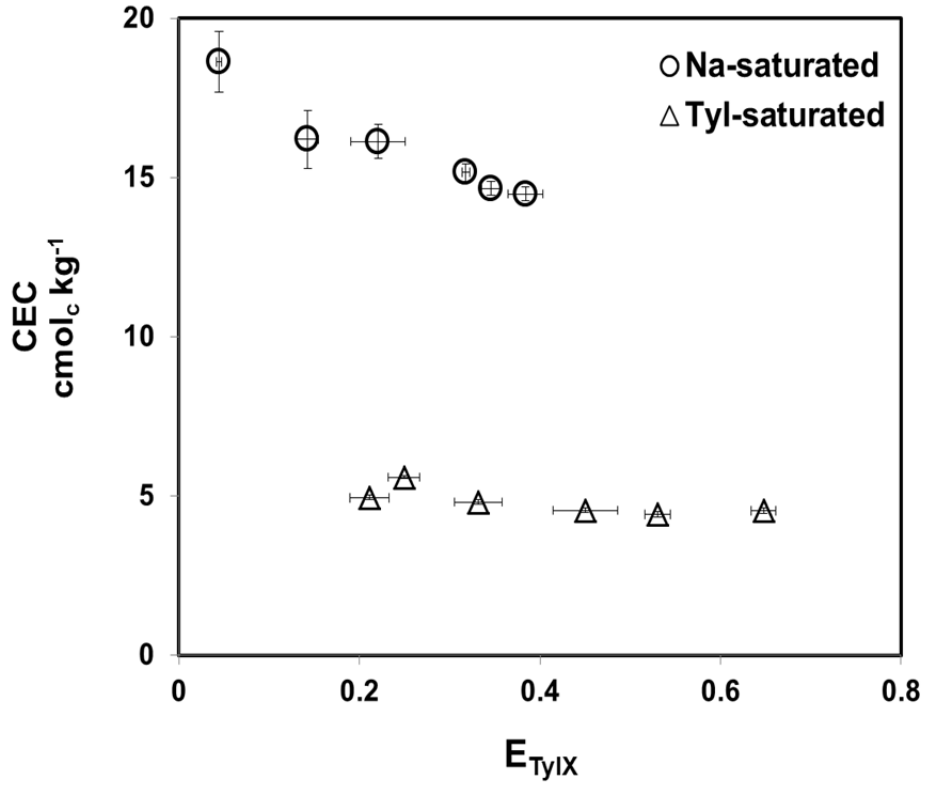

Figure C-10: Cation exchange capacity of TYLX-NaX for 30-46 cm depth of Loring soil.

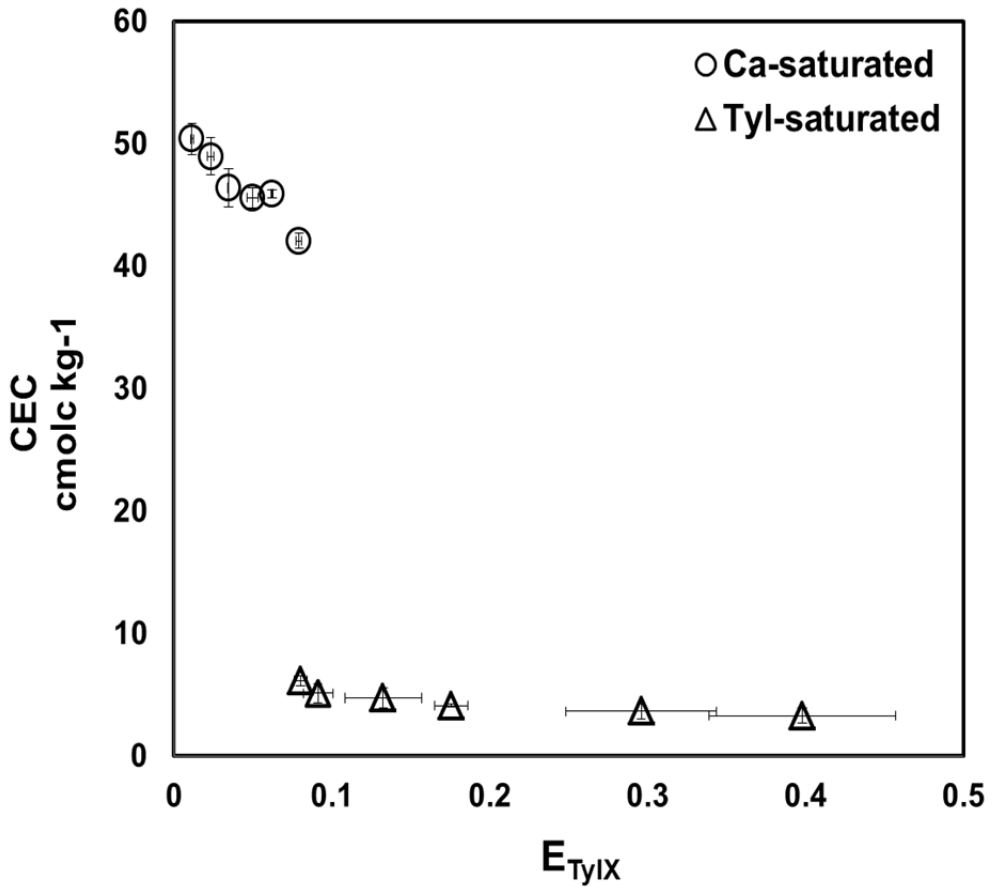

Figure C-11: Cation exchange capacity of TYLX-CaX for 15-30 cm depth of Loring soil.

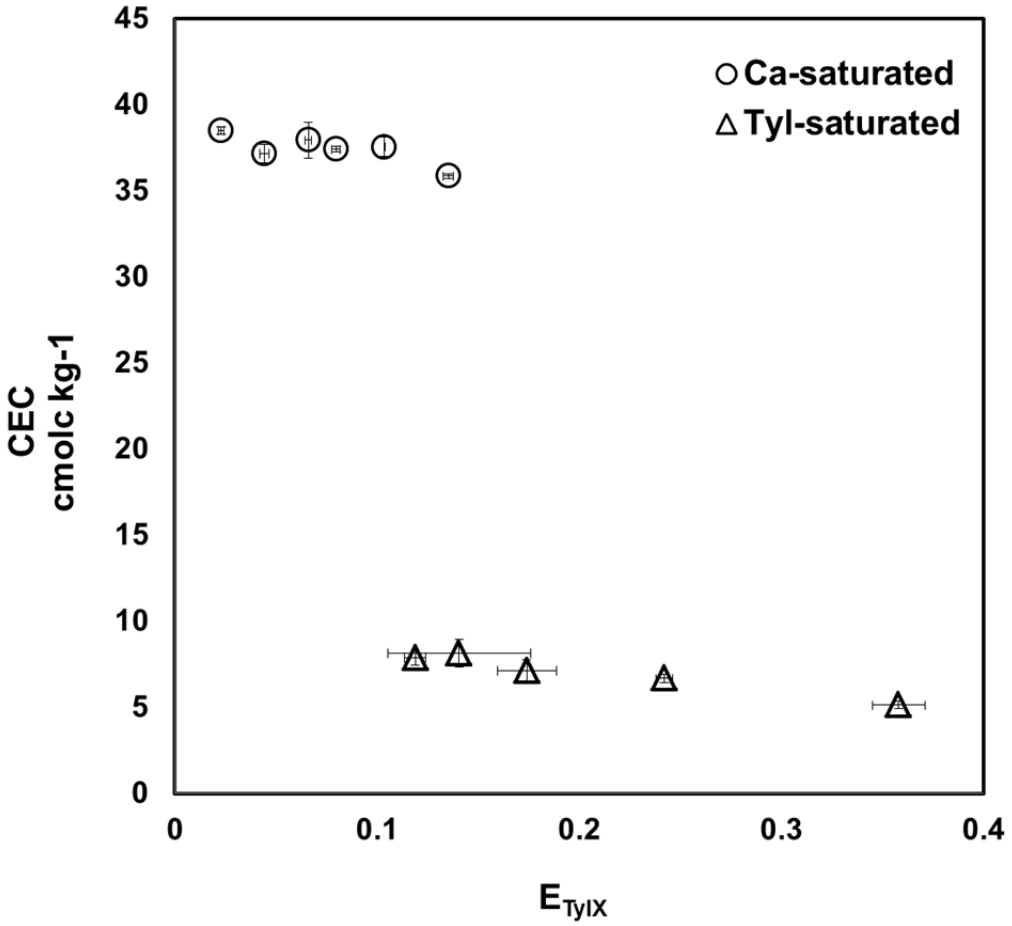

Figure C-12: Cation exchange capacity of TYLX-CaX for 30-46 cm depth of Loring soil.

Table C-4: Adsorption constants generated by applying the partition model to describe the tylosin adsorption isotherms for TYLX-NaX and TYLX-CaX of Loring soil systems.

Exchange	Tylosin	K_P	R^2
Na-saturated soil 15-30 cm depth	total	34	0.94
	exchangeable	12.2	0.98
	nonexchangeable	22	0.87
Na-saturated soil 30-46 cm depth	total	58.3	0.90
	exchangeable	25	0.92
	nonechangeable	33.5	0.83
Ca-saturated soil 15-30 cm depth	total	18.87	0.90
	exchangeable	10.67	0.99
	nonechangeable	8.20	0.31
Ca-saturated soil 30-46 cm depth	total	25.82	0.51
	exchangeable	16.42	0.96
	nonexchangeable	--	--

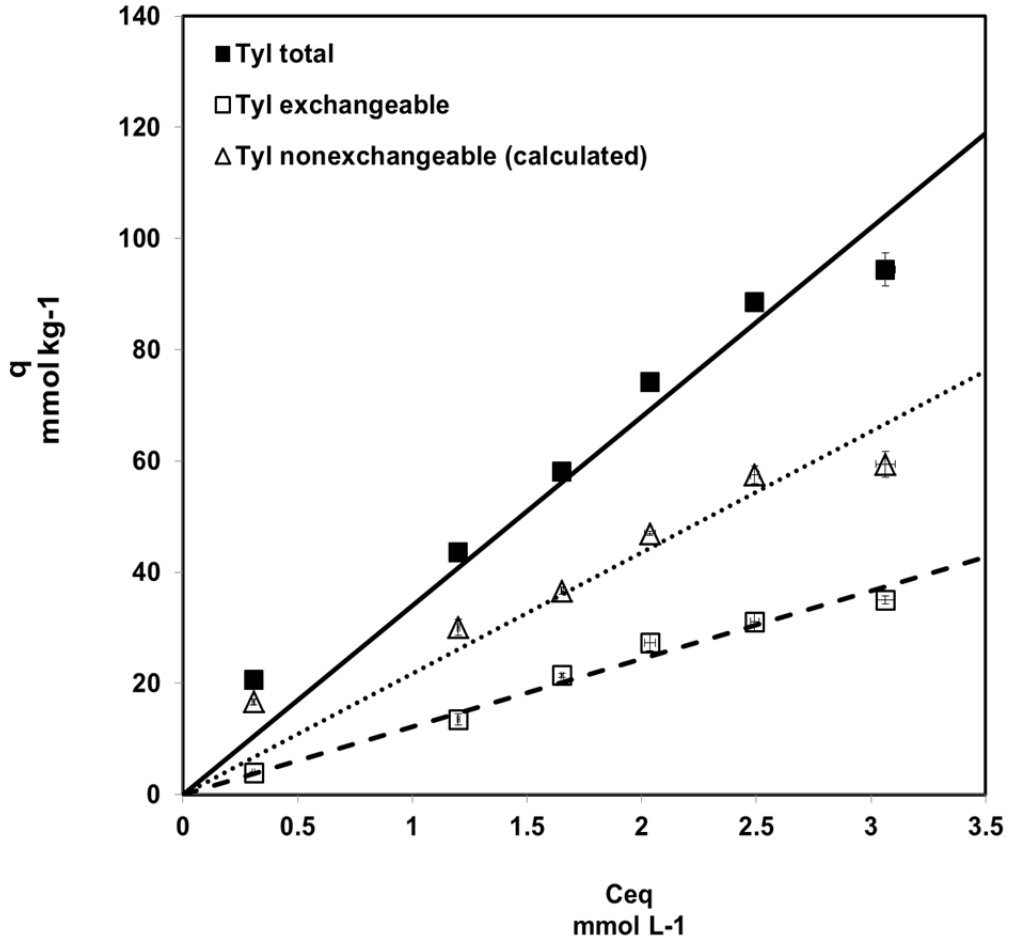

Figure C-13: Adsorption isotherms and partition model of TYLX-NaX for 15-30 cm depth of Loring soil.

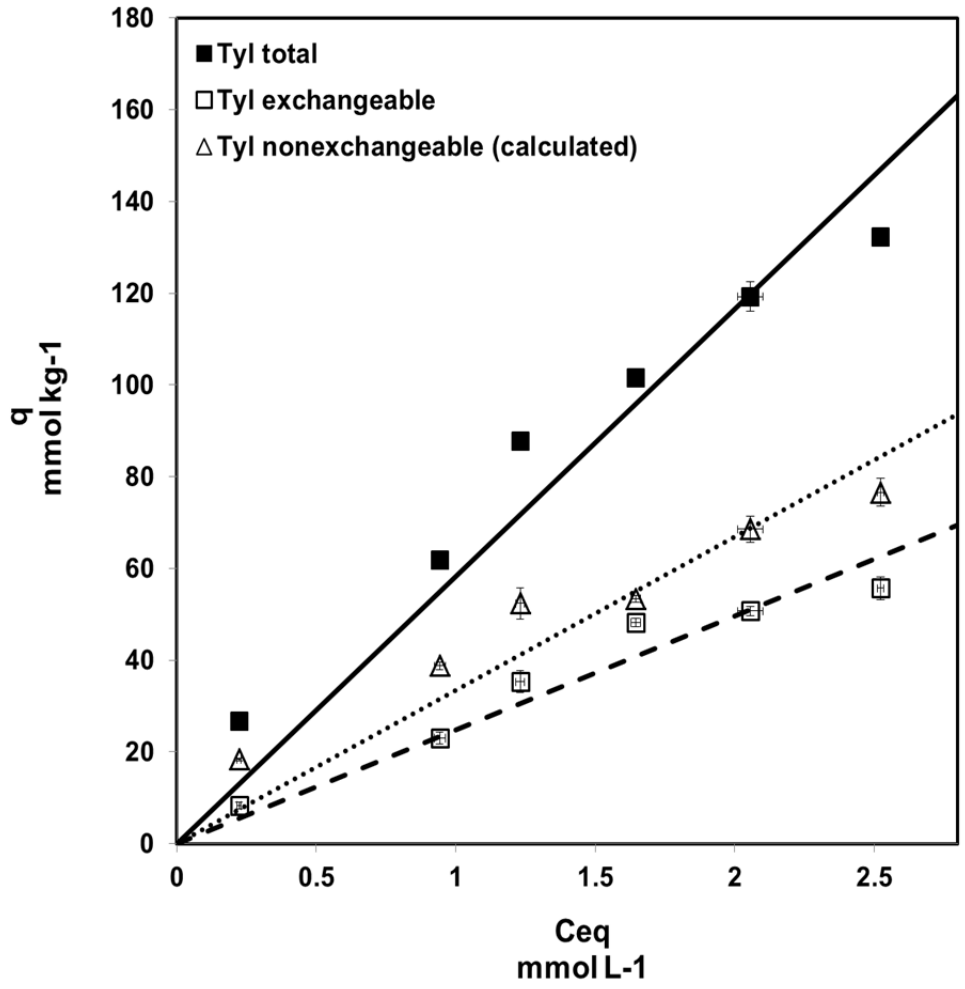

Figure C-14: Adsorption isotherms and partition model of TYLX-NaX for 30-46 cm depth of Loring soil.

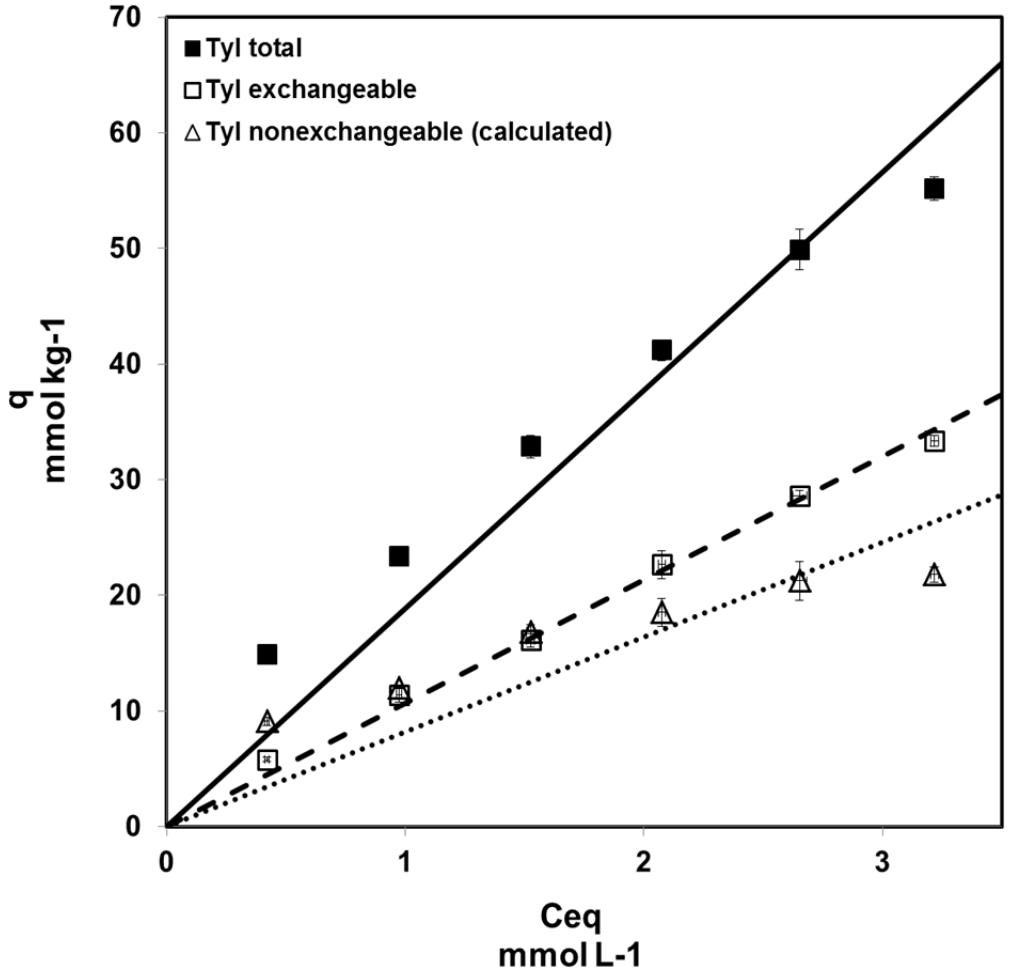

Figure C-15: Adsorption isotherms and partition model of TYLX-CaX for 15-30 cm depth of Loring soil.

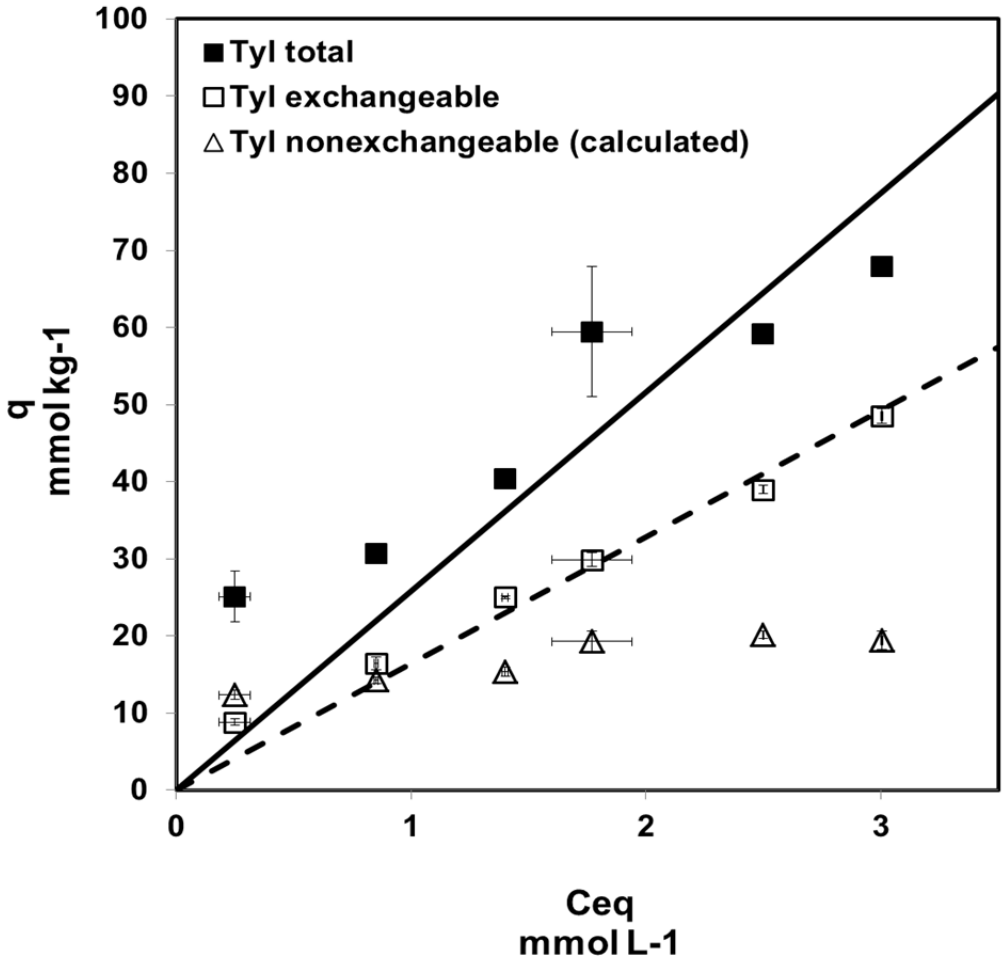

Figure C-16: Adsorption isotherms and partition model of TYLX-CaX for 30-46 cm depth of Loring soil.

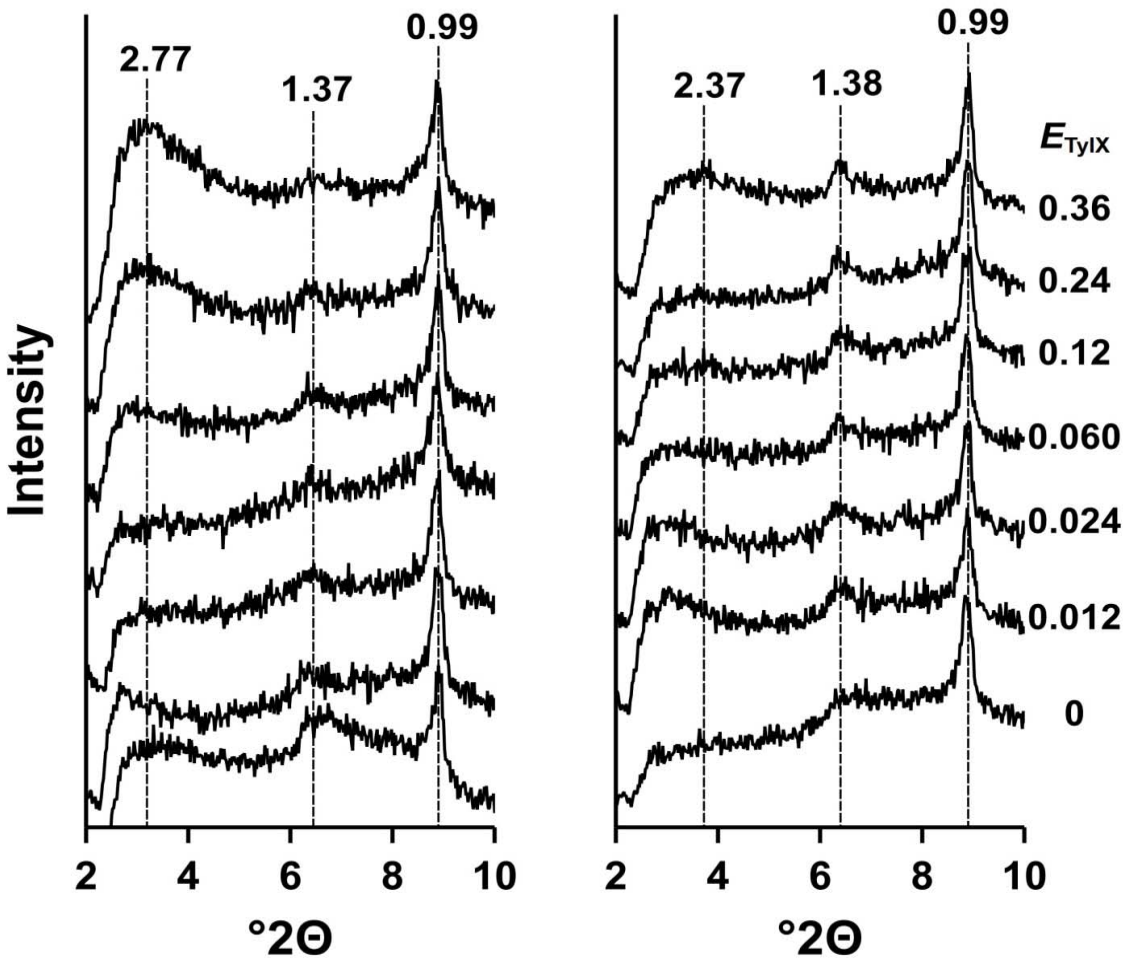

Figure C-17: X-ray diffractograms of TYLX-NaX for 15-30 cm and 30-46 cm depths of the Loring soil. The d-values of diffraction peaks are given in nm.

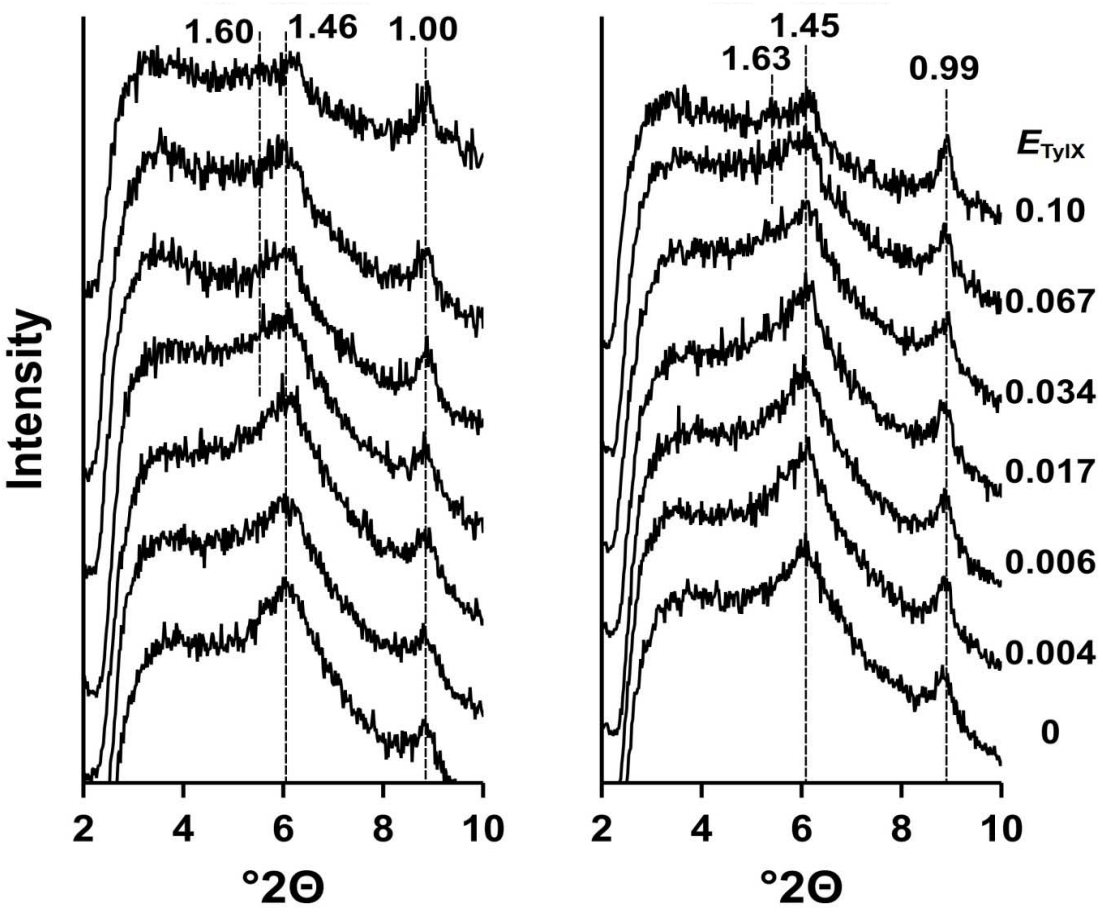

Figure C-18: X-ray diffractograms of TYLX-CaX for 15-30 cm and 30-46 cm depths of the Loring soil. The d-values of diffraction peaks are given in nm.

CHAPTER 4: SUMMARY

Tylosin is a commonly used veterinary antibiotic in animal husbandry that has been found in soil and water environments. The occurrence of TYL in the environment is generally associated with the use of manures as fertilizers. While the U.S. has recently regulated the use of veterinary antibiotics, extensive use as a prophylactic and growth promotor, coupled with inefficient animal metabolism, has resulted in environmental levels that may lead to the development of antibiotic resistant microorganisms.

Tylosin is a large organic molecule that develops a positive charge due to the protonation of a methylamine functional group in the pH range of soils. X-ray diffraction studies have shown large molecules like TYL can intercalate into clay mineral layers. Because of these unique characteristics and its potential mobility in the environment, TYL has been subject to adsorption studies on reference clay minerals and soils. Tylosin adsorption studies have examined TYL adsorption as a function of pH, ionic strength, background electrolyte type, and clay content and type. These studies have shown that an important adsorption mechanism for TYL appears to be outer sphere complexation, or cation exchange. Because TYL is exchangeable, common soil cations, such as Na^{+} and Ca^{2+}, would be in competition with TYL^{+} for the exchange surface.

The exchange selectivity of TYL was examined in the B2t horizons of a west Tennessee soil and in reference vermiculite and montmorillonite systems. Binary exchange isotherms involving TYL-Ca and TYL-Na were developed to establish exchange preference and to determine the distribution between exchangeable and

nonexchangeable forms of the adsorbed TYL. The exchange isotherms were modeled with the Vanselow selectivity coefficient to generate the exchange constant, K_V. Adsorption isotherms were modeled using the Freundlich and partition models to generate adsorption constants K_F and N, and K_P respectively. An XRD study was performed to examine the intercalation of TYL into clay layers.

Tylosin participated in cation exchange with the STx-1 reference clay and with the surface and subsurface depths of the Loring soil. The participation of TYL in cation exchange in the Libby vermiculite systems was minor; most likely due to its higher charged surface and limited layer expansion. Exchange equilibrium for TYL was reached after 2 h and constant total TYL adsorption was achieved by 12 h. For both the TYLX-NaX and TYLX-CaX STx-1 systems, TYL^+ was preferred over Na^+ and Ca^{2+}, contradicting studies that show bivalent cations are generally preferred over monovalent cations by montmorillonite. The Loring soil showed no preference for TYL in the surface 15 to 30 cm depth and minor preference in the subsurface 30-46 depth. The Vanselow selectivity coefficient varied with exchange phase composition for the STx-1 systems, while in the surface and subsurface Loring soils were more constant and less variable with exchange phase composition.

Adsorbed TYL was partitioned into exchangeable and nonexchangeable forms and described by either the Freundlich or partition isotherm. Exchangeable TYL contributed to half of the total adsorbed in both depths of the Loring soil for the TYLX-CaX system and the 30-46 cm depth in the TYLX-NaX system. Exchangeable TYL also dominated the TYLX-NaX system on STx-1. However, nonexchangeable TYL dominated the 15-30 cm depth in the TYLX-NaX system of the soil and in the TYLX-

CaX systems of STx-1. The introduction of a bivalent cation in the TYLX-CaX on STx-1 systems increased surface charge competition; therefore, exchangeable TYL was adsorbed less even though nonexchangeable TYL adsorption increased with surface coverage. The exchangeable TYL was modeled by the partition model for TYLX-NaX and TYLX–CaX exchange of the Loring soil systems. The exchangeable TYL was also modeled by the partition model for the TYLX-NaX STx-1 and 0.01 N TYLX-CaX STx-1 systems. For the 0.004 N TYLX-CaX STx-1 system, exchangeable TYL was modeled using the Freundlich. As total normality increased from 0.004 N to 0.01 N the Freundlich adsorption constant increased. The constant increased with a change in cation from Ca^{2+} to Na^{+},

X-ray diffraction illustrated the intercalation of TYL into the STx-1 and the Loring soil interlayers, with the d-value of the 00l plane increasing with increasing E_{TYLX}. Tylosin is adsorbed by reference montmorillonite clay and subsurface Loring soils by intercalation into the clay layers.

Tylosin is generally thermodynamically preferred by the smectite and soil exchange phase. The Vanselow selectivity coefficient (K_V) does not change with surface composition in the binary TYLX-NaX soil system; however, K_V is variable with composition in the TYLX-CaX soil system. Thus, in soil environments, which are commonly dominated by Ca^{2+}, K_V cannot be used as a predictive tool. The intercalation of tylosin into smectite interlayers may also provide a level of protection for the tylosin molecule, reducing bioaccessibilty and increasing longevity in affected soils.

LIST OF REFERENCES

Alcock, R. E., Sweetman, A., and Jones, K.C. (1999). Assessment of organic contaminant fate in waste water treatment plants; I: selected compounds and physiochemical properties. Chemosphere, 38 (10), 2247-2262.

Alexiades, C. A., and Jackson, M. L. (1965). Quantitative determination of vermiculite in soils. Soil Science Society of America Journal, 29, 522-527

Allaire, S.E., Del Castillo, J. and Juneau, V. (2006). Sorption kinetics of chlortetracycline and tylosin on sandy loam and heavy clay soils. Journal of Environmental Quality, 35, 969-972.

Aristilde, L., Landson, B., Miehe-Brendle, J., Marichal, C., and Laurent, C., (2016). Enhanced interlayer trapping of a tetracycline antibiotic within montmorillonite layers in the presence of Ca and Mg. Journal of Colloid and Interface Science, 464, 153-149.

Batchelder, A.R. (1982). Chlortetracycline and oxytetracycline effects on plant growth and development in soil systems. Journal of Environmental Quality, 11(4), 675-678.

Beausse, J. (2004). Selected drugs in solid matrices: a review of environmental determination, occurrence, and properties of principal substances. Trends in Analytical Chemistry, 23(10-11), 753-761.

Borden, D and Giese, R. F. (2001) Baseline studies of the clay minerals society source clays: cation exchange capacity measurements by the ammonia-electrode method. Clays and Clay Minerals 49 (50), 444-445.

Change, P.H., Li, Z., Jiang, W.T., and Jean, J.S. (2009). Adsorption and intercalation of tetracycline by swelling clay minerals. Applied Clay Science, 46, 27-36.

Chipera, S.J. and Bish, D. L. (2001) Baseline studies of the clay minerals society source clays: powder X-ray diffraction analyses. Clays and Clay Minerals 49(5), 398-409.

Cohen, M. L. (1998). Antibiotic use. In Antimicrobial Resistance: Issues and Options. Workshop Report. National Academy Press. Washington DC.

European Commission. (2003). Regulation (EC) No. 1831/2003 of the European Parliament and of the Council of 22 September 2003 on Additives for Use in Animal Nutrition.

Essington, M. E. (2015). Soil and water chemistry: An integrative approach, 2nd ed. CRC press, Boca Raton.

Essington, M. E., Lee, J., and Seo, Y. (2010). Adsorption of antibiotics by montmorillonite and kaolinite. Soil Science Society of America Journal, 74(5), 1577-1588.

Fejer, I., Mihaly, K., Istvan, E. and Dekany, I. (2002). Interaction of monovalent cationic drugs with montmorillonite. Colloid and Polymer Science, 280, 372-379.

Fish, B.J. and Carr, G.P.R. (1986). Pharmacopoeial procedure for the determination of tylosin factors by high-performance liquid chromatography. Journal of Chromatography, 353, 39-50.

Fitch, A., Du, J., Gan, H. and Stucki, J.W. (1995). Effect of clay charge on swelling: A clay-modified electrode study. Clays and clay minerals, 43(5), 607-614.

Fletcher, P., Sposito, G., and LeVesque, C.S. (1984). Sodium-calcium-magnesium exchange reactions on a montmorillonitic soil: I: Binary exchange reactions. Soil Science Society of America Journal, 48(5), 1016-1021.

Gustafsson, J.P. (2014). Visual MINTEQ (Version 3.1). http://vminteq.lwr.kth.se/.

Jackson, M. L. (2005). Soil chemical analysis: advanced course. UW-Madison Libraries Parallel Press.

Halling-Sorensen, B., Nors Nielson, S., Lanzky, P.F., Ingerslev, F., Holten Lutzhoft, H.C., and Jorensen, S.E. (1998). Occurrence, fate, and effects of pharmaceutical substances in the environment – a review. Chemosphere, 36, 357-393.

Harris, S.J., Cormican, M., and Cummins E. (2012). Antimicrobial residues and antimicrobial-resistant bacteria: impact on the microbial environment and risk to human health – a review. Human and Ecological Risk Assessment, 18, 767-809.

Hou, Y., Wu, P., Huang, Z., Ruan, B., Liu, P., and Zhu, N. (2014). Successful intercalation of DNA into CTAB-modified clay minerals for gene protection. Journal of Materials Science, 49(20), 7273-7281.

Hsu, P.H. and Bates, T.F. (1964). Fixation of hydroxy-aluminum polymers by vermiculite. Soil Science Society of America Journal, 28(6), 763-769.

Hu, D., and Coats, J. R. (2009). Laboratory evaluation of mobility and sorption for the veterinary antibiotic, tylosin, in agricultural soils. Journal of Environmental Monitoring, 11(9), 1634-1638.

Kaur, M. and Datta, M. (2013). Adsorption equilibrium and kinetics of toxic dye-erythrosine B adsorption onto montmorillonite. Separation Science and Technology, 38, 1370-1381.

Kedzierski, M., Janiszewska, J., and Moszumanska, I. (2016). Dendrimeric peptide – montmorillonite intercalation compound. Polimery, 61(10), 677-682.

Kemper, N. (2008). Veterinary antibiotics in the aquatic and terrestrial environment. Ecological Indicators, 8(1), 1-13.

Kolpin, D. W., Furlong, E. T., Meyer, M. T., Thurman, E. M., Zaugg, S. D., Barber, L. B., and Buxton, H. T. (2002). Pharmaceuticals, hormones, and other organic wastewater contaminants in US streams, 1999-2000: A national reconnaissance. Environmental Science & Technology, 36(6), 1202-1211.

Kolz, A.C., Ong, S.K., and Moorman, T.B. (2005). Sorption of tylosin onto swine manure. Chemosphere, 60, 284-289.

Kumar, K., Gupta, S.C., Baidoo, S.K., Chander, Y., and Rosen, C.J. (2005). Antibiotic uptake by plants from soil fertilized with animal manure. Journal of Environmental Quality, 34, 2082-2085.

Kummerer, K. (2003). Significance of antibiotics in the environment. Journal of Antimicrobial Chemotherapy, 52(1), 5-7.

Lee, J., Seo, Y., and Essington, M. E. (2014). Sorption and transport of veterinary pharmaceuticals in soil - a laboratory study. Soil Science Society of America Journal, 78(5), 1531-1543.

Levy, S.B. (1992) The antibiotic paradox. Plenum Press, New York.

Loke, M-L., Tjornelund, J., and Halling-Sorensen, B. (2002). Determination of the distribution coefficient (log K_d) of oxytetracycline, tylosin A, olaquindox and metronidazole in manure. Chemosphere, 48, 351-361.

Lv, G., Li, Z., Jiang, W.T., Change, P.H., and Liao, L. (2015). Interlayer configuration of ionic liquids in a ca-montmorillonite as evidenced by FTIR, TG-DTG, and XRD analyses. Materials Chemistry and Physics, 162, 417-424.

Madsen, F. T. (1977). Surface area measurements of clay minerals by glycerol sorption on a thermobalance. Thermochimica Acta, 21, 89-93.

Malekani, K., Rice, J.A., and JAR-SYoNG, L.I.N. (1996). Comparison of techniques for determing the fractal dimensions of clay minerals. Clays and clay minerals, 44(5), 677-685.

McFarland, J.W., Berger, C.M., Froshauer, S.A., Hayashi, S. F., Hecker, S.J., Jaynes, B.H., Jefson, M.R., Kamicker, B.J., Lipinski, C.A., Lundy, K.M., Reese, C.P., and Vu, C.B. (1997). Quantitative structure - activity relationships among macrolide antibacterial agents: in vitro and in vivo potency against Pasteurella multocida. Journal of Medicinal Chemistry, 40 (9), 1340-1346.

Mercier, L. and Detellier, C. (1994). Intercalation of tetraalkylammonium cations into smectites and its application to internal surface area measurements. Clays and Clay Minerals, 42, 71-76.

Michelini, L., Reichel, R., Werner, W., Ghisi, R., and Thiele-Bruhn, S. (2012). Sulfadiazine uptake and effects on *Salix fragilis* L. and *Zea mays* L. plants. Water, Air, and Soil Pollution, 223, 5243-5257.

Parolo, M.E., Savini, M.C., Valles, J.M., Baschini, M.T., and Avena, M.J. (2008). Tetracycline adsorption on montmorillonite: pH and ionic strength effects. Applied Clay Science, 40, 179-186.

Porubcan, L.S., Serna, C.J., White, J.L., and Hem, S.L. (1977). Mechanism of adsorption of clindamycin and tetracycline by montmorillonite. Journal of Pharmaceutical Sciences, 67(8), 1081-1087.

Sarmah, A.K., Meyer, M.T., Boxall, A.B.A. (2006). A global perspective on the use, sales, exposure pathways, occurrence, fate and effects of veterinary antibiotics (VAs) in the environment. Chemosphere. 65, 725-759.

Sassman, S. A., Sarmah, A. K., and Lee, L. S. (2007). Sorption of tylosin A, D, and Aaldol and degradation of tylosin A in soils. Environmental Toxicology and Chemistry, 26(8), 1629-1635.

Sposito, G., Holtzclaw, K. M., Jouany, C., and Charlet, L. (1983). Cation selectivity in sodium-calcium, sodium-magnesium, and calcium-magnesium exchange on Wyoming bentonite at 298 K. Soil Science Society of America Journal, 47(5), 917-921.

Sun, Z., Park, Y., Zheng, S., Ayoko, G.A., and Frost, R.L. (2013). XRD, TEM, and thermal analysis of Arizona ca-montmorillonite modified with didodecyldimethylammonium bromide. Journal of Colloid and Interface Science, 408, 75-81.

Ter Laak, T.L., Gebbink, W.A., and Tolls, J. (2006). The effect of pH and ionic strength on the sorption of sulfachloropyridzine, tylosin, and oxytetracycline to soil. Environmental Toxicology and Chemistry, 25(4), 904-911.

Teuber, M., 1999. Spread of antibiotic resistance with food-borne pathogens. Cell Mol. Life Sci. 56, 755–763.

Teuber, M., 2001. Veterinary use and antibiotic resistance. Curr. Opin. Mikrobiol. 4, 493–499.

Thiele-Bruhn, S. (2003). Pharmaceutical antibiotic compounds in soils - a review. Plant Nutrition and Soil Science, 166, 145-167.

U.S. Food and Drug Administration. (2015). Veterinary Feed Directive, 80 FR 31707 (3 June 2015). Federal Register: The Daily Journal of the United States. Web. 25 January 2017.

Wang, C.J, Li, Z., Jiang, W.T., Jean, J.S., and Liu, C.C. (2010). Cation exchange interaction between antibiotic ciprofloxacin and montmorillonite. Journal of Hazardous Materials, 183, 309-314.

Wang, Q. and Yates, S.R. (2008). Laboratory study of oxytetracycline degradation kinectics in animal manure and soil. Journal of Agricultural and Food Chemistry, 56, 1683-1688.

APPENDIX D: EXPERIMENTAL RAW DATA

Table D-1: Raw data for the Na-saturated TYLX-NaX STx-1 system.

Sample	NaX ppm	NaX*df	TylX mM	TylX µM*df	Na+ ppm	Na+*df	Tyl+ µM	Tyl mM*df
1	3.2933	6.5866	347.938	695.876	15.680	78.4	207.713	1038.565
2	3.6463	7.2926	311.327	622.654	16.486	82.43	152.018	760.09
3	5.3377	10.6754	247.064	494.128	17.824	89.12	110.506	552.53
4	6.8448	13.6896	172.129	344.258	18.264	91.32	84.327	421.635
5	7.8095	15.619	98.011	196.022	19.936	99.68	51.777	258.885
6	8.8903	17.7806	36.51	73.02	19.696	98.48	24.446	122.23
7	3.3068	6.6136	346.232	692.464	15.165	75.825	235.085	1175.425
8	3.9481	7.8962	321.428	642.856	16.386	81.93	157.543	787.715
9	4.6293	9.2586	255.686	511.372	17.355	86.775	115.679	578.395
10	6.7966	13.5932	173.429	346.858	18.156	90.78	77.374	386.87
11	8.534	17.068	97.534	195.068	18.272	91.36	39.225	196.125
12	9.266	18.532	36.801	73.602	18.961	94.805	21.933	109.665
13	3.3781	6.7562	376.264	752.528	15.161	75.805	239.066	1195.33
14	4.706	9.412	321.572	643.144	17.119	85.595	145.392	726.96
15	5.6986	11.3972	248.47	496.94	17.949	89.745	110.735	553.675
16	6.9907	13.9814	167.411	334.822	19.179	95.895	76.5	382.5
17	8.0596	16.1192	100.883	201.766	19.226	96.13	50.372	251.86
18	9.0289	18.0578	35.938	71.876	19.704	98.52	24.732	123.66
					2.8537	14.2685	805.704	4028.52
					5.5511	27.7555	654.359	3271.795
					8.3073	41.5365	539.96	2699.8
	amt. Tyl	pH	pH av	Tyl+	11.193	55.965	406.869	2034.345
	30	6.40	6.279072	94.3282942	13.278	66.39	275.206	1376.03
	30	6.29			16.038	80.19	137.586	687.93
	30	6.37			2.9218	14.609	825.35	4126.75
	30	6.13			5.7668	28.834	692.317	3461.585
	5	6.43			8.5715	42.8575	542.923	2714.615
	5	6.16			11.157	55.785	420.448	2102.24
	5	6.24			13.578	67.89	273.158	1365.79
	5	6.31			16.707	83.535	137.946	689.73

Table D-2: Raw data for the TYL-saturated TYLX-NaX STx-1 system.

Sample	NaX ppm	NaX*10df	TylX mM	TylX µM*20df	Sample	pH	Na+ ppm	Na+*10df	Tyl+ µM	Tyl mM*10df
1	16.985	169.85	10.19101	203.8202	1	6.04	3.725	37.25	22.85943	228.5943
2	26.849	268.49	14.67291	293.4582	2	6	3.359	33.59	44.17296	441.7296
3	34.683	346.83	19.37396	387.4792	3	6.53	2.889	28.89	74.20499	742.0499
4	38.497	384.97	20.55583	411.1166	4	6.33	2.487	24.87	105.23199	1052.3199
5	42.847	428.47	22.10154	442.0308	5	6.5	1.942	19.42	153.72532	1537.2532
6	43.428	434.28	22.53033	450.6066	6	6.52	1.407	14.07	189.68626	1896.8626
7	20.688	206.88	11.59583	231.9166	7	6.09	3.782	37.82	25.2603	252.603
8	29.966	299.66	16.01201	320.2402	8	6.09	3.411	34.11	47.04704	470.4704
9	34.857	348.57	18.89604	377.9208	9	6.11	3.006	30.06	76.51334	765.1334
10	38.898	388.98	21.26826	425.3652	10	6.23	2.519	25.19	110.06024	1100.6024
11	42.407	424.07	21.99224	439.8448	11	6.66	1.989	19.89	158.97437	1589.7437
12	42.847	428.47	22.19999	443.9998	12	6.53	1.442	14.42	192.24038	1922.4038
13	20.871	208.71	11.5312	230.624	13	6.07	3.88	38.8	26.00416	260.0416
14	29.008	290.08	15.29482	305.8964	14	6.17	3.579	35.79	46.83264	468.3264
15	35.295	352.95	19.63284	392.6568	15	6.23	3.11	31.1	78.72897	787.2897
16	40.429	404.29	20.75642	415.1284	16	6.69	2.092	20.92	112.08586	1120.8586
17	40.692	406.92	21.92061	438.4122	17	6.39	2.118	21.18	156.86698	1568.6698
18	43.828	438.28	43.828	438.28	18	6.53	1.549	15.49	203.62503	2036.2503
					19		4.881	48.81	0	0
					20		4.225	42.25	54.54681	545.4681
					21		3.578	35.78	102.21606	1022.1606
					22		2.954	29.54	147.99888	1479.9888
					23		2.338	23.38	194.26487	1942.6487
					24		1.726	17.26	245.72731	2457.2731
					25		5.007	50.07	0	0
					26		4.672	46.72	55.40238	554.0238
					27		4.027	40.27	103.00975	1030.0975
					28		3.377	33.77	152.28254	1522.8254
					29		2.728	27.28	193.11926	1931.1926
					30		2.042	20.42	241.61448	2416.1448

Table D-3: Raw data for the Ca-saturated 0.004 total normality TYLX-CaX STx-1 system.

Sample	CaX ppm	CaX*2df	TylX mM	TylX µM*2df	Sample	Ca2+ ppm	Ca2+*5df	Tyl+ µM	Tyl mM*5df	pH
1	14.61	29.22	93.188	186.376	1	8.008	40.04	366.22	1831.1	6.16
2	15.84	31.68	80.587	161.174	2	9.958	49.79	295.88	1479.4	6.25
3	16.62	33.24	64.239	128.478	3	11.32	56.6	224.74	1123.7	
4	17.64	35.28	48.31	96.62	4	13.09	65.45	138.46	692.3	
5	18.17	36.34	31.851	63.702	5	14.83	74.15	63.173	315.865	
6	19.06	38.12	11.101	22.202	6	15.71	78.55	10.177	50.885	
7	11.43	22.86	94.402	188.804	7	7.763	38.815	379.94	1899.7	
8	15.67	31.34	84.226	168.452	8	10.41	52.05	169.85	849.25	
9	14.16	28.32	61.965	123.93	9	11.15	55.75	230.56	1152.8	
10	15.55	31.1	51.917	103.834	10	12.78	63.9	143.84	719.2	
11	16.05	32.1	32.711	65.422	11	14.58	72.9	64.284	321.42	
12	16.78	33.56	11.16	22.32	12	15.44	77.2	9.94	49.7	
13	12.27	24.54	97.969	195.938	13	7.739	38.695	392.98	1964.9	
14	13.04	26.08	80.037	160.074	14	9.377	46.885	308.38	1541.9	
15	14.14	28.28	63.995	127.99	15	11.37	56.85	228.45	1142.25	
16	14.83	29.66	48.578	97.156	16	13.02	65.1	142.15	710.75	
17	16.89	33.78	32.085	64.17	17	14.5	72.5	56.527	282.635	
18	16.72	33.44	10.971	21.942	18	15.33	76.65	10.102	50.51	
					19	0	0	825.97	4129.85	
					20	2.562	12.81	705.35	3526.75	
					21	5.183	25.915	546.08	2730.4	
					22	7.984	39.92	412.89	2064.45	
					23	10.87	54.35	280.28	1401.4	
					24	13.48	67.4	137.43	687.15	
					25	0	0	838.17	4190.85	
					26	2.619	13.095	690.5	3452.5	
					27	5.28	26.4	560.03	2800.15	
					28	8.021	40.105	410.47	2052.35	
					29	10.56	52.8	275.42	1377.1	
					30	13.58	67.9	136.92	684.6	

Table D-4: Raw data for the TYL-saturated 0.004 total normality TYLX-CaX STx-1 system.

Sample	CaX ppm	CaX*5df	TylX mM	TylX µM*20df	Sample	pH	Ca2+ ppm	Ca2+*10df	Tyl+ µM	Tyl mM*10df
1	3.517	17.585	9.347	186.94	1	5.18	2.755	27.55	107.11	1071.1
2	3.498	17.49	13.127	262.54	2	5.71	1.592	15.92	156.923	1569.23
3	3.102	15.51	17.697	353.94	3	6.01	0.801	8.01	212.544	2125.44
4	2.869	14.345	22.331	446.62	4	6.17	0.183	1.83	275.79	2757.9
5	2.613	13.065	26.596	531.92	5	6.3	0.05	0.5	348.822	3488.22
6	2.338	11.69	29.349	586.98	6	6.34	0.05	0.5	398.927	3989.27
7	3.859	19.295	9.804	196.08	7	5.24	2.701	27.01	114.064	1140.64
8	3.504	17.52	13.508	270.16	8	6.24	1.574	15.74	164.757	1647.57
9	3.251	16.255	15.306	306.12	9	6.05	0.886	8.86	223.925	2239.25
10	2.933	14.665	20.793	415.86	10	6.21	0.101	1.01	281.288	2812.88
11	2.71	13.55	25.787	515.74	11	6.29	0.05	0.5	352.381	3523.81
12	2.323	11.615	30.257	605.14	12	6.36	0.05	0.5	422.098	4220.98
13	3.56	17.8	9.101	182.02	13	5.26	2.648	26.48	111.192	1111.92
14	3.391	16.955	12.237	244.74	14	6.12	1.472	14.72	173.624	1736.24
15	3.206	16.03	16.044	320.88	15	6.05	0.793	7.93	237.689	2376.89
16	3.001	15.005	20.847	416.94	16	6.14	0.191	1.91	291.508	2915.08
17	2.609	13.045	25.515	510.3	17	6.45	0.05	0.5	344.068	3440.68
18	2.259	11.295	29.585	591.7	18	6.43	0.05	0.5	427.127	4271.27
					19		7.714	77.14	0	0
					20		6.254	62.54	94.507	945.07
					21		4.931	49.31	185.882	1858.82
					22		3.634	36.34	233.156	2331.56
					23		2.393	23.93	383.32	3833.2
					24		1.1015	11.015	468.212	4682.12
					25		7.613	76.13	0	0
					26		6.247	62.47	93.168	931.68
					27		4.985	49.85	188.056	1880.56
					28		3.965	39.65	282.073	2820.73
					29		2.253	22.53	370.69	3706.9
					30		1.07	10.7	467.156	4671.56

Table D-5: Raw data for the Ca-saturated 0.01 total normality TYLX-CaX STx-1 system.

Sample	CaX ppm	CaX*5df	TylX µM	TylX µM*20df	Sample	pH	Ca2+ ppm	Ca2+*10df	Tyl+ µM	Tyl µM*10df
1			3.23622	64.7244	1	6.67	17.85	178.5	59.314	593.14
2	4.603	23.015	5.80925	116.185	2	6.81	14.35	143.5	169.784	1697.8374
3	4.559	22.795	7.98253	159.6506	3	6.88	10.75	107.5	306.942	3069.4234
4	3.959	19.795	11.16649	223.3298	4	6.92	10.7	107	439.809	4398.0905
5	3.821	19.105	14.35888	287.1776	5	6.94	6.44	64.4	581.856	5818.5554
6	3.586	17.93	24.79629	495.9258	6	6.97	6.162	61.62	743.877	7438.7661
7			3.49768	69.9536	7	6.67	17.98	179.8	53.838	538.379
8	4.741	23.705	5.86246	117.2492	8	6.84	14.06	140.6	180.007	1800.074
9	4.366	21.83	8.30803	166.1606	9	6.89	11.59	115.9	299.353	2993.5293
10	3.933	19.665	10.71537	214.3074	10	6.93	9.288	92.88	438.351	4383.51
11	3.852	19.26	15.44323	308.8646	11	6.96	6.508	65.08	581.414	5814.1361
12	3.627	18.135	24.70163	494.0326	12	6.99	6.171	61.71	733.669	7336.6855
13			3.4489	68.978	13	6.67	18.25	182.5	54.578	545.7843
14	4.611	23.055	5.86314	117.2628	14	6.84	15.25	152.5	178.939	1789.3865
15	4.823	24.115	7.83394	156.6788	15	6.9	9.849	98.49	314.856	3148.5631
16	4.146	20.73	11.952	239.04	16	6.88	8.801	88.01	439.713	4397.1281
17	3.824	19.12	14.28727	285.7454	17	6.93	7.422	74.22	598.068	5980.6842
18	3.468	17.34	24.64938	492.9876	18	6.97	6.258	62.58	748.246	7482.46
19a	3.469	17.345			19		16.19	161.9	111.777	1117.7728
19b	3.476	17.38			20		13.64	136.4	343.167	3431.668
19c	3.428	17.14			21		10.26	102.6	506.236	5062.3613
					22		7.076	70.76	705.617	7056.1674
					23		1.379	13.79	886.532	8865.3183
CEC1	6.032	30.16			24		0.24	2.4	1056.483	10564.8299
CEC2	6.241	31.205			25		16.68	166.8	171.085	1710.8474
CEC3	6.136	30.68			26		13.62	136.2	320.811	3208.1074
					27		10.36	103.6	517.881	5178.8141
					28		7.325	73.25	675.556	6755.5552
					29		3.725	37.25	866.210	8662.1023
					30		0.221	2.21	1048.575	10485.7544

Table D-6: Raw data for the TYL-saturated 0.01 total normality TYLX-CaX STx-1 system.

Sample	CaX ppm	CaX*5df	TylX mM	TylX µM*20df	Sample	pH	Ca2+ ppm	Ca2+*10df	Tyl+ µM	Tyl mM*10df
1	4.065	20.325	2.37298	47.4596	1	4.97	16.16	161.6	66.846	668.46
2	3.907	19.535	6.45752	129.1504	2	5.71	13.16	131.6	185.247	1852.47
3	3.625	18.125	9.22272	184.4544	3	6.08	10.61	106.1	317.328	3173.28
4	3.248	16.24	11.66082	233.2164	4	6.33	8.088	80.88	458.557	4585.57
5	2.936	14.68	13.29896	265.9792	5	6.45	5.399	53.99	612.329	6123.29
6	2.617	13.085	14.78285	295.657	6	6.47	2.644	26.44	786.99	7869.9
7	3.999	19.995	3.17565	63.513	7	4.97	15.45	154.5	71.953	719.53
8	3.856	19.28	6.57409	131.4818	8	5.72	13.11	131.1	188.366	1883.66
9	3.516	17.58	9.26724	185.3448	9	6.04	10.58	105.8	319.147	3191.47
10	3.335	16.675	12.48665	249.733	10	6.28	7.897	78.97	466.229	4662.29
11	3.012	15.06	14.37622	287.5244	11	6.45	5.327	53.27	616.759	6167.59
12	2.667	13.335	16.0247	320.494	12	6.55	2.551	25.51	785.592	7855.92
13	4.186	20.93	3.39714	67.9428	13	5.07	15.46	154.6	74.46	744.6
14	3.93	19.65	7.19719	143.9438	14	5.9	12.75	127.5	196.577	1965.77
15	3.407	17.035	9.57496	191.4992	15	6.1	10.45	104.5	322.166	3221.66
16	3.23	16.15	12.59186	251.8372	16	6.29	7.781	77.81	470.99	4709.9
17	2.947	14.735	14.69739	293.9478	17	6.38	5.243	52.43	627.85	6278.5
18	2.495	12.475	16.07553	321.5106	18	6.42	2.566	25.66	798.288	7982.88
					19		19.45	194.5	0	0
					20		16.51	165.1	175.769	1757.69
					21		13.6	136	340.749	3407.49
					22		5.665	56.65	526.824	5268.24
					23		6.795	67.95	703.712	7037.12
					24		3.515	35.15	882.188	8821.88
					25		20.31	203.1	0	0
					26		16.32	163.2	174.186	1741.86
					27		10.24	102.4	352.474	3524.74
					28		5.425	54.25	527.932	5279.32
					29		6.945	69.45	713.67	7136.7
					30		5.383	53.83	893.515	8935.15

Table D-7: Raw data for TYLX-NaX STx-1 system as a function of equilibrium time.

Sample	NaX ppm	NaX*df5	TylX mM	TylX µM*df20	Hour	Sample	Na+ ppm	Na+*df10	Tyl+ µM	Tyl mM*5df
E1	1.58	7.9	10.955	219.1	2	1	8.539	85.39	41.53	207.65
E2	1.544	7.72	10.739	214.78	2	2	8.377	83.77	42.95	214.75
E3	1.624	8.12	11.011	220.22	2	3	8.573	85.73	40.79	203.95
E4	1.755	8.775	11.148	222.96	6	4	8.716	87.16	43.942	219.71
E5	1.778	8.89	11.579	231.58	6	5	8.791	87.91	48.215	241.075
E6	1.882	9.41	11.494	229.88	6	6	8.65	86.5	44.577	222.885
E7	1.453	7.265	6.741	269.64	12	7	8.754	87.54	67.812	339.06
E8	1.392	6.96	6.478	259.12	12	8	8.538	85.38	70.278	351.39
E9	1.391	6.955	6.345	253.8	12	9	8.877	88.77	73.544	367.72
E10	1.849	9.245	11.842	236.84	24	10	8.582	85.82	60.623	303.115
E11	1.931	9.655	12.343	246.86	24	11	8.696	86.96	67.253	336.265
E12	2.16	10.8	12.088	241.76	24	12	8.751	87.51	68.738	343.69
E13	1.761	8.805	10.184	203.68	48	13	8.647	86.47	42.561	425.61
E14	1.967	9.835	12.256	245.12	48	14	8.874	88.74	37.302	373.02
E15	2.151	10.755	11.794	235.88	48	15	8.958	89.58	42.831	428.31
E16	1.719	8.595	12.673	253.46	72	16	8.703	87.03	46.326	463.26
E17	1.87	9.35	13.918	278.36	72	17	8.636	86.36	44.085	440.85
E18	1.792	8.96	13.133	262.66	72	18	8.348	83.48	43.658	436.58
					B2	19	4.878	48.78	475.92	2379.6
					B6	20	4.789	47.89	103.098	2061.96
					B6	21	3.844	38.44	105.278	2105.56
					B12	22	4.675	46.75	105.585	2111.7
					B12	23	4.748	47.48	106.365	2127.3
					B24	24	4.639	46.39	104.242	2084.84
					B24	25	4.755	47.55	106.495	2129.9
					B48	26	4.731	47.31	214.922	2149.22
					B48	27	4.641	46.41	216.443	2164.43
					B72	28	4.641	46.41	217.234	2172.34
					B72	29	4.671	46.71	219.622	2196.22

Table D-8: Raw data for the Na-saturated TYLX-NaX Libby vermiculite system.

Sample	NaX ppm	NaX*20df	TylX mM	TylX µM*20df	Sample	Na+ ppm	Na+*10df	Tyl+ µM	Tyl mM*10df		NaX redo	*df5
1	2.507	50.14	0.924	18.48	1	5.134	51.34	415.191	4151.91	E19	10.28	51.40
2	2.569	51.38	0.753	15.06	2	6.602	66.02	340.705	3407.05	E20	10.81	54.05
3	2.591	51.82	0.524	10.48	3	7.927	79.27	272.605	2726.05	E21	10.71	53.55
4	2.632	52.64	0.234	4.68	4	10.766	107.66	203.898	2038.98	E22	10.88	54.40
5	2.694	53.88	0.188	3.76	5	11.843	118.43	133.073	1330.73	E23	11.27	56.35
6	2.671	53.42	0.121	2.42	6	5.147	51.47	63.099	630.99	E24	11.06	55.30
7	2.572	51.44	1.121	22.42	7	4.568	45.68	408.898	4088.98	E25	10.67	53.35
8	2.615	52.3	0.809	16.18	8	5.765	57.65	343.935	3439.35	E26	10.89	54.45
9	2.589	51.78	0.486	9.72	9	12.645	63.225	270.628	2706.28	E27	10.67	53.35
10	2.717	54.34	0.303	6.06	10	9.194	91.94	363.343	3633.43	E28	10.93	54.65
11	2.812	56.24	0.193	3.86	11	10.234	102.34	131.242	1312.42	E29	11.29	56.45
12	2.81	56.2	0.068	1.36	12	11.452	114.52	65.357	653.57	E30	11.46	57.30
13	2.652	53.04	0.877	17.54	13	4.876	48.76	411.824	4118.24	E31	10.76	53.80
14	2.645	52.9	0.771	15.42	14	6.009	60.09	338.947	3389.47	E32	10.73	53.65
15	2.678	53.56	0.449	8.98	15	7.588	75.88	279.172	2791.72	E33	10.88	54.40
16	2.626	52.52	0.293	5.86	16	8.621	86.21	204.522	2045.22	E34	10.56	52.80
17	2.696	53.92	0.16	3.2	17	9.996	99.96	134.243	1342.43	E35	11.09	55.45
18	2.92	58.4	0.079	1.58	18	11.037	110.37	69.351	693.51	E36	11.36	56.80
					19	2.417	24.17	451.786	4517.86			
	amt. Tyl	pH	pH av	Tyl+	20	4.044	40.44	378.917	3789.17			
	30	7.41	7.613707	43.49162397	21	5.645	56.45	298.313	2983.13			
	30	8.01			22	7.274	72.74	220.116	2201.16			
					23	8.871	88.71	147.504	1475.04			
					24	10.135	101.35	77.198	771.98			
					25	2.391	23.91	444.825	4448.25			
					26	3.911	39.11	366.45	3664.5			
					27	5.402	54.02	293.899	2938.99			
					28	7.082	70.82	217.468	2174.68			
					29	8.602	86.02	141.994	1419.94			
					30	10.217	102.17	69.797	697.97			

Table D-9: Raw data for the TYL-saturated TYLX-NaX Libby vermiculite system.

Sample	NaX ppm	NaX*5df	TylX mM	TylX µM*10df	Sample	pH	Na+ ppm	Na+*10df	Tyl+ µM	Tyl mM*10df
1	3.07	15.35	0.253	2.53	1	6.73	5.135	51.35	8.32869	83.2869
2	2.927	14.635	0.348	3.48	2	6.75	4.464	44.64	54.48729	544.8729
3	2.742	13.71	0.347	3.47	3	6.88	3.787	37.87	99.93419	999.3419
4	2.518	12.59	0.394	3.94	4	6.97	3.329	33.29	144.27009	1442.7009
5	2.515	12.575	0.505	5.05	5	6.65	2.751	27.51	190.60135	1906.0135
6	2.286	11.43	0.554	5.54	6	7.03	2.217	22.17	233.54698	2335.4698
7	2.787	13.935	0.085	0.85	7	6.81	5.221	52.21	8.38637	83.8637
8	2.791	13.955	0.252	2.52	8	6.71	4.62	46.2	54.46275	544.6275
9	2.553	12.765	0.33	3.3	9	6.83	4.071	40.71	99.1152	991.152
10	2.521	12.605	0.377	3.77	10	6.86	3.45	34.5	141.34006	1413.4006
11	2.659	13.295	0.507	5.07	11	6.94	2.901	29.01	190.518	1905.18
12	2.371	11.855	0.698	6.98	12	6.98	2.297	22.97	229.30525	2293.0525
13	2.72	13.6	0.064	0.64	13	6.72	5.384	53.84	8.5191	85.191
14	2.752	13.76	0.161	1.61	14	6.74	4.752	47.52	54.32223	543.2223
15	2.562	12.81	0.291	2.91	15	6.81	4.212	42.12	95.1206	951.206
16	2.471	12.355	0.332	3.32	16	6.95	3.648	36.48	140.29074	1402.9074
17	2.396	11.98	0.466	4.66	17	6.96	3.006	30.06	188.94441	1889.4441
18	2.354	11.77	0.533	5.33	18	6.98	2.42	24.2	227.29431	2272.9431
					19		4.881	48.81	0	0
					20		4.225	42.25	54.54681	545.4681
					21		3.578	35.78	102.21606	1022.1606
					22		2.954	29.54	147.99888	1479.9888
					23		2.338	23.38	194.26487	1942.6487
					24		1.726	17.26	245.72731	2457.2731
					25		5.007	50.07	0	0
					26		4.672	46.72	55.40238	554.0238
					27		4.027	40.27	103.00975	1030.0975
					28		3.377	33.77	152.28254	1522.8254
					29		2.728	27.28	193.11926	1931.1926
					30		2.042	20.42	241.61448	2416.1448

Table D-10: Raw data for the Ca-saturated TYLX-CaX Libby vermiculite system.

Sample	CaX ppm	CaX*10df	TylX mM	TylX µM*2df	Sample	Ca2+ ppm	Ca2+*5df	Tyl+ µM	Tyl mM*5df
1	3.925	39.25	0.716	1.432	1	1.985	9.925	784.93	3924.65
2	4.167	41.67	0.455	0.91	2	4.01	20.05	660.45	3302.25
3	4.873	48.73	0.303	0.606	3	6.313	31.565	504.87	2524.35
4	4.499	44.99	0.233	0.466	4	8.663	43.315	394.32	1971.6
5	4.616	46.16	0.183	0.366	5	11.34	56.7	263.97	1319.85
6	4.589	45.89	0.099	0.198	6	13.58	67.9	127.02	635.1
7	4.335	43.35	0.796	1.592	7	1.984	9.92	767.4	3837
8	4.313	43.13	0.435	0.87	8	3.994	19.97	659.72	3298.6
9	4.36	43.6	0.368	0.736	9	6.354	31.77	528.83	2644.15
10	4.361	43.61	0.228	0.456	10	8.882	44.41	392.94	1964.7
11	4.414	44.14	0.182	0.364	11	12.07	60.35	248.37	1241.85
12	4.405	44.05	0.095	0.19	12	14.59	72.95	130.19	650.95
13	4.253	42.53	0.788	1.576	13	2.08	10.4	756.75	3783.75
14	4.562	45.62	0.476	0.952	14	4.298	21.49	678.64	3393.2
15	4.843	48.43	0.298	0.596	15	6.837	34.185	550.84	2754.2
16	4.882	48.82	0.204	0.408	16	9.23	46.15	397.83	1989.15
17	4.754	47.54	0.174	0.348	17	11.75	58.75	266.26	1331.3
18	4.791	47.91	0.123	0.246	18	14.22	71.1	130.76	653.8
					19	0	0	825.97	4129.85
					20	2.562	12.81	705.35	3526.75
					21	5.183	25.915	546.08	2730.4
	amt. Tyl	pH	pH av	Tyl+	22	7.984	39.92	412.89	2064.45
	30	6.97	7.11066	71.02290371	23	10.87	54.35	280.28	1401.4
	30	7.32			24	13.48	67.4	137.43	687.15
					25	0	0	838.17	4190.85
					26	2.619	13.095	690.5	3452.5
					27	5.28	26.4	560.03	2800.15
					28	8.021	40.105	410.47	2052.35
					29	10.56	52.8	275.42	1377.1
					30	13.58	67.9	136.92	684.6

Table D-11: Raw data for the TYL-saturated TYLX-CaX Libby vermiculite system.

Sample	CaX ppm	CaX*5df	TylX mM	TylX µM*20df	Sample	pH	Ca2+ ppm	Ca2+*10df	Tyl+ µM	Tyl mM*10df
1	5.021	25.105	0.022	0.44	1	6.23	4.731	47.31	5.803	58.03
2	4.713	23.565	0.092	1.84	2	6.44	3.515	35.15	102.555	1025.55
3	4.322	21.61	0.152	3.04	3	6.5	2.908	29.08	194.722	1947.22
4	3.856	19.28	0.283	5.66	4	6.65	2.108	21.08	276.588	2765.88
5	3.289	16.445	0.549	10.98	5	6.77	1.383	13.83	371.991	3719.91
6	2.535	12.675	0.817	16.34	6	6.16	0.632	6.32	469.161	4691.61
7	5.009	25.045	0	0	7	6.23	4.887	48.87	6.939	69.39
8	4.767	23.835	0.095	1.9	8	6.5	3.843	38.43	100.361	1003.61
9	4.457	22.285	0.142	2.84	9	6.65	2.953	29.53	190.816	1908.16
10	4.045	20.225	0.264	5.28	10	6.55	2.153	21.53	286.151	2861.51
11	3.413	17.065	0.523	10.46	11	6.61	1.439	14.39	371.281	3712.81
12	2.827	14.135	0.843	16.86	12	6.73	0.763	7.63	363.344	3633.44
13	4.829	24.145	0	0	13	6.13	4.574	45.74	6.666	66.66
14	4.717	23.585	0.089	1.78	14	6.55	3.556	35.56	102.555	1025.55
15	4.408	22.04	0.135	2.7	15	6.62	2.71	27.1	191.651	1916.51
16	3.948	19.74	0.249	4.98	16	6.67	1.98	19.8	282.206	2822.06
17	3.466	17.33	0.526	10.52	17	6.66	1.311	13.11	368.765	3687.65
18	2.848	14.24	0.735	14.7	18	6.73	0.515	5.15	480.275	4802.75
					19		7.714	77.14	0	0
					20		6.254	62.54	94.507	945.07
					21		4.931	49.31	185.882	1858.82
					22		3.634	36.34	233.156	2331.56
					23		2.393	23.93	383.32	3833.2
					24		1.1015	11.015	468.212	4682.12
					25		7.613	76.13	0	0
					26		6.247	62.47	93.168	931.68
					27		4.985	49.85	188.056	1880.56
					28		3.965	39.65	282.073	2820.73
					29		2.253	22.53	370.69	3706.9
					30		1.07	10.7	467.156	4671.56

Table D-12: Raw data for the 15-30 cm depth of the Na-saturated TYLX-NaX Loring soil system.

Sample	NaX ppm	NaX*2df	TylX mM	TylX µM*2df	Na+ ppm	Na+*5df	Tyl+ µM	Tyl mM*5df	pH
1	7.352	14.704	9.253	18.506	18.551	92.755	59.392	296.96	7.75
2	5.368	10.736	39.912	79.824	16.334	81.67	242.598	1212.99	7.31
3	4.24	8.48	53.631	107.262	17.288	86.44	328.742	1643.71	7.64
4	4.412	8.824	76.809	153.618	15.261	76.305	396.119	1980.595	7.67
5	3.848	7.696	88.359	176.718	14.534	72.67	496.175	2480.875	
6	3.133	6.266	91.545	183.09	11.931	59.655	596.301	2981.505	
7	7.361	14.722	10.449	20.898	18.565	92.825	63.77	318.85	
8	5.585	11.17	32.563	65.126	17.823	89.115	239.884	1199.42	
9	4.159	8.318	55.587	111.174	16.342	81.71	332.697	1663.485	
10	4.407	8.814	62.795	125.59	14.991	74.955	415.999	2079.995	
11	3.598	7.196	74.912	149.824	13.394	66.97	492.411	2462.055	
12	2.882	5.764	86.257	172.514	11.557	57.785	609.87	3049.35	
13	7.502	15.004	10.284	20.568	18.718	93.59	61.626	308.13	
14	5.038	10.076	29.203	58.406	17.359	86.795	238.108	1190.54	
15	4.223	8.446	51.751	103.502	15.255	76.275	330.556	1652.78	
16	3.934	7.868	65.21	130.42	15.353	76.765	409.226	2046.13	
17	3.285	6.57	69.902	139.804	13.063	65.315	507.272	2536.36	
18	2.946	5.892	84.603	169.206	12.237	61.185	631.581	3157.905	
				Blanks	16.81	84.05	119.12	595.6	
				Blanks	12.028	60.14	368.227	1841.135	
				Blanks	10.037	50.185	494.24	2471.2	
				Blanks	7.697	38.485	612.715	3063.575	
				Blanks	5.389	26.945	755.436	3777.18	
				Blanks	2.977	14.885	897.035	4485.175	
				Blanks	17.011	85.055	122.226	611.13	
				Blanks	12.685	63.425	361.426	1807.13	
				Blanks	10.166	50.83	499.16	2495.8	
				Blanks	7.991	39.955	625.781	3128.905	
				Blanks	5.558	27.79	748.19	3740.95	
				Blanks	3.089	15.445	867.743	4338.715	

Table D-13: Raw data for the 15-30 cm depth of the TYL-saturated TYLX-NaX Loring soil system.

Sample	NaX ppm	NaX ppm*2df	TylX mM	TylX µM*2df	Na+ ppm	Na ppm*5df	Tyl+ µM	Tyl mM*5df
1	0.90069	1.80138	32.234	64.468	5.113	25.565	639.061	3195.305
2	1.2208	2.4416	30.005	60.01	6.8904	34.452	484.227	2421.135
3	1.5563	3.1126	21.729	43.458	10.333	51.665	412.632	2063.16
4	1.7843	3.5686	17.587	35.174	12.112	60.56	263.149	1315.745
5	1.9157	3.8314	14.936	29.872	13.863	69.315	133.671	668.355
6	1.7033	3.4066	5.838	11.676	17.234	86.17	29.345	146.725
7	0.82675	1.6535	40.729	81.458	5.2057	26.0285	645.921	3229.605
8	1.2044	2.4088	29.07	58.14	6.9588	34.794	484.734	2423.67
9	1.5461	3.0922	20.369	40.738	9.0806	45.403	373.161	1865.805
10	1.7303	3.4606	21.547	43.094	11.594	57.97	252.559	1262.795
11	1.9112	3.8224	11.405	22.81	13.683	68.415	131.543	657.715
12	1.7626	3.5252	7.081	14.162	16.405	82.025	27.333	136.665
13	0.83446	1.66892	39.217	78.434	5.2667	26.3335	641.888	3209.44
14	1.1324	2.2648	30.34	60.68	7.3141	36.5705	510.997	2554.985
15	1.5238	3.0476	25.833	51.666	10.242	51.21	409.338	2046.69
16	1.8193	3.6386	16.515	33.03	11.343	56.715	131.897	659.485
17	1.8212	3.6424	12.253	24.506	13.1	65.5	129.49	647.45
18	1.6692	3.3384	7.583	15.166	14.995	74.975	26.204	131.02
				Blanks	5.0703	25.3515	684.379	3421.895
pH=7.37				Blanks	8.2028	41.014	617.543	3087.715
				Blanks	10.328	51.64	430.241	2151.205
				Blanks	12.62	63.1	282.091	1410.455
				Blanks	17.587	87.935	163.134	815.67
				Blanks	19.48	97.4	0.062	0.31
				Blanks	5.7472	28.736	781.898	3909.49
				Blanks	8.2165	41.0825	584.666	2923.33
				Blanks	11.653	58.265	465.833	2329.165
				Blanks	14.186	70.93	310.847	1554.235
				Blanks	17.179	85.895	57.021	285.105
				Blanks	20.037	100.185	0.045	0.225

Table D-14: Raw data for the 30-46 cm depth of the Na-saturated TYLX-NaX Loring soil system.

Sample	NaX ppm	NaX*2df	TylX mM	TylX µM*2df	Na+ ppm	Na+*5df	Tyl+ µM	Tyl mM*5df
19	9.028	18.056	16.828	33.656	19.657	98.285	48.505	242.525
20	6.973	13.946	51.555	103.11	18.729	93.645	198.135	990.675
21	6.651	13.302	94.825	189.65	17.11	85.55	247.699	1238.495
22	5.781	11.562	120.327	240.654	15.981	79.905	323.931	1619.655
23	5.261	10.522	128.125	256.25	14.514	72.57	428.792	2143.96
24	4.947	9.894	137.92	275.84	12.679	63.395	508.854	2544.27
25	10.532	21.064	23.336	46.672	19.984	99.92	43.339	216.695
26	7.889	15.778	64.712	129.424	18.522	92.61	183.185	915.925
27	6.746	13.492	96.137	192.274	16.941	84.705	251.606	1258.03
28	5.836	11.672	115.451	230.902	16.028	80.14	337.384	1686.92
29	5.564	11.128	120.827	241.654	14.478	72.39	414.239	2071.195
30	5.101	10.202	153.249	306.498	13.397	66.985	505.566	2527.83
31	11.127	22.254	22.065	44.13	19.012	95.06	41.775	208.875
32	9.098	18.196	56.274	112.548	19.156	95.78	183.813	919.065
33	8.335	16.67	73.7	147.4	17.191	85.955	239.286	1196.43
34	6.213	12.426	125.725	251.45	16.852	84.26	325.866	1629.33
35	5.711	11.422	131.172	262.344	15.54	77.7	390.564	1952.82
36	5.33	10.66	126.33	252.66	13.552	67.76	499.181	2495.905
				Blanks	16.81	84.05	119.12	595.6
				Blanks	12.028	60.14	368.227	1841.135
				Blanks	10.037	50.185	494.24	2471.2
	pH	pH av	Tyl+	Blanks	7.697	38.485	612.715	3063.575
30-46	7.34	7.55655	46.74957	Blanks	5.389	26.945	755.436	3777.18
30-46	7.11			Blanks	2.977	14.885	897.035	4485.175
30-46	7.63			Blanks	17.011	85.055	122.226	611.13
30-46	7.56			Blanks	12.685	63.425	361.426	1807.13
		7.36072	57.94972	Blanks	10.166	50.83	499.16	2495.8
				Blanks	7.991	39.955	625.781	3128.905
				Blanks	5.558	27.79	748.19	3740.95
				Blanks	3.089	15.445	867.743	4338.715

Table D-15: Raw data for the 30-46 cm depth of the TYL-saturated TYLX-NaX Loring soil system.

Sample	NaX ppm	NaX ppm*df	TylX mM	TylX µM*df	Na+ ppm	Na ppm*df	Tyl+ µM	Tyl mM*df
19	0.90078	1.80156	68.949	137.898	4.6251	23.1255	583.841	2919.205
20	1.1873	2.3746	55.268	110.536	7.123	35.615	495.685	2478.425
21	1.4553	2.9106	49.187	98.374	8.922	44.61	386.244	1931.22
22	1.9304	3.8608	35.14	70.28	10.701	53.505	267.387	1336.935
23	2.4624	4.9248	30.958	61.916	13.518	67.59	166.878	834.39
24	2.3383	4.6766	26.102	52.204	15.54	77.7	66.792	333.96
25	0.98923	1.97846	74.678	149.356	5.4386	27.193	641.574	3207.87
26	1.2002	2.4004	56.307	112.614	6.8616	34.308	479.497	2397.485
27	1.5061	3.0122	44.561	89.122	8.8829	44.4145	368.971	1844.855
28	1.7268	3.4536	41.698	83.396	11.613	58.065	279.643	1398.215
29	2.3869	4.7738	35.148	70.296	13.842	69.21	171.495	857.475
30	2.1099	4.2198	29.47	58.94	16.419	82.095	67.565	337.825
31	0.8659	1.7318	76.78	153.56	5.0923	25.4615	640.575	3202.875
32	1.1867	2.3734	64.283	128.566	7.3628	36.814	515.167	2575.835
33	1.3368	2.6736	59.889	119.778	9.693	48.465	405.481	2027.405
34	1.8797	3.7594	42.763	85.526	10.532	52.66	258.303	1291.515
35	2.3805	4.761	38.621	77.242	14.24	71.2	169.263	846.315
36	2.2768	4.5536	22.698	45.396	15.386	76.93	67.318	336.59
				Blanks	5.0703	25.3515	684.379	3421.895
pH=7.13				Blanks	8.2028	41.014	617.543	3087.715
				Blanks	10.328	51.64	430.241	2151.205
				Blanks	12.62	63.1	282.091	1410.455
				Blanks	17.587	87.935	163.134	815.67
				Blanks	19.48	97.4	0.062	0.31
				Blanks	5.7472	28.736	781.898	3909.49
				Blanks	8.2165	41.0825	584.666	2923.33
				Blanks	11.653	58.265	465.833	2329.165
				Blanks	14.186	70.93	310.847	1554.235
				Blanks	17.179	85.895	57.021	285.105
				Blanks	20.037	100.185	0.045	0.225

Table D-16: Raw data for the 15-30 cm depth of the Ca-saturated TYLX-CaX Loring soil system.

Sample	CaX ppm	CaX*100df	TylX mM	TylX µM*2df	Ca2+ ppm	Ca2+*5df	Tyl+ µM	Tyl mM*5df	pH
1	0.3902	39.02	97.989	195.978	6.073	30.365	638.177	3190.885	7.44
2	0.4352	43.52	83.469	166.938	7.405	37.025	518.633	2593.165	7.75
3	0.4197	41.97	68.234	136.468	8.896	44.48	407.655	2038.275	
4	0.4315	43.15	43.758	87.516	10.4	52	311.696	1558.48	
5	0.4469	44.69	34.439	68.878	12.42	62.1	190.668	953.34	
6	0.4764	47.64	17.039	34.078	13.6	68	79.76	398.8	
7	0.3764	37.64	93.43	186.86	5.79	28.95	640.585	3202.925	
8	0.4281	42.81	80.741	161.482	7.321	36.605	529.321	2646.605	
9	0.4336	43.36	68.928	137.856	8.863	44.315	419.432	2097.16	
10			47.61	95.22	10.5	52.5	305.743	1528.715	
11	0.511	51.1	32.398	64.796	10.75	53.75	193.864	969.32	
12	0.5048	50.48	16.233	32.466	12.95	64.75	85.433	427.165	
13	0.4033	40.33	92.21	184.42	5.783	28.915	651.459	3257.295	
14	0.4405	44.05	84.795	169.59	7.458	37.29	543.364	2716.82	
15	0.4596	45.96	57.66	115.32	9.21	46.05	417.538	2087.69	
16	0.474	47.4	48.338	96.676	10.48	52.4	297.991	1489.955	
17	0.4921	49.21	28.744	57.488	11.97	59.85	199.851	999.255	
18	0.5298	52.98	14.806	29.612	13.08	65.4	87.254	436.27	
				Blanks	0.1319	0.6595	842.422	4212.11	
				Blanks	2.848	14.24	706.379	3531.895	
				Blanks	5.347	26.735	556.992	2784.96	
				Blanks	8.023	40.115	415.229	2076.145	
				Blanks	10.54	52.7	270.492	1352.46	
				Blanks	12.48	62.4	132.744	663.72	
				Blanks	0.1622	0.811	812.061	4060.305	
				Blanks	2.338	11.69	687.021	3435.105	
				Blanks	5.608	28.04	547.44	2737.2	
				Blanks	8.221	41.105	414.157	2070.785	
				Blanks	10.51	52.55	274.823	1374.115	
				Blanks	12.82	64.1	134.946	674.73	

Table D-17: Raw data for the 15-30 cm depth of the TYL-saturated TYLX-CaX Loring soil system.

Sample	CaX ppm1	CaX*20df	TylX mM	TylX µM*df2	Ca2+ ppm1	Ca2+*5df	Tyl+ µM	Tyl mM*df5
1	0.189	3.78	2.279	4.558	9.145	45.725	200.58	1002.9
2	0.313	6.26	2.473	4.946	6.179	30.895	314.127	1570.635
3	0.134	2.68	3.165	6.33	4.002	20.01	415.639	2078.195
4	0.203	4.06	4.21	8.42	2.591	12.955	493.875	2469.375
5	0.091	1.82	6.37	12.74	1.343	6.715	572.119	2860.595
6	0.075	1.5	8.887	17.774	0.469	2.345	659.204	3296.02
7	0.034	0.68	11.767	23.534	0	0	744.365	3721.825
8	0.219	4.38	2.34	4.68	9.328	46.64	210.984	1054.92
9	0.257	5.14	2.55	5.1	6.278	31.39	306.66	1533.3
10	0.253	5.06	3.103	6.206	4.07	20.35	389.752	1948.76
11	0.18	3.6	4.481	8.962	1.474	7.37	467.5	2337.5
12	0.207	4.14	6.595	13.19	0.858	4.29	580.754	2903.77
13	0.175	3.5	8.856	17.712	0.485	2.425	662.997	3314.985
14	0	0	11.466	22.932	0	0	756.351	3781.755
15	0.345	6.9	2.569	5.138	9.393	46.965	223.134	1115.67
16	0.336	6.72	2.816	5.632	6.692	33.46	302.141	1510.705
17	0.307	6.14	3.297	6.594	4.336	21.68	417.936	2089.68
18	0.207	4.14	3.815	7.63	2.737	13.685	495.458	2477.29
				Blanks	16.17	80.85	0	0
	pH	pH av	Tyl+	Blanks	13.621	68.105	128.563	642.815
6-12	5.92	6.1068614	96.1128	Blanks	11.153	55.765	254.665	1273.325
6-12	6.85			Blanks	8.137	40.685	365.415	1827.075
6-12	5.79			Blanks	5.576	27.88	511.194	2555.97
6-12	6.79			Blanks	2.773	13.865	647.886	3239.43
				Blanks	0	0	772.742	3863.71
				Blanks	16.124	80.62	0	0
				Blanks	13.534	67.67	118.196	590.98
				Blanks	11.059	55.295	253.961	1269.805
				Blanks	8.215	41.075	382.303	1911.515
				Blanks	5.853	29.265	511.252	2556.26
				Blanks	2.789	13.945	644.295	3221.475
				Blanks	0	0	788.784	3943.92

Table D-18: Raw data for the 30-46 cm depth of the Ca-saturated TYLX-CaX Loring soil system.

Sample	CaX ppm	CaX*100df	TylX mM	TylX µM*2df	Ca2+ ppm	Ca2+*5df	Tyl+ µM	Tyl mM*5df
19	0.315	31.5	132.334	264.668	4.71	23.55	598.935	2994.675
20	0.3451	34.51	116.387	232.774	6.086	30.43	499.958	2499.79
21	0.3476	34.76	80.215	160.43	7.967	39.835	385.95	1929.75
22	0.3729	37.29	69.795	139.59	7.463	37.315	274.151	1370.755
23	0.351	35.1	48.221	96.442	11.2	56	166.777	833.885
24	0.3859	38.59	21.67	43.34	12.86	64.3	62.702	313.51
25	0.3141	31.41	142.734	285.468	4.901	24.505	602.354	3011.77
26	0.3283	32.83	107.259	214.518	6.321	31.605	500.023	2500.115
27	0.7544	75.44	125.814	251.628	8.332	41.66	285.494	1427.47
28	0.3341	33.41	67.795	135.59	9.445	47.225	284.107	1420.535
29	0.3729	37.29	45.943	91.886	11.32	56.6	170.707	853.535
30	0.7987	79.87	18.314	36.628	13.07	65.35	23.71	118.55
31	0.314	31.4	142.011	284.022	8.848	44.24	600.877	3004.385
32	0.3499	34.99	115.665	231.33	6.097	30.485	498.943	2494.715
33	0.3496	34.96	87.322	174.644	7.553	37.765	390.703	1953.515
34	0.3705	37.05	69.01	138.02	9.334	46.67	282.567	1412.835
35	0.358	35.8	39.873	79.746	11.51	57.55	173.472	867.36
36	0.3787	37.87	24.932	49.864	13.14	65.7	63.997	319.985
				Blanks	0.1319	0.6595	842.422	4212.11
				Blanks	2.848	14.24	706.379	3531.895
				Blanks	5.347	26.735	556.992	2784.96
	pH	pH av	Tyl+	Blanks	8.023	40.115	415.229	2076.145
12-18	7.29	7.1967345	66.78096	Blanks	10.54	52.7	270.492	1352.46
12-18	7.12			Blanks	12.48	62.4	132.744	663.72
				Blanks	0.1622	0.811	812.061	4060.305
				Blanks	2.338	11.69	687.021	3435.105
				Blanks	5.608	28.04	547.44	2737.2
				Blanks	8.221	41.105	414.157	2070.785
				Blanks	10.51	52.55	274.823	1374.115
				Blanks	12.82	64.1	134.946	674.73

Table D-19: Raw data for the 30-46 cm depth of the TYL-saturated TYLX-CaX Loring soil system.

Sample	CaX ppm1	CaX*20df	TylX mM	TylX µM*df2	Ca2+ ppm1	Ca2+*5df	Tyl+ µM	Tyl mM*df5
19	0.208	4.16	6.339	12.678	1.498	7.49	571.115	2855.575
20	0.191	3.82	8.781	17.562	0.583	2.915	659.791	3298.955
21	0.135	2.7	10.941	21.882	0	0	757.486	3787.43
22	0.323	6.46	9.494	18.988	7.568	37.84	239.011	1195.055
23	0.38	7.6	5.178	10.356	3.695	18.475	339.861	1699.305
24	0.275	5.5	7.209	14.418	2.157	10.785	416.435	2082.175
25	0.287	5.74	9.653	19.306	1.14	5.7	476.808	2384.04
26	0.223	4.46	12.662	25.324	0.384	1.92	538.644	2693.22
27	0.136	2.72	15.597	31.194	0	0	630.093	3150.465
28	0.042	0.84	15.853	31.706	0	0	729.081	3645.405
29	0.367	7.34	3.807	7.614	6.944	34.72	259.546	1297.73
30	0.344	6.88	5.099	10.198	3.588	17.94	350.078	1750.39
31	0.409	8.18	7.076	14.152	1.67	8.35	425.771	2128.855
32	0.317	6.34	9.876	19.752	0.887	4.435	476.592	2382.96
33	0.215	4.3	13.317	26.634	0.28	1.4	539.121	2695.605
34	0.147	2.94	15.481	30.962	0	0	628.888	3144.44
35	0.044	0.88	16.209	32.418	0	0	732.474	3662.37
36	0.496	9.92	5.525	11.05	7.989	39.945	231.976	1159.88
37	0.429	8.58	5.151	10.302	3.612	18.06	360.598	1802.99
38	0.344	6.88	6.859	13.718	2.104	10.52	410.291	2051.455
39	0.34	6.8	10.519	21.038	1.009	5.045	470.366	2351.83
40	0.257	5.14	12.574	25.148	0.36	1.8	545.529	2727.645
41	0.258	5.16	16.297	32.594	0.055	0.275	624.382	3121.91
42	0.17	3.4	17.645	35.29	0	0	723.847	3619.235
				Blanks	16.17	80.85	0	0
	pH	pH av	Tyl+	Blanks	13.621	68.105	128.563	642.815
12-18	5.4	5.7533917	98.2393	Blanks	11.153	55.765	254.665	1273.325
12-18	6.35			Blanks	8.137	40.685	365.415	1827.075
12-18	6.8			Blanks	5.576	27.88	511.194	2555.97
12-18	5.39			Blanks	2.773	13.865	647.886	3239.43
12-18	6.79			Blanks	0	0	772.742	3863.71
				Blanks	16.124	80.62	0	0
				Blanks	13.534	67.67	118.196	590.98
				Blanks	11.059	55.295	253.961	1269.805
				Blanks	8.215	41.075	382.303	1911.515
				Blanks	5.853	29.265	511.252	2556.26
				Blanks	2.789	13.945	644.295	3221.475
				Blanks	0	0	788.784	3943.92

VITA

Jaime Call was born in Decatur, Georgia, to the parents of Robert and Helen Wilson. She is the middle of three daughters: Rebecca and Amber. Her family moved to Madisonville, Tennessee when she was very young. She attended Madisonville Elementary School, Madisonville Middle School, and Sequoyah High School. After high school graduation in May 1999, she attended the University of Tennessee in Knoxville for three years. She transferred to Thomas Edison State University in New Jersey in August 2002 after she married Benjamin Call in May 2002. She traveled throughout the United States and abroad with her husband who was an officer in the United States Air Force. She finally graduated with a Bachelor of Arts degree in March 2006 from Thomas Edison State University. In December 2006, Jaime and her husband permanently moved to Knoxville, TN where Jaime began working full time at the University of Tennessee, Knoxville as an administrative assistant. In August 2009, she started an undergraduate degree in Environmental and Soil Science and in August 2010, Benjamin and Jaime welcomed their first daughter, Rose. Jaime graduated with a Bachelor of Science in May 2013 and in August 2013, the couple welcomed their second daughter, Marisa. Soon after, in January 2014, Jaime accepted a Graduate Teaching Assistantship at the University of Tennessee, Knoxville in the Biosystems Engineering and Soil Science Department working with Dr. Michael Essington. Jaime graduated with a Master of Science degree in Environmental and Soil Science in May 2017. She is currently working as a Research Coordinator with Dr. Sindhu Jagadamma at the University of Tennessee, Knoxville.